Electron transport in Fermi liquids and beyond

Dmitrii L. Maslov and Joshua Covey

Department of Physics, University of Florida

(Dated: August 4, 2025)

CONTENTS

I. CLASSICAL MEMORY EFFECTS IN APPLICATION TO RESISTIVE ANOMALIES NEAR SECOND-ORDER PHASE TRANSITIONS

The Boltzmann equation (BE) in the presence of a time-independent and spatially non-uniform electric and magnetic field reads

$$\frac{\partial f_{\mathbf{k}}(\mathbf{r},t)}{\partial t} + \mathbf{v}_{\mathbf{k}} \cdot \boldsymbol{\nabla}_{\mathbf{r}} f_{\mathbf{k}}(\mathbf{r},t) - e\left[\mathbf{E}(\mathbf{r},t) + \mathbf{v}_{\mathbf{k}} \times \mathbf{B}(\mathbf{r},t)\right] \cdot \frac{\partial f_{\mathbf{k}}(\mathbf{r},t)}{\partial \mathbf{k}} = I_{ee}\left[f_{\mathbf{k}}\right] + I_{eph}[f_{\mathbf{k}}] + I_{ei}\left[f_{\mathbf{k}}\right], \quad (1.1)$$

where $\mathbf{v}_{\mathbf{k}} = \partial\varepsilon_{\mathbf{k}}/\partial\mathbf{k}$ is the group velocity, I_{ee}, I_{ee}, and I_{ei} are the collision integrals, describing electron-electron, electron-phonon, and electron-impurity interactions, respectively.

A. Basics of electron-impurity scattering

1. *What is the correct form of the Boltzmann equation for elastic scattering?*

Contrary to the popular opinion, the *most* general form of the the electron-impurity collision integral is [1–3]

$$I_{ei}[f_{\mathbf{k}}] = -\int_{\mathbf{k}'} \left(w_{\mathbf{k},\mathbf{k}'} f_{\mathbf{k}} - w_{\mathbf{k}',\mathbf{k}} f_{\mathbf{k}'}\right) \delta(\varepsilon_{\mathbf{k}} - \varepsilon_{\mathbf{k}'}), \quad (1.2)$$

where $f_{\mathbf{p}} \equiv f_{\mathbf{p}}(\mathbf{r},t)$, $\int_{\mathbf{p}} \equiv \int d^d p/(2\pi)^d$ and $w_{\mathbf{k}',\mathbf{k}}$ is proportional to the probability of scattering from $\mathbf{k}'$ to $\mathbf{k}$. The delta function expresses energy conservation: Electron-impurity collisions are elastic. [1] Equation (1.2) is valid both for fermions and bosons.

In general, $w_{\mathbf{k}',\mathbf{k}} \neq w_{\mathbf{k},\mathbf{k}'}$.[2] Indeed, if the system is invariant on time-reversal, then

$$w_{\mathbf{k},\mathbf{k}'} = w_{-\mathbf{k}',-\mathbf{k}}. \quad (1.3)$$

[1] This is not really true, as impurities are not infinitely heavy, and scattering at them can emit a phonon. This is a triple scattering event though (electron-impurity-phonon), and the corresponding probability is small.

[2] In the first Born approximation, this relation is valid regardless of the symmetries of the system. However, it is not valid beyond the first Born approximation [3].

If, in addition, the system has spatial inversion symmetry, then

$$w_{\mathbf{k},\mathbf{k}'} = w_{-\mathbf{k},-\mathbf{k}'}. \tag{1.4}$$

Applying *both* (1.3) and (1.4), one arrives at what is known as the microreversibility property

$$w_{\mathbf{k}',\mathbf{k}} = w_{\mathbf{k},\mathbf{k}'}. \tag{1.5}$$

But if either one or both symmetries are broken, (1.5) is not satisfied.

Why is this important? Note that (1.2) is different from an often quoted form

$$\tilde{I}_{ei}[f_\mathbf{k}] = -\int_{\mathbf{k}'} \left[w_{\mathbf{k},\mathbf{k}'} f_\mathbf{k}(1 \mp f_{\mathbf{k}'}) - w_{\mathbf{k}',\mathbf{k}} f_{\mathbf{k}'}(1 \mp f_\mathbf{k})\right] \delta(\varepsilon_\mathbf{k} - \varepsilon_{\mathbf{k}'}), \tag{1.6}$$

where $\mp$ applies to fermions/bosons. [3] If (1.5) is satisfied, the bilinear terms in (1.6) cancel out, and it reduces back to (1.2). However, what if (1.5) is not satisfied? Well, then we have a non-linear integral equation to solve. The consequences of non-linearity is that, sooner or later, the system will run into an instability. But wait, we are talking about impurity scattering here; hence, there is just an electron moving in a given potential. One can solve the Schrodinger equation for this system, and the result will be (in the semiclassical limit) an absolutely unambiguous prediction about the state of the system at later time t, given its state at $t = 0$. This is why the most general form of the collision integral is (a simpler) (1.2), rather than (a more complicated) (1.6): The former is valid even if (1.5) is not satisfied.

In the simplest case of point-like impurities, when scattering is isotropic, $w_{\mathbf{k}',\mathbf{k}} = \text{const}$. Recalling that $\int_{\mathbf{k}'} \delta(\varepsilon_{\mathbf{k}'} - \varepsilon_\mathbf{k}) = \nu(\varepsilon_\mathbf{k})$, where $\nu(\varepsilon)$ is the density of states (per flavor), and defining the mean free time via $1/\tau(\varepsilon_\mathbf{k}) = w\nu(\varepsilon_\mathbf{k})$, we simplify (1.2) to

$$I_{ee}[f_\mathbf{k}] = -\frac{f_\mathbf{k} - \bar{f}}{\tau}, \tag{1.7}$$

where $\bar{f}$ is the angular average of the distribution function at a given energy.

Let's compare (1.7) with another popular form of the collision integral, known as the "relaxation time approximation" (RTA):

$$I_{RTA}[f_\mathbf{k}] = -\frac{f_\mathbf{k} - f_0}{\tau^*}, \tag{1.8}$$

[3] The mere fact that (1.6) distinguishes between fermions and bosons should raise an alarm. We have a single particle bouncing off potential scatterers. There is no way to tell if the particle is a fermion or boson, unless other particles are present.

where f_0 is the equilibrium distribution function. Despite an obvious similarity, (1.7) and (1.8) describe very different physics. Indeed, (1.7) describes relaxation towards an *isotropic* but *not* equilibrium state. Elastic scattering conserves energy, so the best it can do is to completely randomize directions of electron velocities. A full equilibrium can be reached only via inelastic processes. In contrast, RTA implies full equilibration. The problem with RTA is that it violates several conservation laws.

In the BE framework, conservation laws are reflected as follows. Suppose that a certain property–$q(\mathbf{k})$–is conserved. For example, $q(\mathbf{k}) = 1$ is the particle number, $q(\mathbf{k}) = \mathbf{k}$ is the momentum, $q(\mathbf{k}) = \varepsilon_{\mathbf{k}}$ is the energy, etc. Multiplying BE by $q(\mathbf{k})$, we obtain

$$\frac{dQ}{dt} = \frac{d}{dt}\int_{\mathbf{k}} q(\mathbf{k}) f_{\mathbf{k}} = \int_{\mathbf{k}} q(\mathbf{k}) I[f_{\mathbf{k}}]. \tag{1.9}$$

If Q is conserved, then $\int_{\mathbf{k}} q(\mathbf{k}) f_{\mathbf{k}} = \int_{\mathbf{k}} q(\mathbf{k}) I[f_{\mathbf{k}}] = 0$.

For the case of elastic scattering, there are two conserved quantities: the number of particles at given energy, equal to $\bar{f}$, and total energy, equal to $\int_{\mathbf{k}} \varepsilon_{\mathbf{k}} f_{\mathbf{k}}$. It is easy to see that the collision integral in (1.7) does satisfy both these properties while the RTA collision integral does not. This is a serious drawback, as in the long-time limit (1.8) cannot describe diffusion. Namely, we should expect the Fourier transform $f(\mathbf{k}, \mathbf{q}, \omega)$ to exhibit a diffusion pole for $\omega\tau \ll 1$ and $qv_F\tau \ll 1$:

$$f(\mathbf{k}, \mathbf{q}, \omega) \propto \frac{1}{Dq^2 - i\omega}, \tag{1.10}$$

where $D = v_F^2\tau/d$ is the diffusion coefficient. As shown in Appendix A, collision integral (1.7) satisfies this property but collision integral (1.8) does not. Using the RTA approximation gives incorrect results, e.g., for ultrasound absorption by free electrons, which is proportional to the conductivity at finite wavenumber, $\sigma(\mathbf{q}, \omega)$.[4]

However, the Boltzmann equation with the "correct" form of the collision integral, Eq. (1.7), has a problem on its own. Namely, if the electric field is weak, we tend to expand the force term, $-e\mathbf{E} \cdot \partial_{\mathbf{k}} f_{\mathbf{k}}$ around equilibrium, i.e., replacing it with $-e\mathbf{E} \cdot \partial_{\mathbf{k}} f_{0\mathbf{k}} = -e\mathbf{E} \cdot \mathbf{v}_{\mathbf{k}} \partial_{\varepsilon} f_{0\mathbf{k}}$. However, since there is no notion of the equilibrium distribution for elastic scattering, we need to expand the force term around the *angular average* of $f_{\mathbf{k}}$, rather than around $f_{0\mathbf{k}}$. Doing so, we obtain the following equation

$$-e(\mathbf{E} \cdot \mathbf{v}_{\mathbf{k}}) \frac{\partial \bar{f}}{\partial \varepsilon_{\mathbf{k}}} = -\frac{f_{\mathbf{k}} - \bar{f}}{\tau}. \tag{1.11}$$

[4] For correct treatment, see Ref. [4].

It can be readily see that this equation is solved by

$$f_{\mathbf{k}} = \bar{f} + e(\mathbf{E}\cdot\mathbf{v}_{\mathbf{k}})\frac{\partial \bar{f}}{\partial \varepsilon_{\mathbf{k}}}, \tag{1.12}$$

which leaves $\bar{f}$ undetermined. Therefore, (1.11) does not have a unique solution.

To make a solution unique, we need to introduce inelastic processes that do equilibrate electrons with the thermostat [5]. For this purpose, RTA collision integral (1.8) can be used as a toy model. Once we invoked the equilibrium distribution via RTA, the LHS can be linearized around $f_{0\mathbf{k}}$, and we obtain the following equation (with $f'_{0\mathbf{k}} \equiv \partial_{\varepsilon_{\mathbf{k}}} f_{0\mathbf{k}}$:

$$-e(\mathbf{v}_{\mathbf{k}}\cdot\mathbf{E})f'_{0\mathbf{k}} = \frac{\bar{f} - f_{\mathbf{k}}}{\tau} + \frac{f_{0\mathbf{k}} - f_{\mathbf{k}}}{\tau^*}, \tag{1.13}$$

which yields

$$f_{\mathbf{k}} = \frac{1}{\frac{1}{\tau}+\frac{1}{\tau^*}}\left[e(\mathbf{v}_{\mathbf{k}}\cdot\mathbf{E})f'_{0\mathbf{k}} + \frac{\bar{f}}{\tau} + \frac{f_0}{\tau^*}\right]. \tag{1.14}$$

Averaging the last expression over angles, we find that $\bar{f} = f_{0\mathbf{k}}$. Now $f_{\mathbf{k}}$ is determined uniquely

$$f_{\mathbf{k}} = f_{0\mathbf{k}} + \frac{1}{\frac{1}{\tau}+\frac{1}{\tau^*}} e(\mathbf{v}_{\mathbf{k}}\cdot\mathbf{E})f'_{0\mathbf{k}}. \tag{1.15}$$

If the equilibrating time is much longer than than the momentum relaxation time, $\tau^* \gg \tau$, we can safely set $1/\tau^* = 0$:

$$f_{\mathbf{k}} = f_{0\mathbf{k}} + \tau e(\mathbf{v}_{\mathbf{k}}\cdot\mathbf{E})f'_{0\mathbf{k}}. \tag{1.16}$$

From now on, we will be using the following form of the Boltzmann equation for elastic scattering

$$-e(\mathbf{v}_{\mathbf{k}}\cdot\mathbf{E})f'_{0\mathbf{k}} = \frac{\bar{f} - f_{\mathbf{k}}}{\tau}, \tag{1.17}$$

with the understanding that inelastic processes were implicitly taken into account when the LHS was linearized around $f_{0\mathbf{k}}$.

The electric current is found as

$$\mathbf{j} = -2e\int_{\mathbf{k}} \mathbf{v}_{\mathbf{k}} f_{\mathbf{k}} = 2e^2 \int_{\mathbf{k}} \tau \mathbf{v}_{\mathbf{k}}(\mathbf{v}_{\mathbf{k}}\cdot\mathbf{E})(-f'_{0\mathbf{k}}). \tag{1.18}$$

For $T \ll \varepsilon_F$, we the corresponding conductivity is given by [5]

$$\sigma = \frac{2}{d}e^2\nu_F v_F^2 \tau_F, \tag{1.19}$$

where ν_F is the density of states at the Fermi energy per spin and τ_F is evaluated at $\varepsilon = \varepsilon_F$.[6]

[5] Note that this result is valid for an isotropic but otherwise arbitrary electron spectrum.

[6] Note that $\tau(\varepsilon)\nu(\varepsilon) = \text{const}$ for point-like impurities.

Note that had we used (1.8) with $\tau^* = \tau$ from the very beginning, we would have obtained the same result for the conductivity. Equations (1.7) and (1.8) lead to same result because both $f_{0\mathbf{k}}$ and $\bar{f}$ depend only on the energy, and thus drop out from the current.

What if scattering is anisotropic while the electron spectrum is still isotropic (this would be the case for free electrons being scattered by impurities of finite size). Because there is no preferred direction in the scattering process, the scattering probability can only depend on the angle between $\mathbf{k}$ and $\mathbf{k}'$: $w_{\mathbf{k},\mathbf{k}'} = w(\theta_{\mathbf{k}\mathbf{k}'})$. In linear response to the electric field, the non-equilibrium part of $f_{\mathbf{k}}$ must be linearly proportional to $\mathbf{E}$. But $\mathbf{E}$ is a vector, while $f_{\mathbf{k}}$ is a scalar, so $\mathbf{E}$ must be dotted into some other vector. Since the system is isotropic, the only such vector is $\mathbf{k}$ or $\mathbf{v}_{\mathbf{k}}$, as they are parallel to each other. Then we can write

$$f_{\mathbf{k}} = f_1(\varepsilon_{\mathbf{k}}) - e(\mathbf{v}_{\mathbf{k}} \cdot \mathbf{E})g(\varepsilon_{\mathbf{k}}), \tag{1.20}$$

where $f_1(\varepsilon_{\mathbf{k}})$ is an arbitrary function of energy only (which one – does not matter, as it cancels on substituting (1.20) into (1.2)). Substituting (1.20) into the linearized BE,

$$-e(\mathbf{v}_{\mathbf{k}} \cdot \mathbf{E})f'_{0\mathbf{k}} = -\int_{\mathbf{k}'} w(\theta_{\mathbf{k}\mathbf{k}'})(f_{\mathbf{k}} - f_{\mathbf{k}'})\delta(\varepsilon_{\mathbf{k}} - \varepsilon_{\mathbf{k}'}), \tag{1.21}$$

and solving for g, we obtain the conductivity

$$\sigma = \frac{2}{d}e^2\nu_F v_F^2 \tau_{\mathrm{tr},F}, \tag{1.22}$$

where $\tau_{\mathrm{tr}}(\varepsilon)$ is the *transport scattering time*, defined by

$$\frac{1}{\tau_{\mathrm{tr}}(\varepsilon)} = \nu(\varepsilon)\int \frac{d\Omega}{\Omega_d} w(\theta)(1 - \cos\theta). \tag{1.23}$$

where $d\Omega$ is the element of the solid angle and $\Omega_d = 2\pi$ in 2D and 4π in 3D. The factor $1 - \cos\theta = q^2/2k_F^2$, where $q = |\mathbf{k} - \mathbf{k}'|$, is known as a "transport factor". Its role is to discriminate against small-angle scattering events which are inefficient in relaxing the current. For comparison, the single-particle lifetime, which determines the width of the spectral function, is given by a similar integral but without the transport factor:

$$\frac{1}{\tau_{\mathrm{sp}}(\varepsilon)} = \nu(\varepsilon)\int \frac{d\Omega}{\Omega_d} w(\theta). \tag{1.24}$$

If $w(\theta)$ is strongly peaked at small θ, one can expand $1 - \cos\theta \approx \theta^2/2$, in which case $1/\tau_{\mathrm{tr}} \ll 1/\tau_{\mathrm{sp}}$. In the opposite case of isotropic scattering, $w(\theta) = \mathrm{const}$, $\cos\theta$ drops out and $\tau_{\mathrm{tr}} = \tau_{\mathrm{sp}} = \tau$, where τ is the same as in (1.7).

Long-range disorder (with correlation length $\xi \gg 1/k_F$) brings about several effects which are not captured by the conventional Boltzmann equation in Eq. (1.1), in particular, magnetoresistance due to classical memory effects [6] and resistive anomalies near second-order phase transitions [7] (cf. Sec.). Also, if ξ is much longer than electron-electron mean free path, the system enters into a hydrodynamic regime, when the electron flow can be described by the Navier-Stokes equation [8]. Therefore, it is important what kind of disorder (long- or short-range) is present in a given system. Experimentally, one typically extracts $\tau_{\rm tr}$ from mobility and $\tau_{\rm sp}$ from the amplitude of de Haas-van Alphen or Shubnikov-de Haas oscillations. The ratio of the two allows one to estimate the product $k_F\xi$.

Despite its simple appearance, (1.23) reflects the gauge symmetry. Indeed, if disorder is infinitely long-ranged, it does not scatter at all, which implies that $w(\theta) \propto \delta(\theta)$. The factor $1-\cos\theta$ guarantees that in this case $\sigma \propto \tau_{\rm tr} = \infty$, as infinitely long-range disorder is just a constant shift of the chemical potential, which should have no effect on transport.

As a rule, if $\tau_{\rm tr} \neq \tau_{\rm sp}$, it is the former that enters all transport quantities. The reason can be understood from classical mechanics. Indeed, our BE should be applicable to a completely classical case, when both statistics and dynamics of particles are governed by classical laws. In this case, $1/\tau_{\rm sp}$ is proportional to the total scattering cross-section, $A_{\rm tot} = \int d\Omega dA(\Omega)/d\Omega$, while $1/\tau_{\rm sp}$ is proportional to the transport cross-section, $A_{\rm tr} = \int d\Omega(1-\cos\theta)dA(\Omega)/d\Omega$, where $dA(\Omega)/d\Omega$ is the differential cross-section. But if the interaction potential extends to all distances from the center, the total cross-section is infinite, no matter how rapidly the potential decreases with r,[7] while $A_{\rm tr}$ is finite for potentials decreasing faster than $1/r$. Therefore, transport quantities, which can be observed both in classical and quantum systems, can contain only a finite cross-section, i.e., $A_{\rm tr}$. In contrast, quantum effects–such as the spectral function and quantum magnetooscillations–may contain $A_{\rm tot}$, which is finite in quantum mechanics for sufficiently rapidly decaying potentials.

What if we have a lattice system, but impurities are point-like, i.e, $w_{\mathbf{k}',\mathbf{k}} = w = \text{const}$? In this case, (1.2) gives

$$I_{ei}[f_{\mathbf{k}}] = -w\int_{\mathbf{k}'}\delta(\varepsilon_{\mathbf{k}}-\varepsilon_{\mathbf{k}'})(f_{\mathbf{k}}-f_{\mathbf{k}'}) = -\frac{w}{(2\pi)^d}\int d\varepsilon_{\mathbf{k}'}\oint\frac{da_{\mathbf{k}'}}{v_{\mathbf{k}'}}\delta(\varepsilon_{\mathbf{k}}-\varepsilon_{\mathbf{k}'})(f_{\mathbf{k}}-f_{\mathbf{k}'})$$
$$= -\frac{w}{(2\pi)^d}\oint\frac{da_{\mathbf{k}'}}{v_{\mathbf{k}'}}(f_{\mathbf{k}}-f_{\mathbf{k}'})\Big|_{\varepsilon_{\mathbf{k}'}=\varepsilon_{\mathbf{k}}} = -\frac{f_{\mathbf{k}}-\bar{f}}{\tau}, \tag{1.25}$$

[7] Indeed, $dA = 2\pi b db$, where b is the impact parameter [9]. If the potential is not artificially cut off at some distance, the total cross-section $A_{\rm tot} = 2\pi\int_0^\infty b db = \infty$.

where

$$\frac{1}{\tau} \equiv \frac{w}{(2\pi)^d} \oint \frac{da_{\mathbf{p}}}{v_{\mathbf{p}}} \tag{1.26}$$

$$\bar{f} \equiv \frac{\int \frac{da_{\mathbf{k}'}}{v_{\mathbf{k}'}} f_{\mathbf{k}'}\Big|_{\varepsilon_{\mathbf{k}'}=\varepsilon_{\mathbf{k}}}}{\oint \frac{da_{\mathbf{p}}}{v_{\mathbf{p}}}\Big|_{\varepsilon_{\mathbf{p}}=\varepsilon_{\mathbf{k}}}} \tag{1.27}$$

where $da_{\mathbf{p}}$ is the surface (line) element. As we see, we are back to (1.7).

Finally, what if we are on a lattice and scattering is anisotropic? Then we are out of luck. We can only say that (up to an arbitrary function of energy) $f_{\mathbf{k}} = \mathbf{u}_{\mathbf{k}} \cdot \mathbf{E}$, where $\mathbf{u}_{\mathbf{k}}$ is an odd function of $\mathbf{k}$, but it is not equal to either $\mathbf{k}$ or $\mathbf{v}_{\mathbf{k}}$, as there are many directions on the lattice where vector $\mathbf{v}_{\mathbf{k}}$ can point. In this case, there is no way of avoiding solving an integral equation numerically [10].

In the literature, the situation described above–lattice+anisotropic scattering–is often fixed by employing a version of RTA with

$$I_{RTA} = -\frac{f_0 - f_{\mathbf{k}}}{\tau_{\mathbf{k}}}, \tag{1.28}$$

where $\tau_{\mathbf{k}}$ depends on $\mathbf{k}$, i.e, on the point on the Fermi surface. In contrast to an isotropic case, this approximation is never consistent with the original BE: there is no magic trick that reduces an integral equation to an algebraic one. Using RTA in this case leads to results which differ significantly from the correct ones, especially for more complicated properties than just a *dc* conductivity, e.g., thermoelectric power and Nersnt effect [11], see Fig. 1.

2. *Kubo formula*

The same results can be obtained from the Kubo formula. Suppose that the disorder potential is Gaussian-distributed with $\langle U \rangle = 0$ and $\langle U(\mathbf{r})U(0)\rangle = W(r)$. Let's pick one realization of disorder, $U(\mathbf{r})$. The corresponding exact Green's function (in Matsubara representation) is $G_{\omega_n}(\mathbf{r}, \mathbf{r}')$ with $\omega_n = \pi(2n+1)T$. Now we apply a weak uniform, time-dependent electric field $\mathbf{E}_{\Omega_m} = -\Omega_m \mathbf{A}_{\Omega_m}$, where $\mathbf{A}$ is the vector-potential and $\Omega_m = 2\pi m T$. Assuming for simplicity a parabolic electron spectrum with effective mass m^*, the charge current to linear order in $\mathbf{E}$ is given by [12]:

$$\mathbf{j}_{\Omega_m}(\mathbf{r}) = \frac{e^2}{m^{*2}} T \sum_{\omega_n} (\boldsymbol{\nabla}_{\mathbf{r}} - \boldsymbol{\nabla}_{\mathbf{r}'}) \int d^d r_1 G_{\omega_n+\Omega_m}(\mathbf{r}, \mathbf{r}_1) (\mathbf{A}_{\Omega_m} \cdot \boldsymbol{\nabla}_{\mathbf{r}_1}) G_{\omega_n}(\mathbf{r}_1, \mathbf{r}')\Big|_{\mathbf{r}'=\mathbf{r}} - \frac{\mathcal{N}e^2}{m^*} \mathbf{A}_{\Omega_m}, \tag{1.29}$$

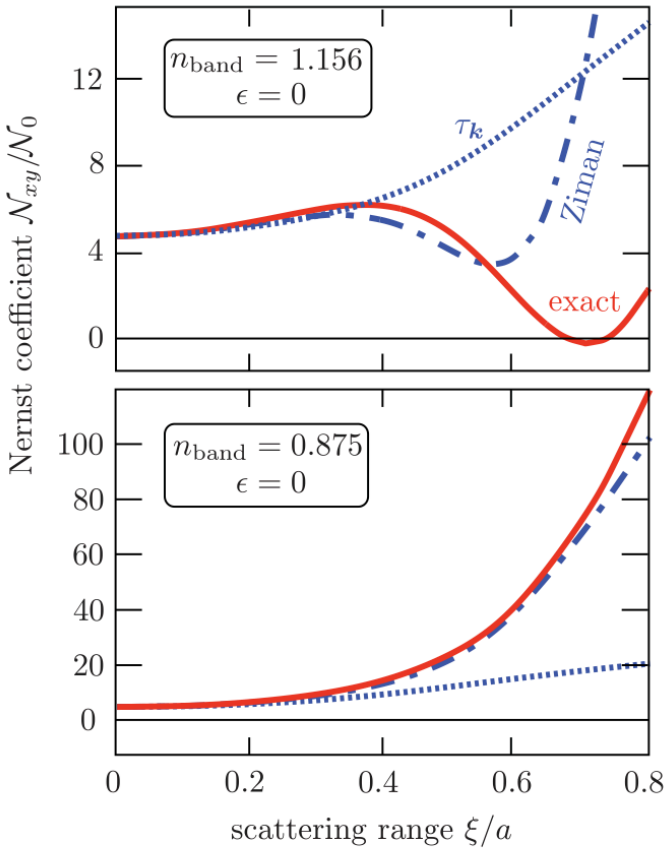

FIG. 3. (Color online) Dependence of the Nernst coefficient on the range ξ of the scattering potential for an undistorted square lattice ($\epsilon = 0$). Two values of the band filling are shown in the upper and lower panel. The three curves in each panel correspond to the exact solution of the linearized Boltzmann equation (solid), the relaxation-time approximation (dotted), and Ziman's improvement on the relaxation-time approximation (dash-dotted).

FIG. 1. Transverse Nernst coefficient, N_{xy}, calculated within the relaxation time approximation and via numerical solution of the Boltzmann equation for a tight-binding model on a square lattice with first, second, and third neighbors hopping. The Nernst coefficient is measured as an electric field E_x, induced by the temperature gradient along y, $-\partial T/\partial y$, in the presence of magnetic field along z: $N_{xy} = E_x/B(-\partial T/\partial y)$. Reproduced from Ref. [11].

where $\mathcal{N}$ is the electron number density. For *dc* case, we need only the first ("gradient") part of the current. Carrying out analytic continuation $i\Omega_m \to \Omega + i0^+$, taking the limit $\Omega \to 0$, and averaging over disorder, we obtain the averaged conductivity

$$\begin{aligned}\sigma_{\alpha\beta} &= \frac{2e^2}{m^*}\int \frac{d\omega}{\pi}\left(-f_0'(\omega)\right)\int d^dr'\partial_{r_\alpha}\partial_{r'_\beta}\langle \mathrm{Im}G^R_\omega(\mathbf{r},\mathbf{r}')\mathrm{Im}G^R_\omega(\mathbf{r}',\mathbf{r})\rangle \\ &= \left(-\frac{1}{4}\right)\frac{2e^2}{m^*}\int \frac{d\omega}{\pi}\left(-f_0'(\omega)\right)\int d^dr'\partial_{r_\alpha}\partial_{r'_\beta} \\ &\quad\times\left[\langle G^R_\omega(\mathbf{r},\mathbf{r}')G^R_\omega(\mathbf{r}',\mathbf{r})\rangle + \langle G^A_\omega(\mathbf{r},\mathbf{r}')G^A_\omega(\mathbf{r}',\mathbf{r})\rangle - \langle G^R_\omega(\mathbf{r},\mathbf{r}')G^A_\omega(\mathbf{r}',\mathbf{r})\rangle - \langle G^A_\omega(\mathbf{r},\mathbf{r}')G^R_\omega(\mathbf{r}',\mathbf{r})\rangle\right]\end{aligned} \tag{1.30}$$

where $G^R_\omega(\mathbf{r},\mathbf{r}')$ is the retarded Green's function, $\langle\ldots\rangle$ stands for averaging over disorder, and where we used a relation $\mathrm{Im}G^R = (G^R - G^A)/2i$ at the last step. Equation (1.30) is exact with respect to disorder. Diagrammatically, $\sigma_{\alpha\beta}$ is expressed by the sum of closed bubbles in Fig. (2).

Now we develop a perturbation theory in disorder. The Greens function is obtained by summing the series, depicted in Fig. (3)

$$\begin{aligned}G^R_\omega(\mathbf{r},\mathbf{r}') = G^R_{0\omega}(\mathbf{r}-\mathbf{r}') &+ \int d^dr_1 G^R_{0\omega}(\mathbf{r}-\mathbf{r}_1)U(\mathbf{r}_1)G^R_{0\omega}(\mathbf{r}_1-\mathbf{r}') \\ &+ \int d^dr_1\int d^dr_2 G^R_{0\omega}(\mathbf{r},\mathbf{r}_1)U(\mathbf{r}_1)G^R_{0\omega}(\mathbf{r}_1-\mathbf{r}_2)U(\mathbf{r}_2)G^R_{0\omega}(\mathbf{r}_2-\mathbf{r}')+\ldots\end{aligned} \tag{1.31}$$

where $G^R_{0\omega}(\mathbf{r})$ is the free Green's function. On substituting series (1.31) into (1.30), we obtain averages of two types. In the first type, shown in Fig. 4a, points $\mathbf{r}_1, \mathbf{r}_2 \ldots$ belong to the same side of the bubble; in the second type, they belong to opposite sides. A dashed line connecting two points $\mathbf{r}_i$ and $\mathbf{r}_j$ represent the disorder correlator, $W(|\mathbf{r}_i - \mathbf{r}_j|)$.

Summing up only the averages of the first type, we obtain a bubble, formed by two *averaged* Green's functions, $\langle G^R_\omega(\mathbf{r},\mathbf{r}')\rangle$. Since averaging restores translational invariance, $\langle G^R_\omega(\mathbf{r},\mathbf{r}')\rangle$ depends only on $\mathbf{r}-\mathbf{r}'$, and we can introduce the momentum:

$$\langle G^R_\omega(\mathbf{k})\rangle = \int d^dr e^{i\mathbf{k}\cdot\mathbf{r}}G^R_\omega(\mathbf{r}) = \frac{1}{\omega - \varepsilon_{\mathbf{k}} - \Sigma^R_\omega(\mathbf{k})}, \tag{1.32}$$

where $\Sigma^R_\omega(\mathbf{k})$ is the self-energy, obtained by re-summing the series shown in Fig. 5.

The corresponding contribution to the conductivity is given by

$$\sigma^{(1)}_{\alpha\beta} = \frac{2e^2}{m^{*2}}\int\frac{d\omega}{\pi}(-f_0'(\omega))\int\frac{d^dk}{(2\pi)^d}k_\alpha k_\beta\left[\mathrm{Im}\langle G^R_\omega(\mathbf{k})\rangle\right]^2. \tag{1.33}$$

Although we initially assumed parabolic spectrum, it is obvious that for a general spectrum the last expression is replaced by

$$\sigma^{(1)}_{\alpha\beta} = 2e^2\int\frac{d\omega}{\pi}(-f_0'(\omega))\int\frac{d^dk}{(2\pi)^d}v_{\mathbf{k},\alpha}v_{\mathbf{k},\beta}\left[\mathrm{Im}G^R_\omega(\mathbf{k})\right]^2. \tag{1.34}$$

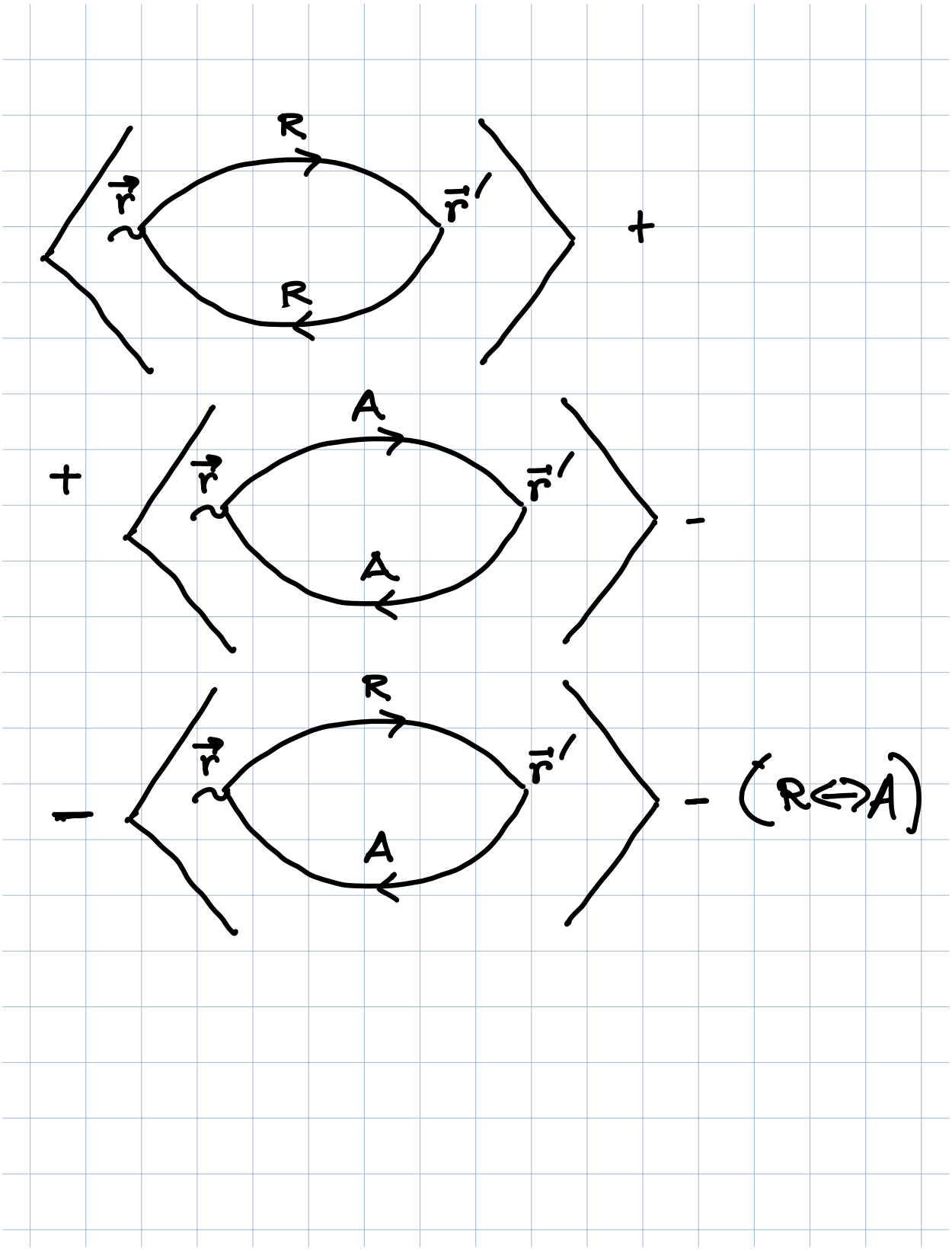

FIG. 2. Closed-bubble diagrams contributing to $\sigma_{\alpha\beta}$.

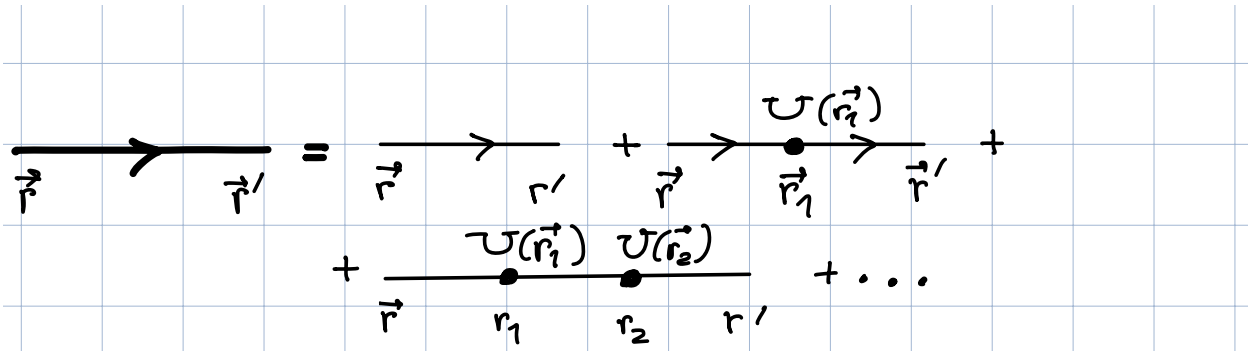

FIG. 3. Diagrammatic representation of series (1.31).

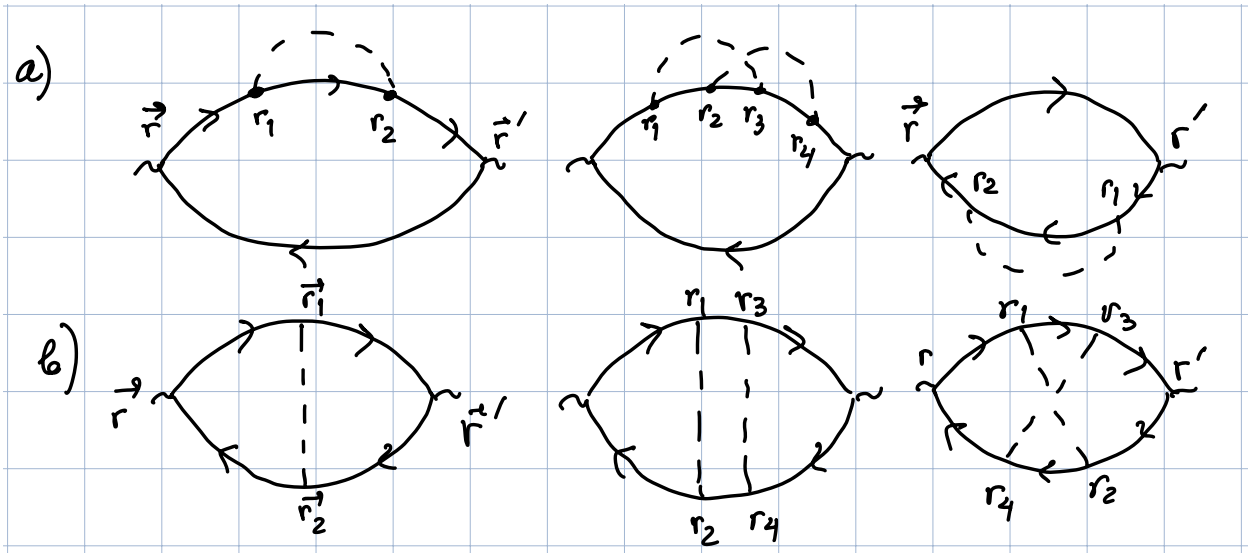

FIG. 4. Two types of disorder averages.

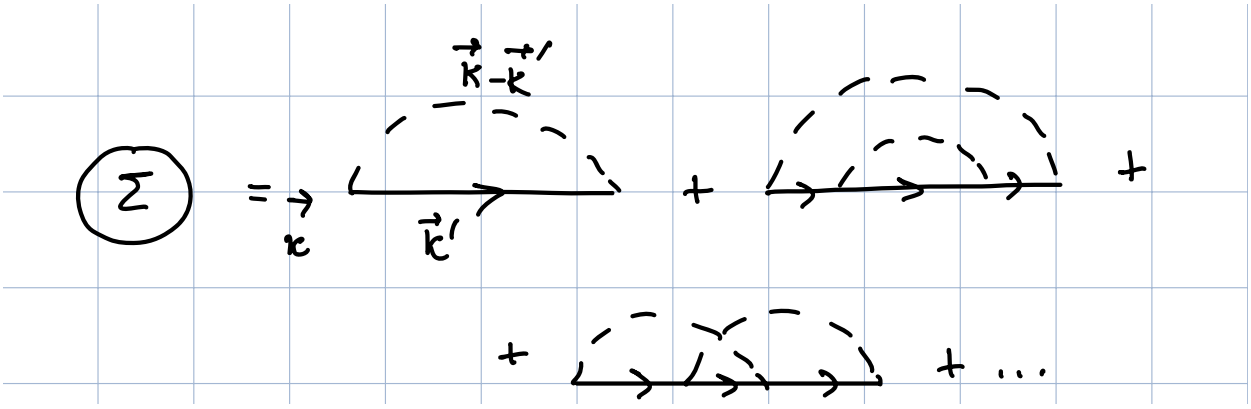

FIG. 5. Electron self-energy for scattering by disorder.

The second type of averaging produces *vertex corrections*.[8] In each of the four terms, we push the vertex corrections to to one side of the bubble (does not matter which one) and call their sum the renormalized current vertex, $\mathbf{V}^{a,b}_{\omega}$, where $a, b = A, R$. After Fourier transform, the corresponding contribution to the conductivity reads

$$\sigma^{(2)}_{\alpha\beta} = 2e^2\left(-\frac{1}{4}\right)\int\frac{d\omega}{\pi}(-f_0'(\omega))\int\frac{d^dk}{(2\pi)^d}v_{\mathbf{k},\alpha} \times\left\{\left[\langle G^R_\omega(\mathbf{k})\rangle\right]^2 V^{R,R}_{\omega,\beta}(\mathbf{k}) + \left[\langle G^A_\omega(\mathbf{k})\rangle\right]^2 V^{A,A}_{\omega,\beta}(\mathbf{k}) -2\langle G^R_\omega(\mathbf{k})\rangle\langle G^A_\omega(\mathbf{k})\rangle V^{R,A}_{\omega,\beta}(\mathbf{k})\right\}. \tag{1.35}$$

Let's now focus on case of isotropic (but not necessarily parabolic) electron spectrum. In what follows, we will be interested in rather weak disorder, such that $\varepsilon_F\tau_{\rm sp} \gg 1$. Then we are interested only in a narrow interval of energies of with $1/\tau_{\rm sp}$ near ε_F, and the integral over the momentum can be simplified as

$$\int\frac{d^dk}{(2\pi)^2}\underbrace{=}_{\text{exact}}\int_0^\infty d\varepsilon_{\mathbf{k}}\nu(\varepsilon_{\mathbf{k}})\int\frac{d\Omega_{\mathbf{k}}}{\Omega_d}\underbrace{=}_{\text{exact}}\int_{-\varepsilon_F}^\infty d\epsilon_{\mathbf{k}}\nu(\epsilon_{\mathbf{k}}+\varepsilon_F)\int\frac{d\Omega_{\mathbf{k}}}{\Omega_d} \underbrace{\approx}_{\text{approximate}}\nu_F\int_{-\infty}^\infty d\epsilon_{\mathbf{k}}\int\frac{d\Omega_{\mathbf{k}}}{\Omega_d}, \tag{1.36}$$

where $\epsilon_{\mathbf{k}} = \varepsilon_{\mathbf{k}} - \epsilon_F$. A major simplification arises from noting that the terms of the type G^RG^R (or G^AG^A) and G^RG^A behave very differently on integrating over $\epsilon_{\mathbf{k}}$. Indeed, the self-energy in (1.32) can be taken on the Fermi surface. Its real part can be absorbed into the chemical potential, while the imaginary part is a constant as well, which–by definition–is equal to (-1/2) of the inverse single-particle lifetime. Then

$$G^{R,A}_\omega(\mathbf{k}) = \frac{1}{\omega - \epsilon_{\mathbf{k}} \pm \frac{i}{2\tau_{\rm sp}}}. \tag{1.37}$$

Now we see that the integrals of the type $\int d\epsilon_{\mathbf{k}}[G^R_\omega(\mathbf{k})]^2G^R$ and $\int d\epsilon_{\mathbf{k}}[G^A_\omega(\mathbf{k})]^2$ vanish, because the poles of the integrands lie in the same half-plane of $\epsilon_{\mathbf{k}}$. Furthermore, for $T \ll \varepsilon_F$, we replace $-f_0' = \delta(\omega)$. Also, an isotropic system has only one component of the conductivity tensor, equal to $\sigma = (1/d)\sum_\alpha\sigma_{\alpha\alpha}$. After these simplifications, Eqs. (1.33) and (1.35) are reduced to

$$\sigma^{(1)} = \frac{e^2}{\pi d}\int\frac{d^dk}{(2\pi)^d}v^2_{\mathbf{k}}\left|G^R_0(\mathbf{k})\right|^2. \tag{1.38a}$$

$$\sigma^{(2)} = \frac{e^2}{\pi d}\int\frac{d^dk}{(2\pi)^d}\left|G^R_0(\mathbf{k})\right|^2\mathbf{v}_{\mathbf{k}}\cdot\mathbf{V}^{RA}_0(\mathbf{k}). \tag{1.38b}$$

[8] Let not the word "correction" confuse you. These "corrections" may be not small.

For weak disorder, we can approximate the self-energy by the first diagram in Fig. 5. Let's look at this diagram in more detail, setting $\omega = 0$, as this is what we need in (1.38a) and (1.38b):

$$\Sigma_0^R(\mathbf{k}) = \int \frac{d^d k'}{(2\pi)^2} G_0^R(\mathbf{k}') W(|\mathbf{k} - \mathbf{k}'|), \tag{1.39}$$

where

$$G_\omega^R(\mathbf{k}) = \frac{1}{\omega - \varepsilon_\mathbf{k} + \varepsilon_F + i0^+} = \frac{1}{\omega - \epsilon_\mathbf{k} + i0^+} \tag{1.40}$$

and $W(q)$ is the Fourier transform of $W(r)$. As we are interested only in the imaginary part,

$$\mathrm{Im}\Sigma_0^R(\mathbf{k}) = -\pi \int \frac{d^d k'}{(2\pi)^2} \delta(\epsilon_{\mathbf{k}'}) W(|\mathbf{k} - \mathbf{k}'|), \tag{1.41}$$

The delta function projects k' onto the Fermi surface. Since we expect only $k \approx k_F$ to be relevant as well, we replace $|\mathbf{k} - \mathbf{k}'| = 2k_F \sin(\theta/2)$. Adopting approximation (1.36), we obtain

$$\mathrm{Im}\Sigma_0^R = -\pi \nu_F W_0 \equiv -\frac{1}{2\tau_{\mathrm{sp}}} \to \tau_{\mathrm{sp}} = 1/2\pi\nu_F W_0, \tag{1.42}$$

where

$$W_0 = \int \frac{d\Omega}{\Omega_d} W\left(2k_F \sin\frac{\theta}{2}\right). \tag{1.43}$$

The next simplification comes from noting that diagrams for $\sigma^{(2)}$ with crossed dashed lines are smaller than the ladder diagrams, under the condition that momenta of all fermions are near k_F. Indeed, consider diagrams a)-c) in Fig. 6. Diagram a) is of the ladder type. Each of the three momenta–$\mathbf{k}$, $\mathbf{k}'$, $\mathbf{k}''$–can be chosen to be near k_F independently of each other. Diagrams b) and c) contain four momenta $\mathbf{k}$, $\mathbf{k}'$, $\mathbf{k}''$, and $\mathbf{k} - \mathbf{k}' + \mathbf{k}''$. If we choose the first three momenta to be equal to k_F, the fourth momentum will be equal to k_F only certain relations between the first three are satisfied: For example, $\mathbf{k}' \approx \mathbf{k}$ or $\mathbf{k}' \approx \mathbf{k}''$, etc. This means that integration phase space is reduced compared to diagram a). The only small parameter in the game is $1/\varepsilon_F\tau_{\mathrm{sp}} \ll 1$, and thus diagrams b) and c) are smaller than a) by this parameter.

Although diagram c) is small compared to a), it turns out that for $1 < d \leq 2$ the next-order diagram of the same type–diagram d)– is equal to diagram b); and the same is true for all other maximally crossed diagrams. This means that the series of maximally crossed diagrams diverges. This is known as weak localization, which is a perturbative manifestation of Anderson localization. We will come back to this point later, but for now let's focus on the infinite sum of ladder diagram, shown in Fig. 7a.

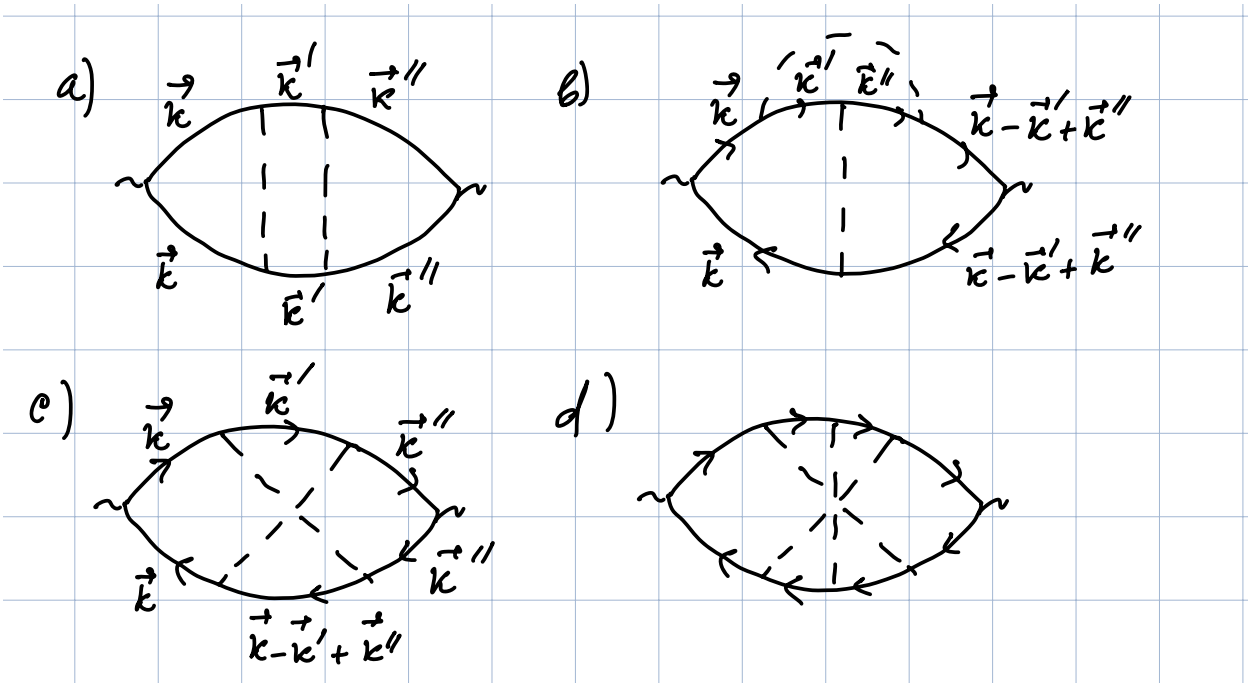

FIG. 6. Non-crossed (a) and crossed (b-d) diagrams for the conductivity.

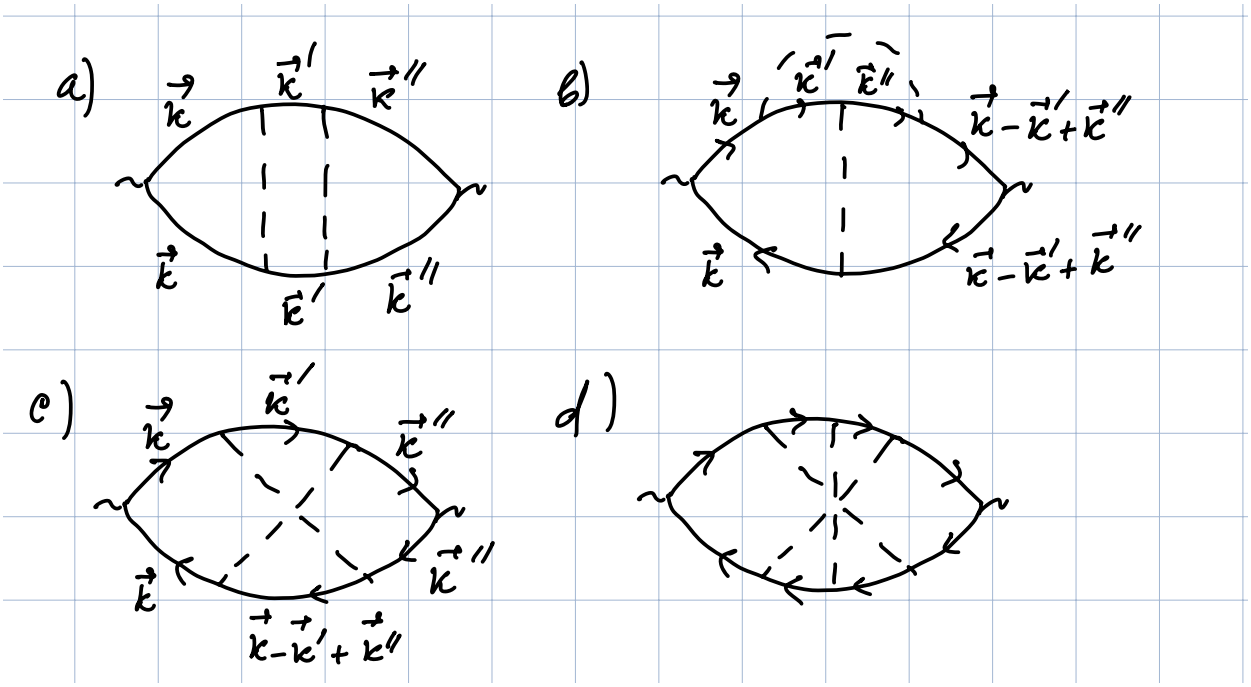

FIG. 7. a) Ladder diagrams for the conductivity. b) Integral equation for the current vertex (1.45).

In the ladder approximation, we add up Eqs.(1.38a) and (1.38b), to obtain the total conductivity as

$$\sigma = \sigma^{(1)} + \sigma^{(2)} = \frac{e^2}{\pi d} \int \frac{d^d k}{(2\pi)^d} \left|G_0^R(\mathbf{k})\right|^2 \mathbf{v}_\mathbf{k} \cdot \boldsymbol{\mathcal{V}}(\mathbf{k}), \tag{1.44}$$

where the renormalized current vertex satisfies an integral equation, shown graphically in Fig. 7b:

$$\boldsymbol{\mathcal{V}}(\mathbf{k}) = \mathbf{v}_\mathbf{k} + \int \frac{d^d k'}{(2\pi)^d} \left|G_0^R(\mathbf{k}')\right|^2 W(|\mathbf{k} - \mathbf{k}'|) \boldsymbol{\mathcal{V}}(\mathbf{k}'). \tag{1.45}$$

In an isotropic system, $\boldsymbol{\mathcal{V}}(\mathbf{k})$ can be directed only along $\mathbf{k}$ or, which is the same, along $\mathbf{v}_\mathbf{k}$. Without loss of generality, we can choose

$$\boldsymbol{\mathcal{V}}(\mathbf{k}) = \mathbf{v}_\mathbf{k} \Gamma(\varepsilon_\mathbf{k}), \tag{1.46}$$

where $\mathcal{V}(\varepsilon_\mathbf{k})$ is a function of energy only. Dotting (1.45) into $\mathbf{v}_\mathbf{k}$, we obtain an equation of Γ:

$$\Gamma(\varepsilon_\mathbf{k}) = 1 + \int \frac{d^d k'}{(2\pi)^d} G_0^R(\mathbf{k}') G_0^A(\mathbf{k}') W(|\mathbf{k} - \mathbf{k}'|) \frac{\mathbf{v}_\mathbf{k} \cdot \mathbf{v}_{\mathbf{k}'}}{v_\mathbf{k}^2} \Gamma(\varepsilon_{\mathbf{k}'}). \tag{1.47}$$

There is no reason to expect $\Gamma(\varepsilon_\mathbf{k})$ to vary rapidly near the Fermi energy. If so, we can put $\varepsilon_\mathbf{k} = \varepsilon_F$ in $\Gamma(\varepsilon_\mathbf{k})$, upon which it becomes a constant, $\Gamma \equiv \Gamma(\varepsilon_F)$. In the integral part, we project the momenta onto the Fermi surface as per (1.36). The solution of the ensuing *algebraic* equation is

$$\Gamma = \frac{1}{1 - RW_1}, \tag{1.48}$$

where, using (1.36),

$$R = \nu_F \int_{-\infty}^{\infty} d\epsilon_{\mathbf{k}'} |G_0^R(\mathbf{k}')|^2 = \nu_F \int_{-\infty}^{\infty} d\epsilon_{\mathbf{k}'} \frac{1}{\epsilon_{\mathbf{k}'}^2 + (1/2\tau_{\rm sp})^2} = 2\pi \nu_F \tau_{\rm sp} = \frac{1}{W_0} \tag{1.49}$$

and

$$W_1 = \int \frac{d\Omega}{\Omega_d} \cos\theta W\left(2k_F \sin\frac{\theta}{2}\right). \tag{1.50}$$

Therefore,

$$\Gamma = \frac{W_0}{W_0 - W_1} \tag{1.51}$$

Substituting the last equation into (1.44) and using (1.49) for the integral of $|G_0^R(\mathbf{k})|^2$, we obtain

$$\sigma = \frac{2e^2}{d} v_F^2 \nu_F \tau_{\rm tr}, \tag{1.52}$$

where

$$\frac{1}{\tau_{\rm tr}} = 2\pi \int \frac{d\Omega}{\Omega_d} (1 - \cos\theta) W\left(2k_F \sin\frac{\theta}{2}\right). \tag{1.53}$$

This result coincides with (1.22), obtained from the Boltzmann equation.

3. *What the Boltzmann equation can and cannot do for you?*

In the previous section we established that the Boltzmann equation gives the same results as the ladder approximation for the Kubo formula. Now it would be easier to understand what the Boltzmann equation is missing.

We already touched on one class of phenomena: weak localization, which arises from quantum interference between electron waves scattered by different impurities. This is a well-researched subject, and I refer you to a number of books and reviews for further study [13–15].

Given the Boltzmann equation is semi-classical by construction, it is not surprising that it cannot capture quantum-mechanical effects. What's more surprising though is that it misses some entirely classical effects which go beyond the usual assumption about the Markovian nature of scattering processes, i.e., that the memory of previous scattering events is erased by the time the next one occurs. This becomes especially important when scatterers are finite-size, rather than point-like, objects. This will be our main subject in Sec. I C but, just to wet your appetite, I give two examples here.

The first one is the Lorentz-gas model, in which scatterers are finite-size spheres or disks distributed randomly over space (without overlaps). Suppose that a point particle starts its motion with some velocity $\mathbf{v}(0)$. Pretty soon the direction of the velocity will be completely random (while its magnitude is still equal to $v(0)$). The degree of randomization can be quantified by the velocity-velocity correlation function, $\langle \mathbf{v}(t) \cdot \mathbf{v}(0) \rangle$. [9] The Boltzmann equation predicts that at long times the velocity-velocity correlator decays exponentially with time: $\langle \mathbf{v}(t) \cdot \mathbf{v}(0) \rangle \propto e^{-t/\tau_{\rm tr}}$, where $\tau_{\rm tr}$ is the corresponding transport time for spheres or disks. However, an exact solution shows that, in fact, the behavior at long times is power law, rather than exponential: $\langle \mathbf{v}(t) \cdot \mathbf{v}(0) \rangle \propto t^{-(1+d/2)}$ [16, 17]. This immediately implies that the optical conductivity should behave in a non-analytic way at small Ω: $\mathrm{Re}\sigma(\Omega) \propto |\Omega|^{d/2}$ [6, 7, 18]. This discrepancy occurs because, for finite-size scatterers, the probability for a particle to return to the same scatterer is also finite, as shown by a red arrow in Fig. 8. The conventional BE cannot capture this effect.

The effect of (classical!) self-returns is amplified in the presence of the magnetic field, which curves electron orbits, thus sending electrons to the same scatterers time and again. In 2D, a strong enough magnetic field leads to complete localization of electrons which move around scatterers on rosette-like trajectories [19, 20], see Fig. 9.

[9] For charged particles, the Fourier transform $\int dt e^{i\Omega t} \langle \mathbf{v}(t) \cdot \mathbf{v}(0) \rangle$ is proportional to the conductivity at frequency Ω.

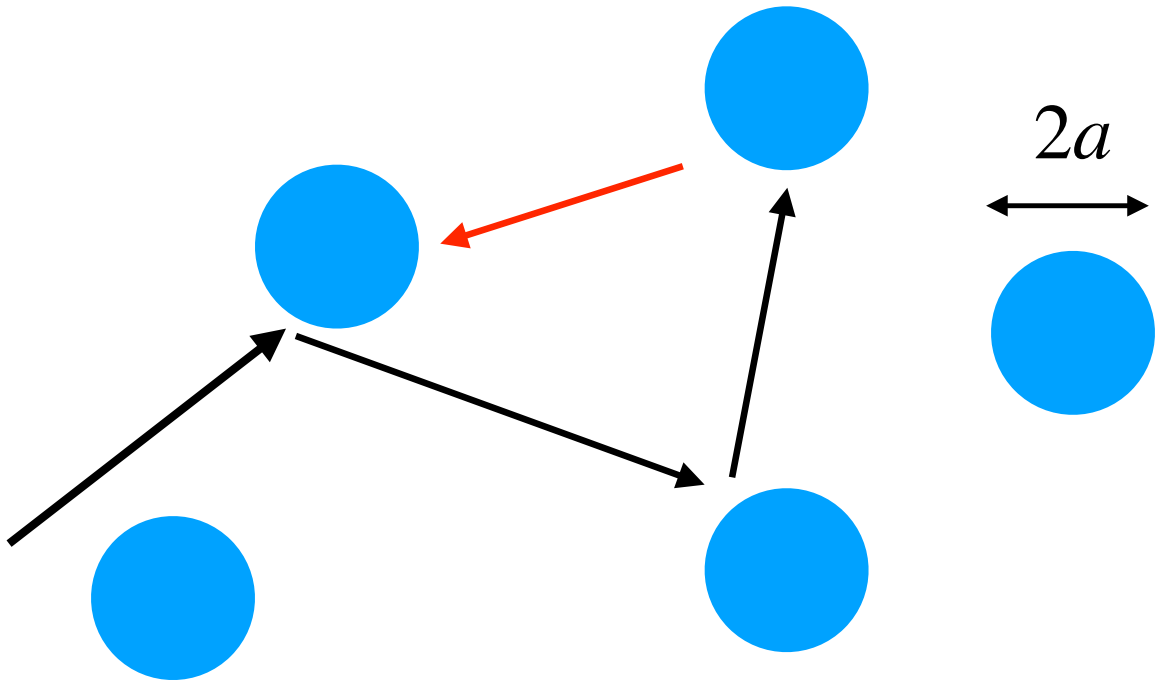

FIG. 8. Lorentz-gas model.

But even in weaker fields, there are pronounced discrepancies betweeen predictions of Boltzmann theory and more sophisticated theories/experiment. You may recall that a simple Drude model [21] predicts that while the conductivity is affected by the magnetic field, the resistivity remains equal to its zero field value. I leave it to you to show that the Boltzmann equation for parabolic electron spectrum but anisotropic scattering probability gives the same result, namely (for simplicity, in 2D with **B** being along the normal to the plane and **E** being in-plane)

$$\sigma_{xx} = \sigma_{yy} = \frac{\sigma}{1 + (\omega_c \tau_{\rm tr})^2}$$
$$\sigma_{xy} = -\sigma_{yx} = \frac{\omega_c \tau_{\rm tr} \sigma}{1 + (\omega_c \tau_{\rm tr})^2}, \tag{1.54}$$

where $\omega_c = eB/m$ and σ is the zero-field conductivity, given by (1.22). Calculating $\hat{\rho} = \hat{\sigma}^{-1}$, you will find that $\rho_{xx} = 1/\sigma$, which means that magnetoresistance is absent. With a little more effort, one can show that the same is true not only for parabolic but any isotropic spectrum. Nevertheless, many real materials with almost isotropic spectrum do show strong magnetoresistance. Theoretically, one obtains this effect by going beyond the conventional Boltzmann equation scheme

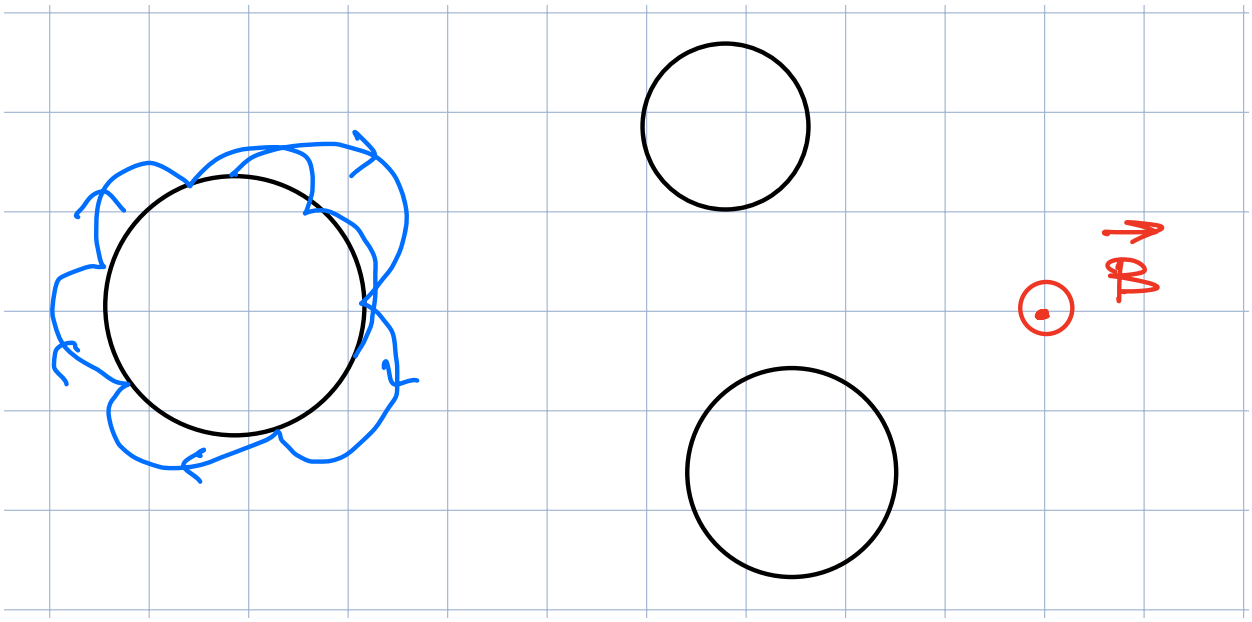

FIG. 9. Classical localization of 2D electrons by a magnetic field.

[4, 6, 22, 23].

B. Electron-phonon interaction

Before turning to the subject of resistive anomalies, let me first make a few straightforward observations about the electron–phonon interaction.

1. *The main rule about phonons: They are always there.*

Rule # 1. Phonons are always there.

Rule # 2. If you think that phonons are not there, see Rule #1.

2. *Phonons are needed to maintain the linear response regime.*

As far as charge transport is concerned, phonons play two roles. First, even if the temperature is so low that electron-phonon scattering is much weaker than electron-impurity one, phonons are ultimately responsible for dissipation. In the previous section, we analyzed electron-impurity scattering in detail. Regardless of the model, we arrived at the conclusion that, at low enough

temperatures and, formally, even at $T = 0$, the conductivity is finite and controlled solely by impurities. Well, Maxwell's law are blind to microscopic mechanisms of conduction. All they say is that, as long as the conductivity is finite, there must be Joule heat, in the amount of $\dot{Q} = \sigma E^2$ Joules released per unit volume per unit time. But wait a second, electron-impurity scattering is elastic, thus no energy is transferred from electrons to the lattice. How come the sample is getting warmer? The answer is that it is still phonons that dissipate energy. Although phonons don't enter the linear response formula $j = \sigma E$ directly, they define the condition on the electric field up to which this formula is valid. If not for phonons, electric field would do work on electrons, which leads to increase of their energy and this heating, when electron and lattice are at different temperatures: T_e and T_{ph}.

The energy balance can be expressed as [24]

$$\frac{\pi^2}{6}\nu_F\left(T_e^2 - T_{ph}^2\right) = \tau_{\rm eph}\sigma E^2, \tag{1.55}$$

where $\tau_{\rm eph}$ is energy relaxation time of electrons due to e-ph interaction. The condition for the absence of heating of electrons is

$$\Delta T = T_e - T_{ph} \ll T_{ph}. \tag{1.56}$$

Re-writing $T_e^2 - T_{ph}^2 \approx 2\Delta T T_{ph}$, (1.56) implies that

$$\Delta T/T_{ph} = \frac{3}{\pi^2}\frac{\tau_{\rm eph}\sigma E^2}{\nu_F T_{ph}^2} \ll 1. \tag{1.57}$$

For acoustic phonons at low T and in 3D, $\tau_{\rm eph} \propto T^{-3}$, and thus (1.57) implies that

$$E \ll A T_{ph}^{2/5}, \tag{1.58}$$

where $A = $ const. That is, at given T the electric field has to be weak enough to satisfy (1.58).

3. *Resistivity controlled by electron-phonon interaction*

The second role of phonons is to control the resistivity directly, via electron-phonon scattering. There are two temperature regimes for electron-phonon scattering: equipartition, for $T \gg T_0$, and inelastic, for $T \ll T_0$. The meaning of T_0 is different for scattering by acoustic and optical phonons. For acoustic phonons, the maximum phonon momentum equals to $2k_F$, thus the frequency of such a phonon equals to $2k_F s$, where s is the speed of sound. The Bloch-Grueneisen

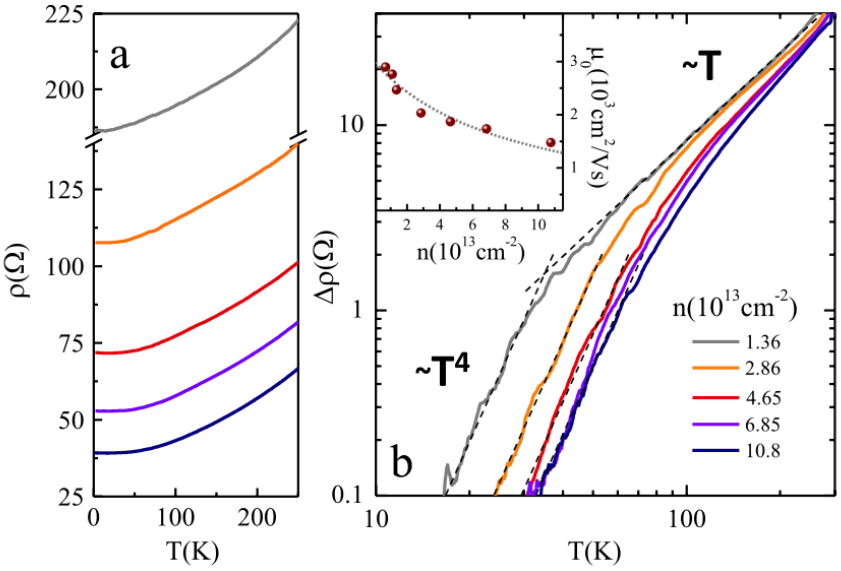

FIG. 2 (color online). (a) Temperature dependence of the resistivity for different charge carrier densities of sample G8A4. (b) The temperature dependent part of the resistivity $\Delta\rho(T)$ scales as T^4 in the low T range and smoothly crosses over into a linear T dependence at higher T. The dashed lines represent fits to the linear T and T^4 dependencies, respectively. The inset shows the mobility μ_0 at $T = 2$ K as a function of the density n. The gray line is the theoretically expected mobility due to short and long range impurity scattering.

FIG. 10. Electron-phonon interaction in monolayer graphene. Reproduced from Ref. [25].

temperature is defined as such frequency (in appropriate units): $T_{BG} = 2k_F s$. [10] For $T \gg T_{BG}$, the phonon mode is in the equipartition regime, when its occupation number scales linearly with T: $1/(e^{\omega/T} - 1) \approx T/\omega$. The corresponding contribution to the resistivity is also linear in T: $\rho \propto T$. For $T \ll T_{BG}$, the number of phonons with $\omega \sim T_{BG}$ is exponentially small, and electrons scatter primarily at thermal phonons with momenta $q_T \sim T/s \ll k_F$. Therefore, scattering is of the forward-scattering type. For deformation-potential scattering by acoustic phonons, the T scaling of the single-particle scattering rate tracks the spatial dimensionality; in 3D, $1/\tau_{\rm sp} \propto T^3$. However, the transport scattering rate acquires as small factor $1 - \cos\theta \approx \theta^2/2 \sim q_T^2/k_F^2 \propto T^2$. As the result, the transport scattering rate scales as $1/\tau_{\rm tr} \propto T^5$.

Note that T_{BG} coincides (in order fo magnitude) with the Debye temperature, $T_D = s/a$, where a is the lattice constant, only in good metals with high number density, where $k_F \sim 1/a$. In low-carrier density systems (semiconductors, semimetals), $k_F \ll 1/a$ and $T_{BG} \ll T_D$. Depending on the number density, at can be as low as few tens of or even few Kelvin. Even in high-density metals, the real crossover between the equipartition and inelastic regimes is lower than the nominal T_{BG} due to numerical factors. A rule of thumb is the linear scaling of the ρ extends down to $T_{BG}/4$.

4. *Equipartition regime is quasi-elastic regime*

One feature of the equipartition regime ($T \gg T_{BG}$) needs to be stressed: although the scattering time depends on temperature, electron-phonon scattering in this regime is almost elastic (quasi-elastic). Consider a typical electron with energy within the interval T around the Fermi energy. Because there are many phonons with $q \sim k_F$, the electron momentum is relaxed quickly. However, the energy of a typical phonon $\sim T_{BG} \ll T$, and thus energy relaxation is slow. The rate of energy relaxation can be estimated in the diffusion model. Because scattering is almost isotropic, $\tau_{\rm sp} \sim \tau_{\rm tr} \propto 1/T$. At each scattering event, the electron energy changes by T_{BG}, which means that the electron energy diffuses with the diffusion coefficient $D_\varepsilon \sim T_{BG}^2/\tau_{\rm sp}$. The energy relaxation time is estimated as [24, 26, 27]

$$\sqrt{D_\varepsilon \tau_\varepsilon} \sim T \to \tau_\varepsilon \sim \tau_{\rm sp}(T/T_{BG})^2 \propto T, \tag{1.59}$$

while the ratio $\tau_\varepsilon/\tau_{\rm sp} \sim (T/T_{BG})^2 \gg 1$, which implies that scattering is elastic.

[10] The factor of 2 is superficial, but I keep it for historical reasons.

To summarize, electron-phonon scattering in the equipartition regime is isotropic and (quasi) elastic. This means that phonons in this regime play a role of point-like impurities, with the scattering cross-section proportional to T. This is easy to understand on physical grounds. An electron moving through the lattice at speed $v_F \ll s$ is "seeing" a snapshot of ions displaced from the equilibrium positions. The rms displacement of an ion $\langle \delta^2 r \rangle \propto T$, which explains the linear scaling of ρ.

Quasieleastic electron-phonon scattering has one more interesting consequence. According to the Wiedemann-Franz law (WFL), the charge and thermal conductivities of a metal are related to each other as $\kappa/\sigma = L_0 T$, where $L_0 = (\pi^2/3)(k_B/e)^2$ is the Lorentz ratio for degenerate electrons. Sometimes you can hear that WFL manifests the Fermi-liquid nature of a system. In fact, WFL applies strictly only to elastic scattering [10], win which can it can be derived without any limitations on the type of scattering (isotropic vs anisotropic) and band structure. In the low-T regime, when electron-impurity scattering is the dominant one, WFL is obviously applicable. But now we also see that it should applicable for $T \gg T_{BG}$, as phonons act as impurities in this regime. Now you would not find it surprising to notice Gustav Wiedemann and Rudolph Franz discovered their law experimentally in 1853–well before any cryogenic techniques were available. In fact, they measured κ and σ only at two temperatures: room and ice. But both temperatures are high enough for copper and aluminum to be in the equipartition regime.

Following the same lines, a curious reader might recall that weak localization (and related phenomena) becomes observable at sufficiently low temperatures, such that the impurity mean free time, τ_i, is much shorter than the *phase-breaking time*, τ_φ. The latter comes from inelastic processes (electron-electron and electron-phonon) and becomes longer at T decreases. But, by the same token, $\tau_\varphi \gg \tau_{\rm sp}$ in the equipartition regime, and thus one should expect phase-coherent phenomena to occur in this regime as well [26]. To date, an experimental confirmation of this idea is still lacking.

5. *How do phonons get rid of extra momentum?*

And the last observation about phonons. In order to control the charge transport, phonons need a mechanism to relax the extra momentum they receive from electrons. In the absence of such mechanism, the electron and phonon subsystems will be accelerated by the electric field and steady-state transport would be impossible. This phenomenon is known as "phonon drag".

Phonon-phonon scattering can relax the momentum but only if it involves umklapp, such that the phonon quasimomenta satisfy the condition $\mathbf{q}_1 + \mathbf{q}_2 = \mathbf{q}_1' + \mathbf{q}_2' + n\mathbf{b}$, where $\mathbf{b}$ is the reciprocal lattice vector. In good metals with $k_F \sim a^{-1}$, umklapp scattering is allowed for $T \gtrsim T_{BG} \sim T_D$, but not for $T \lesssim T_{BG}$, when typical phonon momenta $\sim q_T \sim T/s \ll k_F \sim a^{-1}$. In a disorder-free metal, that would imply that the resistivity becomes exponentially small, in proportion to $\exp(-T_{BG}/T)$. However, such a reduction of the resistivity is observed only in ultra-pure samples. In a typical sample, there is enough disorder to take away the extra momentum from phonons. All one needs is to guarantee that the rate at which the momentum flows from electrons to phonons is slower that the rate at which the momentum flows from phonons to disorder. This condition is satisfied even if phonons are scattered by small defects, of dimensions smaller than the phonon wavelength, $\lambda_T \sim 1/q_T \sim s/T$. In this case, the phonon-impurity scattering rate obeys Rayleigh's law: $1/\tau_{\text{phi}} \propto T^4$, while the electron-phonon scattering rate scales as T^5, i. e., slower. In addition, the exponent in the Rayleigh's law depends on the dimensionality of the scattering object, $\mathcal{D}$, and decreases as one moves from point defects ($\mathcal{D} = 0$) to line defects ($\mathcal{D} = 1$), when $1/\tau_{\text{phi}} \propto T^3$. In short, enough junk in a sample make the problem of phonon relaxation go away. Again, as it was the case with "hidden phonons" in the linear-response formula, the junk that scatters phonons does now show up in the results explicitly, but you have to have enough of it in order to forget about it.

C. Classical memory effect: Resistive anomaly near a classical second-order phase transition

1. *History and model*

Finally, we cam to the subject of resistive anomalies near classical second-order phase transitions, of which I will focus on the ferromagnetic ones. For the first time, such a anomaly was observed in Ni by Walther Gerlach (same Gerlach as in the Gerlach-Stern experiment), back in 1932–see Fig. 11. More examples are shown in Fig. 12.

Theoretically, the resistive anomaly was first addressed by de Gennes and Friedel (dGF) in 1958 [30], who formulated a model which I am also going to use. Namely, T_c is assumed to be higher than T_{BG}, such that electron-phonon interaction is in the equipartition regime, when–as we now know–phonons play a role of point-like elastic scatterers with T-dependent cross-section. Because we will be interested only in the narrow vicinity of T_c, all non-critical quantities can be evaluated right at T_c, in which case the T-dependence of the phonon contribution to the resistivity

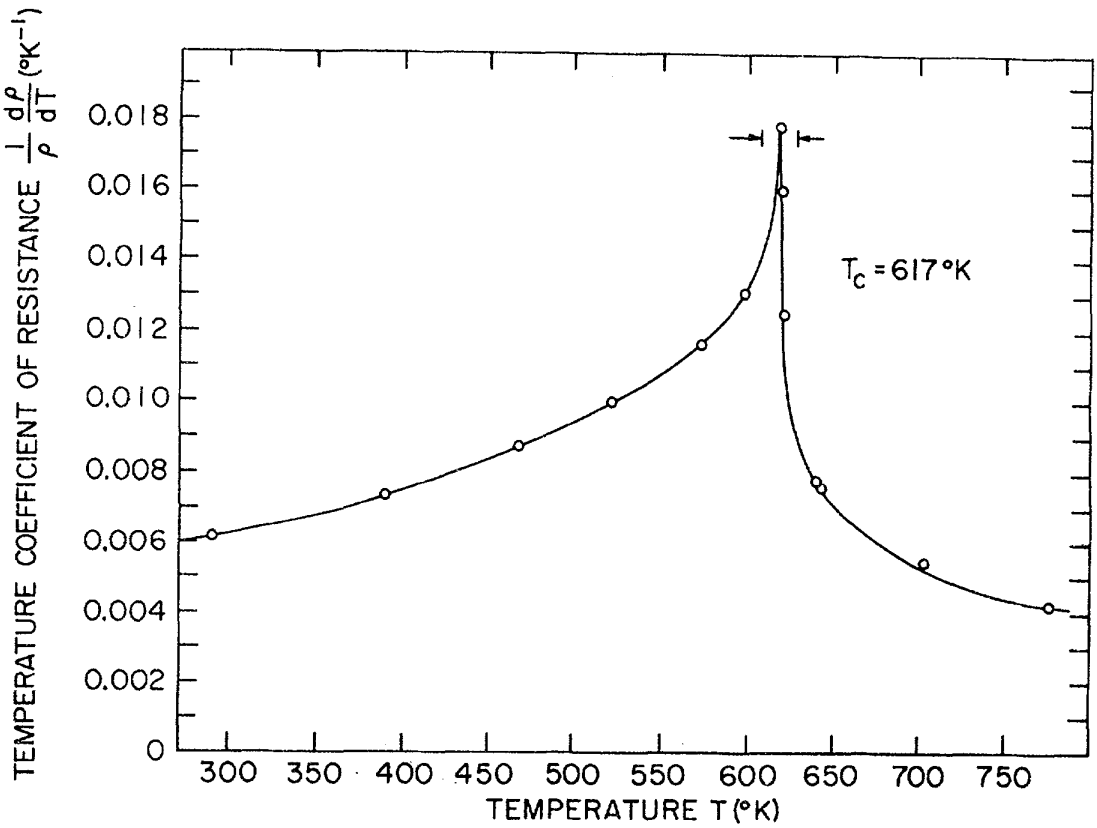

FIG. 11. $d\rho/dT$ in Ni. Reproduced from Ref. [28].

does not play any role. In addition to phonons, there are also real impurities, which are also assumed to be point-like. These two kinds of disorder–real and thermal– are lumped together into one short-range disorder (SRD), characterized by a mean free time $\tau_{\rm sp} = \tau_{\rm tr} \equiv \tau_s$. Scattering of electrons at localized magnetic moments is also assumed to be elastic–this is a reasonable assumption as the ordering degree of freedom (magnetization) exhibits critical slowing down near T_c. Therefore, spin-flip scattering can also be viewed as another kind of disorder. However, in contrast to impurities and phonons, the magnetic disorder is of a very long range near T_c, because its correlation length, ξ, diverges at T_c. This will be modeled as long-range disorder (LRD) with known correlation function, $W(q)$, which we will eventually borrow from the theory of classical phase transitions. We will also assume that LRD is weaker than SRD, and thus treat the former as a correction to the latter.

So, we have two kinds of disorder, what's the total resistivity of the metal? dGF believed into the conventional Boltzmann equation, which would describe this situation by the sum of two collision integrals: due to SRD and LRD. The ensuing Matthiessen rule then says that the total resistivity is proportional to the sum of scattering rates:

$$\rho = \frac{m^*}{e^2 \mathcal{N}} \left(\frac{1}{\tau_s} + \frac{1}{\tau_l} \right), \tag{1.60}$$

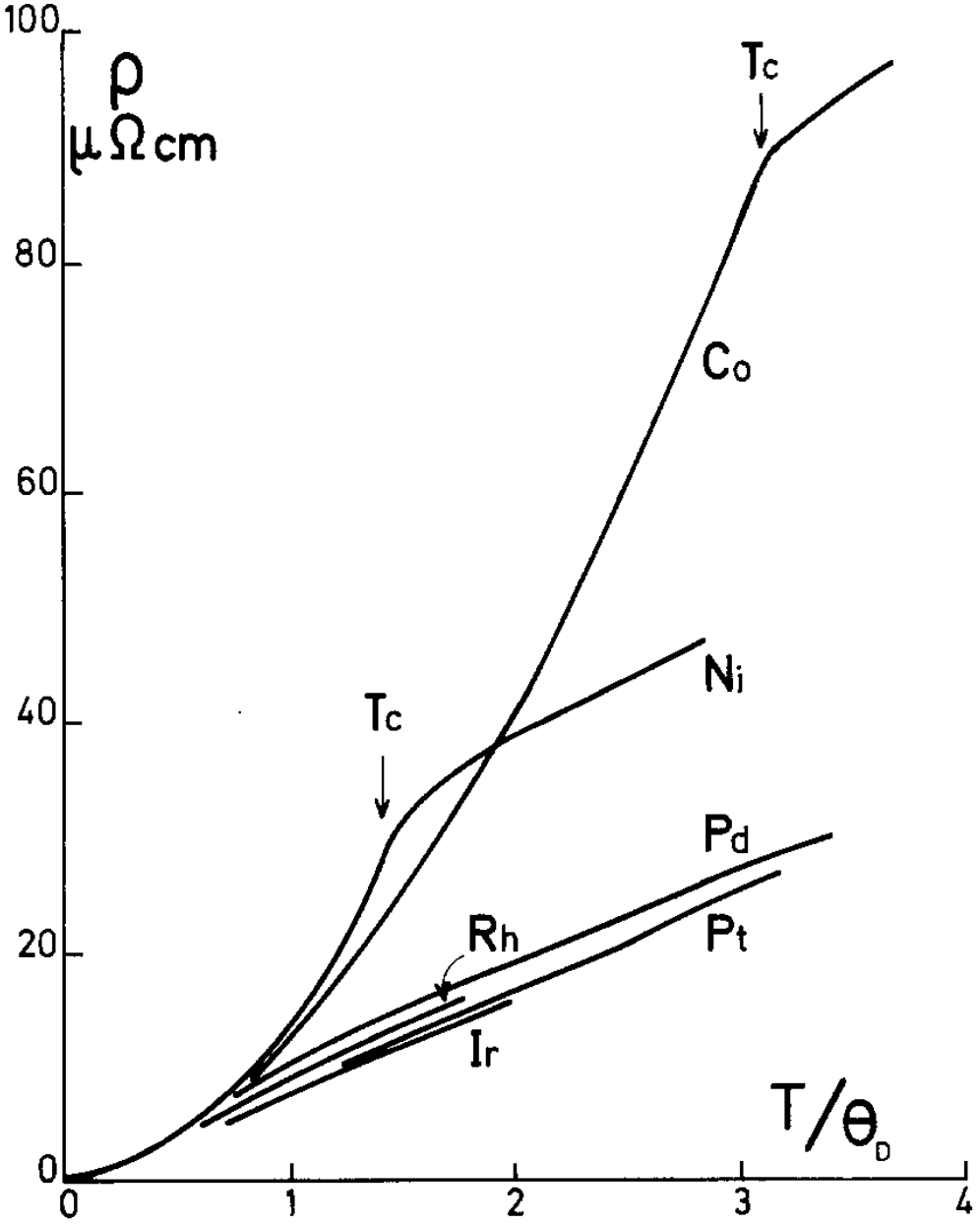

FIG. 12. $\rho(T)$ in Ni and Co, along with some non-magnetic metals. Reproduced from Ref. [29].

where τ_l is the transport scattering time due to LRD. dGF then invoked the Fermi Golden Rule (FRG), according to which (in 3D)

$$\frac{1}{\tau_l} = 2\pi \int_0^{2k_F} \frac{dqq^2}{(2\pi)^3} W(q) \frac{q^2}{2k_F^2} \Delta t(q), \tag{1.61}$$

where I just took a liberty to denote the angular average of the energy-conserving delta function as

$$\Delta t(q) = \int d\Omega_{\mathbf{q}} \delta(\varepsilon_{\mathbf{k}} - \varepsilon_{\mathbf{k}+\mathbf{q}}). \tag{1.62}$$

with $d\Omega_{\mathbf{q}}$ being the element of solid angle subtended by $\mathbf{q}$. Note, however, that $\Delta t(q)$ does have units of time, and we will clarify its meaning later. Applying (1.62) for $q \ll k_F$, we obtain

$\Delta t(q) \sim 1/v_F q$.

At the mean-field level,

$$W(q) \propto \frac{1}{q^2 + \xi^{-2}}, \tag{1.63}$$

where $\xi \propto |\theta|^{-1/2}$ and $\theta = (T - T_c)/T_c \ll 1$. Power-counting the integrand, we see that integral is controlled by $q \sim k_F$, i.e., by short-range physics. Subtracting off this contribution, dGF obtained the universal part, coming from $q \sim \xi^{-1}$:

$$\frac{1}{\tau_l} \propto C - \xi^{-2} \int_0^{2k_F} \frac{dqq}{q^2 + \xi^{-2}} = C - |\theta| \ln \frac{1}{|\theta|}. \tag{1.64}$$

This is now known as "de Gennes-Friedel" scaling.

Ten years later, Fisher and Langer (FL) [31] re-visited the same problem and pointed out several issues with dGF solution. First–and obvious–issue was the dGF theory contradicted the experimental results, at least those that had been know prior to 1968. Indeed, (1.64) predicts that the ρ itself has an upward cusp, while $d\rho/dT$ diverges as $\ln |\theta|^{-1}$. However, ρ of Ni and Co [cf. Fig. (12)] increases monotonically with T, exhibiting a knee, rather than a cusp, at T_c, while $d\rho/dT$ exhibits a cusp. Second, FL argued that Matthiessen's rule is not applicable if the mean free path due to SRD, $\ell_s = v_F \tau_s$, is shorter than ξ, which is guaranteed to be the case close enough to T_c. They did not fix this problem, however, but merely pointed out that "smearing" of electron states by SRD should weaken the dGF singularity, and the issue had remained unresolved until recently. Finally, they rolled yet another counter-argument, beautiful in its simplicity. This argument is about short-range contribution–the C term in (1.64)–which was discarded by dGF as "uninteresting". However, FL argued that this term is, in fact, very interesting as it does encode a singular dependence on θ. Indeed, in a metallic FM, such as Ni or Co, $k_F \sim a^{-1} = a_M^{-1}$, where a_M is the distance between localized magnetic moments. This means that the upper-limit contribution to the integral in (1.61) is coming from the same region as the magnetic internal energy,

$$U(T) = -J \sum_n \langle \mathbf{S}_0 \mathbf{S}_n \rangle \propto - \int_0^{1/a} dqq^2 W(q), \tag{1.65}$$

for a short-range Heisenberg exchange interaction. The temperature derivative of $U(T)$ is the magnetic part of the specific heat, which, beyond the mean-field level, is a non-analytic function of θ: $C(T) \propto |\theta|^{-\alpha}$. Here comes the relation, now known as "Fisher-Langer scaling"

$$\frac{d\rho}{dT} \propto \frac{dU}{dT} = C(T) \propto |\theta|^{-\alpha}, \tag{1.66}$$

or $\rho \propto \mathrm{sgn}\theta |\theta|^{1-\alpha}$. A cusp in $d\rho/dT$ is consistent with the behavior observed in Ni and Co.

2. Revisiting the Fermi Golden Rule

Although the FL contribution is always there, it turns out there is still a universal contribution, missed by dGF. This contribution becomes larger than the FL sufficiently close to T_c [7]. To find this contribution, we need to get back to Eq. (1.61) and clarify the meaning of $\Delta t(q)$.

In the current version of (1.61), there is no mentioning of SRD, which presumes that two kinds of disorder act independently of each other. When is this valid? Let's look at the relation $\Delta t(q) = 1/v_F q$ and understand its meaning. By uncertainty principle, momentum transfer q occurs in the region of size $1/q$. Then $1/v_F q$ is the time it takes to accomplish the momentum transfer–let dub it as the "interaction time". SRD is irrelevant if momentum transfer occurs in the region which is much smaller than the mean free path due to SRD. For the universal contribution, $q \sim 1/\xi$ and thus the condition is $\xi \ll \ell_s$. This is the ballistic regime, where the dGF scaling is valid. In the opposite, diffusive regime, when $\xi \gg \ell_s$, two effects occur. First–as FL pointed out–scattering by SRD smears out electron states. This means that the delta function in (1.62) must be replaced by a Lorentzian of width τ_s. Accordingly, $\Delta t(q) \sim \tau_s = \text{const}$, which adds an extra factor of q to the integrand of the second term in (1.64). This, indeed, weakens the singularity, as FL conjectured. More important, however, is the second effect of diffusion: now the time to traverse a region of size $1/q$ is $\Delta t(q) \sim 1/D_s q^2$, where $D_s = (1/3)v_F^2 \tau_s$ is the diffusion coefficient due to SRD. The diffusive $\Delta t(q)$ is more singular than the ballistic one, which *removes* a factor of q from the integrand in (1.64). Extracting the FL singularity from the first (C) term in this equation, we obtain the resistive anomaly as

$$\delta\rho = a\,\mathrm{sgn}(\theta)|\theta|^{1-\alpha} + b|\theta|^{1/2} \tag{1.67}$$

or

$$\frac{d\rho}{dT} = a'|\theta|^{-\alpha} + b'\,\mathrm{sgn}(\theta)|\theta|^{-1/2}. \tag{1.68}$$

If $\alpha < 1/2$, the second, "diffusive" term is larger than the FL one.

Of course, such a comparison is not really correct, as $\alpha = 0$ at the mean-field level. To see what replaces the mean-field exponent of $1/2$ in the diffusive term, one can invoke the asymptotic form of the exact correlation function [32, 33]

$$W(q) = q^{-2+\eta}\left[A + B_\pm\,\mathrm{sgn}\,\theta\left(\frac{|\theta|}{q^{1/\nu}}\right)^{1-\alpha} + C_\pm\frac{|\theta|}{q^{1/\nu}} + \ldots\right] \tag{1.69}$$

Universality class	ν	η	α	2β	γ	ζ
O(3), $d = 3$ [35]	0.71	0.038	-0.13	0.738	1.40	0.39
O(2), $d = 3$ [36]	0.67	0.038	-0.015	0.698	1.32	0.31
Ising, $d = 3$ [37, 38]	0.63	0.037	0.11	0.652	1.24	0.24
Ising, $d = 2$ [34]	1	1/4	0	1/4	7/4	3/4

TABLE I. Critical exponents for common universality classes. ν governs the correlation length, η is defined in Eq. (1.69), α is the specific heat exponent, β describes the order parameter (2β governs Bragg peak intensity), γ is the susceptibility exponent, and $\zeta = \nu(2-\eta) - 1$. For the $d = 2$ Ising model, $\alpha = 0$ implies a logarithmic divergence. Exponents for $d = 3$ are rounded to two significant digits.

with $A > 0$, and $B_\pm$, $C_\pm$ being generally different above and below T_c. For a general form of $W(q)$, the critical part of ρ in the diffusive limit becomes

$$\delta\rho = a\mathrm{sgn}(\theta)|\theta|^{1-\alpha} + \int dq q^2 W(q) \tag{1.70}$$

Substituting (1.69) into the second term in (1.70), and integrating over the interval $\xi^{-1} \lesssim q \lesssim 1/\ell_s$, we obtain

$$\delta\rho = a\mathrm{sgn}(\theta)|\theta|^{1-\alpha} + b|\theta|^{2\beta} \tag{1.71}$$

where β is the order-parameter exponent, defined by $\langle M\rangle \propto \Theta(-\theta)(-\theta)^\beta$ and related to other exponents via $2\beta = (d-2+\eta)\nu$. Using the hyperscaling relation, $\nu d = 2 - \alpha$ [34] , 2β can be re-written as

$$2\beta = 1 - \alpha - \zeta, \tag{1.72}$$

where $\zeta = (2-\eta)\nu - 1$. As long as $\zeta > 0$, $2\beta < 1 - \alpha$, the second term in (1.71) is more singular than the first one. The critical exponents for most common universality classes are listed in Table I. Form the last column, we see that, indeed, $\zeta > 0$ for all cases.

Hand-waving arguments of given above can be made rigorous in two ways: by straightforward analysis of Feynman diagrams and via the stochastic Liouville equation.

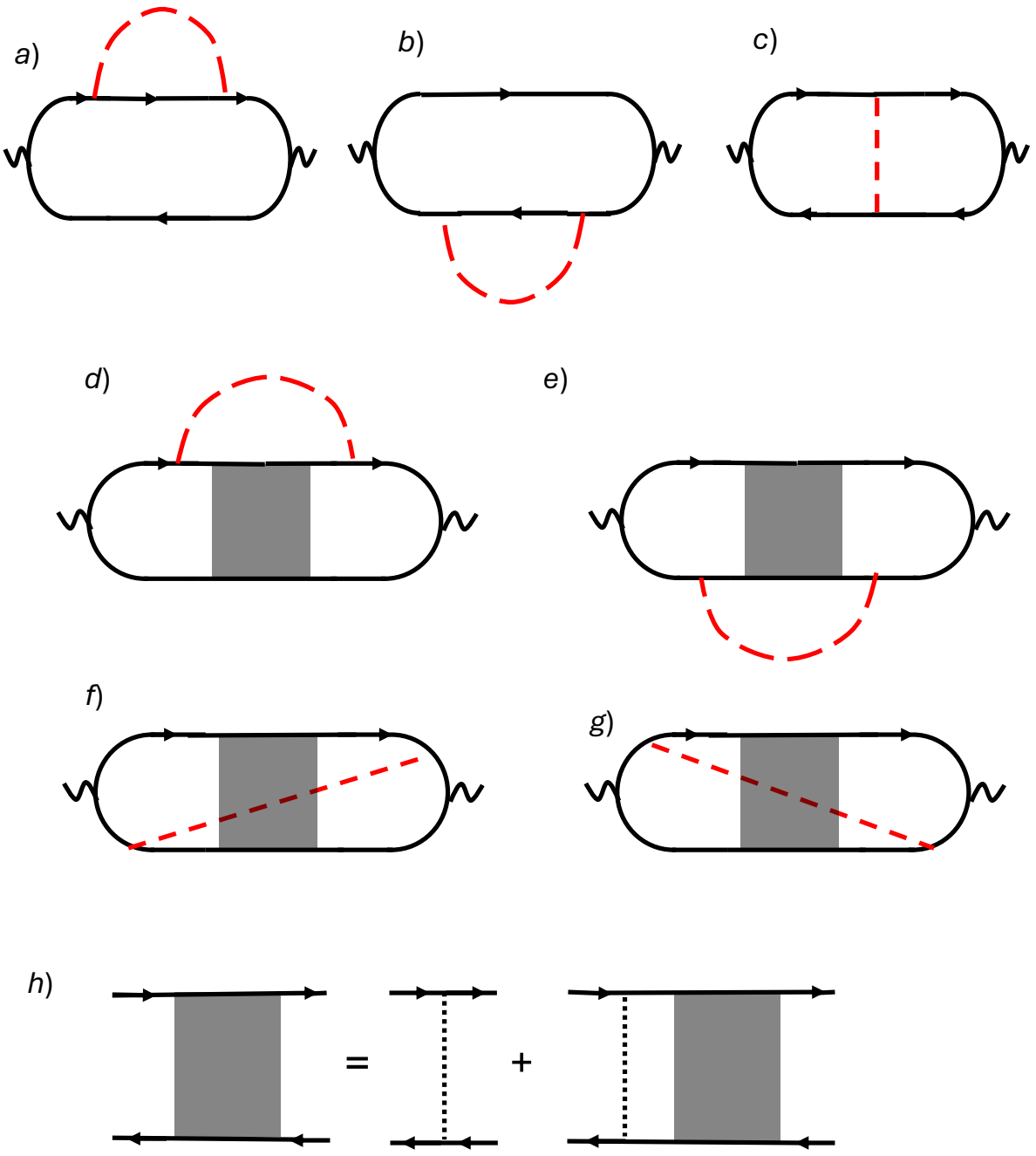

FIG. 13. Lowest-order corrections to the conductivity due to long-range disorder. Solid lines: Green's functions averaged over realizations of short-range disorder; wiggly lines: current vertices, dashed line: correlation function of long-range disorder; dotted line: correlation function of short-range disorder; shaded box: diffuson ladder, satisfying the equation shown graphically by diagram *h*.

3. Resistive anomaly from diagrams

Relevant diagrams are shown in Fig. 13. The solid lines are the Green's functions averaged over SRD:

$$\langle G^{R,A}_{\mathbf{k}}(\omega)\rangle = \frac{1}{\omega - \epsilon_{\mathbf{k}} \pm \frac{i}{2\tau_s}}, \tag{1.73}$$

where $\epsilon_{\mathbf{k}} = \varepsilon_{\mathbf{k}} - \varepsilon_F$. The dashed line is the LRD correlation function, $W(q)$, while the dotted line is (momentum-independent) SRD correlation function. The shaded box is the infinite sum of ladder diagrams, known as "diffuson", $\Lambda^R(q,\Omega)$, derived in Appendix B. As the name suggests, the diffuson exhibits a diffusion pole for $\omega\tau_s$ and $q\ell_s \ll 1$:

$$\Lambda^R(q,\Omega) \propto \frac{1}{D_s q^2 - i\Omega}. \tag{1.74}$$

In the ballistic limit $\xi \ll \ell_s$, diagrams a)-c) reproduce the Fermi Golden Rule in (1.61), and the corresponding singular contribution coincides with that predicted by dGF, modulo replacing the mean-field critical exponent $1/2$ by an exact one, ν. In the diffusive limit ($\xi \gg \ell_s$), diagrams a)-c) become subleading, while the leading ones are diagrams d)-g) with diffuson insertions. For the *dc* conductivity, the diffuson enters the result as $\Lambda(q,0) \propto 1/D_s q^2$, which is precisely the diffusive limit of the interaction time, $\Delta t(q)$. The sum of diagrams d)-g) reproduces the diffusion resistive anomaly, the second term in (1.71). Calculations are rather straightforward, and I refer the reader to Ref. [7] for details.

The interpretation of the resistive anomaly in the diffusive regime as a classical memory effect is confirmed by calculating the optical conductivity. For $\Omega \ll D_s/\xi^2$, the optical conductivity exhibits an non-analytic scaling: $\mathrm{Re}\sigma(\Omega) \propto |\Omega|^{d/2}$, which corresponds to the power-law tail in the velocity-velocity correlation function: $\langle \mathbf{v}(t)\cdot\mathbf{v}(0)\rangle \propto t^{-(1+d/2)}$, cf. the discussion in Sec. I A 3.

4. Resistive anomaly from the stochastic Liouville equation

We saw that the approach based on the conventional Boltzmann equation fails to describe the most interesting (diffusive) regime of the resistive anomaly: according to this equation, the scattering rates due to SRD and LRD simply add, as in (1.60). Why does it fail and can it still be made to work?

Why it fails: The conventional Boltzmann equation assumes a memory loss between consequitive collisions. But for a LRD the very notion of "collision" does not make sense: the collision

never ends. As to how it can still work, we need to return to the exact Liouville equation, describing the motion of a particle in a given realization of LRD, $U(\mathbf{r})$. LRD is now modeled by the random force on the RHS: $-\mathbf{v}_\mathbf{k} \cdot \boldsymbol{\nabla} U(\mathbf{r}) \cdot \partial_\mathbf{k} f_\mathbf{k}$. Because the LRD force is non-uniform, we must also to keep the gradient term, $\mathbf{v} \cdot \boldsymbol{\nabla}_\mathbf{r} f_\mathbf{k}$, even though the external electric field is still assumed to be uniform and weak, such that the corresponding force term can be linearized. For generality though, I will keep the time-dependence of $\mathbf{E}$. Scattering by SRD can be still described by a collision integral–which means that our distribution function is already averaged over SRD and exact with respect to LRD. However, it is imperative now to use the correct form of the collision integral, as in (1.7), rather than its RTA version. Finally, we need to recall that the system is still non-uniform even in the absence of the electric field, which means that the equilibrium distribution is $f_0(\varepsilon + U(\mathbf{r}))$. Collecting everything together, we obtain a stochastic Liouville equation

$$\frac{\partial f_\mathbf{k}}{\partial t} + \mathbf{v}_\mathbf{k} \cdot \boldsymbol{\nabla}_\mathbf{r} f_\mathbf{k} - \boldsymbol{\nabla}_\mathbf{r} U(\mathbf{r}) \cdot \frac{\partial f_\mathbf{k}}{\partial \mathbf{k}} + \frac{f_\mathbf{k} - \bar{f}}{\tau_s} = e(\mathbf{v}_\mathbf{k} \cdot \mathbf{E}(t) f_0'(\varepsilon_\mathbf{k} + U(\mathbf{r})) \equiv S_\mathbf{k}(\mathbf{r}), \tag{1.75}$$

If the Green's function of (1.75) is known, the distribution function *averaged* over LRD is found as

$$\langle f_\mathbf{k}(\mathbf{r}, t)\rangle = \int d^d k' \int d^d r' \int dt' \langle \mathcal{G}(\mathbf{k}, \mathbf{r}, t|\mathbf{k}', \mathbf{r}', t') S_{\mathbf{k}'}(\mathbf{r}', t')\rangle. \tag{1.76}$$

Note that both $\mathcal{G}$ and $S_\mathbf{k}$ depend on $U(\mathbf{r})$, and thus it is their product that needs to be averaged. From Eq. (1.76), we find the average current at point $\mathbf{r}$. But since averaging restores translational invariance, the current must be same at all points, and we can choose $\mathbf{r} = 0$:

$$\begin{aligned}\langle \mathbf{j}(t)\rangle &= -2e \int \frac{d^d k}{(2\pi)^d} \mathbf{v}_\mathbf{k} \langle f_\mathbf{k}(0, t)\rangle \\ &= -2e \int \frac{d^d k}{(2\pi)^d} \int d^d k' \int d^d r' \int dt' \langle \mathcal{G}(\mathbf{k}, 0, t|\mathbf{k}', \mathbf{r}', t') S_{\mathbf{k}'}(\mathbf{r}', t')\rangle \mathbf{v}_\mathbf{k}\end{aligned} \tag{1.77}$$

The perturbation theory is developed by expanding $\mathcal{G}$ and $S_\mathbf{k}$ to second order in $U(\mathbf{r})$, and collecting all terms. The diagrammatic technique can be formulated directly for the conductivity in terms of the Green's function of (1.75) without $U(\mathbf{r})$, which is derived in Appendix A. Thanks to using the correct form of the collision integral, this Green's function has a diffusion pole, and thus captures the right physics.

The leading order diagrams for the conductivity are shown in Fig. 14. Evaluating these diagrams, one again reproduces the second term in (1.71) [39]

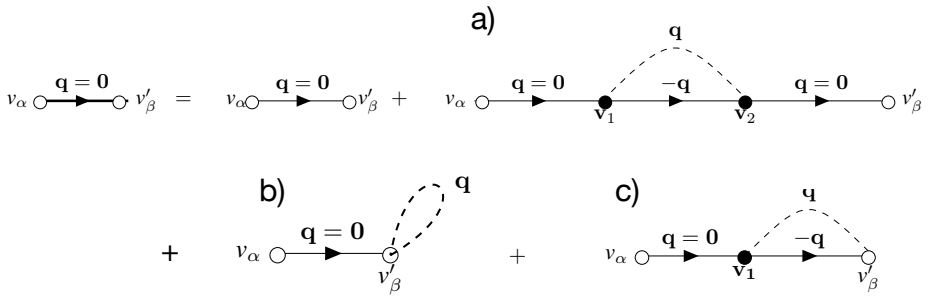

FIG. 14. Diagrams for the conductivity to second order in LRD. Solid line: the Green's function of (**??**) in the absence of LRD, $g(\mathbf{q},\omega;\mathbf{k},\mathbf{k}')$, cf. Eqs. (A5a)-(A5c). Blank circles: Cartesian components of $\mathbf{v}_\mathbf{k}$; filled circles: vertices of scattering by LRD, $-\vec{\nabla}U\cdot\partial/\partial\mathbf{k}$; dashed line: the correlation function of LRD. The first (unlabeled) term on the RHS is the Drude conductivity in the presence of SRD only. Diagrams a)-c) are corrections due to LRD. Diagram a) comes from expanding G to $O(U^2)$, while neglecting U in $S_\mathbf{k}$. Diagram b) comes from expanding $S_\mathbf{k}$ to order $O(U^2)$, while neglecting U in G. Diagram c) comes from expanding both G and $S_\mathbf{k}$ to $O(U)$ and keeping the cross-term.

II. HOMEWORK PROBLEMS FOR SECTION I

1. Consider a Boltzmann equation for 2D electrons in the presence of an in-plane electric field and out-of-plane magnetic fields. The electric field is weak enough for the left-hand side to be linearized, but the magnetic field is arbitrarily strong (in the classical sense, i.e., $\omega_c\tau_{\rm tr}$ is arbitrary). Assume that the electron spectrum is parabolic, while the probability of elastic scattering is an arbitrary function of the scattering angle, $w(\theta_{\mathbf{k}\mathbf{k}'})$. With these assumptions, the Boltzmann equation reads

$$-\frac{eB}{m}(\mathbf{k}\times\mathbf{B})\cdot\frac{\partial f_\mathbf{k}}{\partial\mathbf{k}}-\frac{e}{m}(\mathbf{k}\cdot\mathbf{E})f_0'=-\int\frac{d^2k'}{(2\pi)^2}w(\theta_{\mathbf{k}\mathbf{k}'})(f_\mathbf{k}-f_{\mathbf{k}'})\delta(\varepsilon_\mathbf{k}-\varepsilon_{\mathbf{k}'}). \qquad (2.1)$$

Derive Eqs. 1.54. *Hint*: In transverse geometry ($\mathbf{E}\cdot\mathbf{B}$=0) and to linear order in $\mathbf{E}$, one can form only two scalars out of vectors $\mathbf{k}$, $\mathbf{E}$, and $\mathbf{B}$, namely, $\mathbf{k}\cdot\mathbf{E}$ and $\mathbf{k}\cdot(\mathbf{E}\times\mathbf{B})$. This means that the non-equilibrium part of $f_\mathbf{k}$ can be represented by the sum of two terms:

$f_{\mathbf{k}} = f_1(\varepsilon_{\mathbf{k}}) + C_1(B)\mathbf{k}\cdot\mathbf{E} + C_2(B)\mathbf{k}\cdot(\mathbf{E}\times\mathbf{B})$, where $f_1(\varepsilon_{\mathbf{k}})$ is an arbitrary function of electron energy and $C_{1,2}(B)$ are arbitrary functions of the magnitude B.

2. Consider a Boltzmann equation with an arbitrarily strong electric field and elastic scattering by point impurities

$$-e\mathbf{E}\cdot\frac{\partial f_{\mathbf{k}}}{\partial \mathbf{k}} = -\frac{f_{\mathbf{k}} - \bar{f}}{\tau}. \tag{2.2}$$

Show that, if i) the electron spectrum is parabolic and ii) τ is independent of energy, the electric current is strictly linear in $\mathbf{E}$, regardless of how strong the electric field is. *Hint*: multiply both sides of (2.2) by $\mathbf{v}_{\mathbf{k}}$ and integrate over $\mathbf{k}$, using the fact that $\int_{\mathbf{k}} f_{\mathbf{k}} = \mathcal{N}$, where $\mathcal{N}$ is the number density.

3. Following the energy diffusion model of Sec. I B 4, derive the phase breaking time under the conditions of quasielastic scattering. *Hint*: assume that the phase of an electron wave function is related to electron energy via $\varphi(t) = \int_0^t dt' \delta\varepsilon(t')$, where $\delta\varepsilon(t)$ is the average gain or a loss of energy acquired by time t.

4. Derive a 2D analog of de Gennes-Friedel scaling in Eq. (1.64).

III. TRANSPORT IN NORMAL AND "STRANGE" FERMI LIQUIDS

A. Introduction

The Pauli principle dictates that the scattering rate of two electrons in a Fermi gas scales as $1/\tau_{ee} \propto T^2$. This observation is a foundation, rather than a consequence, of the Landau Fermi-liquid theory, which, in its original formulation, takes τ_{ee} to infinity [40]. The Landau Fermi liquid is a Fermi gas of *non-interacting* quasi-particles with renormalized parameters: m^*, g^*, etc. The original Landau Fermi-liquid theory is based on the Boltzmann (kinetic) equation *without* any collision integrals on the RHS:

$$\frac{\partial f_{\mathbf{k}}}{\partial t} + \mathbf{v}_{\mathbf{k}}\cdot\boldsymbol{\nabla} f_{\mathbf{k}} + (\mathcal{F}_{\text{ext}} - \boldsymbol{\nabla}\delta\varepsilon_{\mathbf{k}})\, f_{\mathbf{k}} = 0, \tag{3.1}$$

where $\mathcal{F}_{\text{ext}}$ is the external force, and $\delta_{\mathbf{k}}$ is a change in the quasiparticle energy due a change in the distribution function

$$\delta\varepsilon_{\mathbf{k}}(\mathbf{r},t) = \int_{\mathbf{k}'} F(\mathbf{k},\mathbf{k}')\delta f_{\mathbf{k}}(\mathbf{r},t), \tag{3.2}$$

and $F(\mathbf{k},\mathbf{k}')$ is the Landau interaction function. The interactions that renormalize quasi-particle parameters are accounted for via a self-consistent force on the LHS of the BE. These interactions need not to be weak, the only condition is that the system has to be away of quantum phase transitions towards broken-symmetry states. The Landau theory describes the low-temperature thermodynamics and collective modes (zero-sound, Silin, plasmon, etc.) in the absence of damping. However, it cannot describe transport properties: for that, one needs to include residual interaction between quasi-particles among themselves, as well as with impurities and lattice. This requires adding the corresponding collision integrals to the RHS of (3.2). Therefore, there is no "general" Fermi-liquid theory of transport: what we have is a number perturbative approaches, which do require the interaction between quasi-particles to be weak, and numerical simulations of various complexity.

B. Conservation of current in Galilean-invariant Fermi liquids

Although common wisdom often relates the resistivity of a (charged) Fermi liquid to the Pauli scattering rate as $\rho \propto 1/\tau_{ee} \propto T^2$, this relation is tenuous at the best. An obvious counter example is a Galilean-invariant Fermi liquid, i.e., an electron system with parabolic spectrum. Quasi-particles in such a system do have finite lifetime, and the thermal diffusivity and viscosity are also finite and do scale as $\tau_{ee} \propto 1/T^2$. However, the *dc* conductivity of such a system is infinite, which follows simply from Newton's Second Law. Indeed, the equation of motion for an electron number i reads

$$\frac{d\mathbf{p}_i}{dt} = -e\mathbf{E} + \sum_{j\neq i} \mathbf{F}_{ij}, \tag{3.3}$$

where $\mathbf{F}_{ij}$ is the Coulomb force between electrons i and j. On summing (3.4) over all particles, the internal forces cancel each other, and the total momentum is changing only due to the action the total electric force:

$$\frac{d\mathbf{P}}{dt} = \sum_{i=1}^{N} \frac{d\mathbf{p}_i}{dt} = -eN\mathbf{E} \Rightarrow \mathbf{P} = -eN\mathbf{E}t. \tag{3.4}$$

Accordingly, the center-of-mass velocity also varies linearly with time

$$\mathbf{u} = \frac{\mathbf{P}}{Nm} = -\frac{e}{m}\mathbf{E}t, \tag{3.5}$$

and so does the current density

$$\mathbf{j} = -e\mathcal{N}\mathbf{u} = \frac{e^2\mathcal{N}}{m}\mathbf{E}t \tag{3.6}$$

where $\mathcal{N}$ is the number density. Even for infinitesimaly weak electric field, $j \to \infty$ at $t \to \infty$, which means that teh conductivity is infinite.

if the electric field oscillates in time, the conductivity is finite but purely imaginary

$$\sigma(\Omega) = \frac{e2\mathcal{N}}{mi\Omega}. \tag{3.7}$$

Adding an infinitesimally weak dissipation via $\Omega \to \Omega - i0^+$ gives

$$\sigma(\Omega) = \frac{\pi e^2 \mathcal{N}}{m}\delta(\Omega) + \frac{e^2\mathcal{N}}{mi\Omega}. \tag{3.8}$$

At the quantum level, the Hamiltonian of a system with density-density interaction is given by (the spin indices are omitted for brevity)

$$H = H_0 + H_{int} = \sum_{\mathbf{k}} \varepsilon_{\mathbf{k}} \hat{a}^\dagger_{\mathbf{k}} \hat{a}_{\mathbf{k}} + \frac{1}{2}\sum_{\mathbf{kpq}} U_{\mathbf{q}} \hat{n}_{\mathbf{q}} \hat{n}_{-\mathbf{q}} \tag{3.9}$$

where $\hat{n}_{\mathbf{q}} = \sum_{\mathbf{k}} a^\dagger_{\mathbf{k}-\mathbf{q}} a^\dagger_{\mathbf{k}}$ is the number density. The corresponding current operator is deduced from the continuity equation

$$-e\partial_t \hat{n}_{\mathbf{q}} = i\mathbf{q}\cdot\hat{\mathbf{j}}_{\mathbf{q}}. \tag{3.10}$$

and the Heisenberg equation of motion for the number density

$$\partial_t \hat{n}_{\mathbf{q}} = i[\hat{n}_{\mathbf{q}}, H] = i[\hat{n}_{\mathbf{q}}, H_0] + i[\hat{n}_{\mathbf{q}}, H_{int}]. \tag{3.11}$$

Since $\hat{n}_{\mathbf{q}}$ commutes with H_{int}, we only need the first commutator. Straightforward commutation algebra yields

$$\hat{\mathbf{j}}_{\mathbf{q}} = -e\sum_{\mathbf{k}\sigma} \mathbf{v}_{\mathbf{k}} \hat{a}^\dagger_{\mathbf{k}-\mathbf{q}/2} \hat{a}_{\mathbf{k}+\mathbf{q}/2}. \tag{3.12}$$

Next, we calculate the time derivative of the uniform ($\mathbf{q} = 0$) current (this is left as a homework exercise #1 in Sec. IV)

$$\partial\hat{\mathbf{j}}_0 = i[\hat{\mathbf{j}}_0, H] = -e\frac{i}{2}\sum_{\mathbf{kq}} U_{\mathbf{q}} \left(\mathbf{v}_{\mathbf{k}-\mathbf{q}/2} + \mathbf{v}_{\mathbf{p}+\mathbf{q}/2} - \mathbf{v}_{\mathbf{k}+\mathbf{q}/2} - \mathbf{v}_{\mathbf{p}-\mathbf{q}/2}\right) \hat{a}^\dagger_{\mathbf{k}-\mathbf{q}/2} \hat{a}^\dagger_{\mathbf{p}+\mathbf{q}/2} \hat{a}_{\mathbf{k}+\mathbf{q}/2} \hat{a}_{\mathbf{p}-\mathbf{q}/2}. \tag{3.13}$$

For a Galilean-invariant system, $\mathbf{v} = \mathbf{k}/m$ and thus the combination of the velocities cancel due to momentum conservation.

Note that the non-uniform current, $\mathbf{j}_{\mathbf{q}\neq 0}$, is not conserved, which means that the conductivity at finite q is finite, rather than infinite. For example, for a 2D system with parabolic dispersion and Coulomb interaction, we have [41]

$$\mathrm{Re}\sigma(q,\Omega) = \frac{e^2}{24\pi^2}\frac{q^2\kappa^2}{m^2\Omega^2}\left(1+\frac{4\pi^2T^2}{\omega}\right)\ln\frac{k_F}{\kappa}, \tag{3.14}$$

where κ is the inverse screening radius and $q \ll \Omega/v_F$.

In a disordered system, the total electric field, which is the sum of the applied field and the fields of impurities, is *non-uniform*. This means that in the presence of disorder electron-electron interaction does affect the current–we will be exploring consequences of this observation.

C. Non-Galilean–invariant Fermi liquids without disorder

Now let's move on to lattice systems, which are not Galilean-invariant. Two things change. First, the electron spectrum is now non-parabolic and, generally speaking, anisotropic, and momentum conservation does not imply conservation of the group velocity $\mathbf{v}_\mathbf{k} = \partial_\mathbf{k}\varepsilon_\mathbf{k}$. Second, umklapp scattering, which does not conserve the momentum.

1. *Momentum-conserving scattering in non-Galilean–invariant Fermi liquids*

In this section we will show if the momentum is conserved, electron-electron interaction cannot render the *dc* conductivity finite, no matter how anisotropic the spectrum is. To this end, we need to invoke the Boltzmann equation with the electron-electron collision integral

$$\begin{aligned} I_{ee} = -\int_{\mathbf{k}',\mathbf{p},\mathbf{p}'} W_{\mathbf{k},\mathbf{p}\to\mathbf{k}'\mathbf{p}'}\left[f_\mathbf{k}f_\mathbf{p}\left(1-f_{\mathbf{k}'}\right)\left(1-f_{\mathbf{p}'}\right) - f_{\mathbf{k}'}f_{\mathbf{p}'}\left(1-f_\mathbf{k}\right)\left(1-f_\mathbf{p}\right)\right] \\ \times\delta\left(\varepsilon_\mathbf{k}+\varepsilon_\mathbf{p}-\varepsilon_{\mathbf{k}'}-\varepsilon_{\mathbf{p}'}\right)\delta\left(\mathbf{k}+\mathbf{p}-\mathbf{k}'-\mathbf{p}'\right), \end{aligned} \tag{3.15}$$

If the external electric field is weak, the deviations of the equilibrium are small, and the collision integral can be linearized. It is convenient to parametrize the distribution function as [42]

$$f_\mathbf{k} = f_{0\mathbf{k}} + f_{0\mathbf{k}}\left(1-f_{0\mathbf{k}}\right)g_\mathbf{k} = f_{0\mathbf{k}} - Tf'_{0\mathbf{k}}g_\mathbf{k} \tag{3.16}$$

a. dc conductivity. We start with the *dc* case. Linearizing the LHS of the Boltzmann equation with respect to $\mathbf{E}$ and the RHS with respect to $g_\mathbf{k}$, we arrive at

$$\begin{aligned} e(\mathbf{v}_\mathbf{k}\cdot\mathbf{E})f'_{0\mathbf{k}} = \int_{\mathbf{k}'\mathbf{p}\mathbf{p}'} W_{\mathbf{k},\mathbf{p}\to\mathbf{k}'\mathbf{p}'}\left(g_\mathbf{k}+g_\mathbf{p}-g_{\mathbf{k}'}-g_{\mathbf{p}'}\right)f_{0\mathbf{k}}f_{0\mathbf{p}}\left(1-f_{0\mathbf{k}'}\right)\left(1-f_{0\mathbf{p}'}\right) \\ \times\delta\left(\mathbf{k}+\mathbf{p}-\mathbf{k}'-\mathbf{p}'\right)\delta\left(\varepsilon_\mathbf{k}+\varepsilon_\mathbf{p}-\varepsilon_{\mathbf{k}'}-\varepsilon_{\mathbf{p}'}\right). \end{aligned} \tag{3.17}$$

Mathematically speaking, (3.17) does not have a unique solution. Indeed, observe that, because of momentum conservation, the collision integral is nullified by the combination

$$g^0_{\mathbf{k}} = \mathbf{A}\cdot\mathbf{k} = -C(e\mathbf{E}\cdot\mathbf{k}), \tag{3.18}$$

where $\mathbf{A}$ is $\mathbf{k}$-independent but otherwise arbitrary vector, which are free to choose in a form specified above with C being an arbitrary constant [10]. In mathematical terms, $g^0_{\mathbf{k}}$ is the zero mode of the integral operator in (3.17). Therefore, if we found a partial solution of the inhomogeneous problem, $\tilde{g}_{\mathbf{k}}$, we can always obtain another solution by adding this combination

$$g_{\mathbf{k}} = \tilde{g}_{\mathbf{k}} - C(e\mathbf{E}\cdot\mathbf{k}). \tag{3.19}$$

Accordingly, the current will change by the amount

$$\delta\mathbf{j} = e^2 C\int_{\mathbf{k}} \mathbf{v}_{\mathbf{k}}(\mathbf{E}\cdot\mathbf{k}) f_{0\mathbf{k}}(1-f_{0\mathbf{k}}), \tag{3.20}$$

Notice that C can be arbitrarily large and its sign can correspond to the current flowing in the direction opposite to that of the electric field, which means Joule *cooling* of the sample. and the conductivity by

$$\delta\sigma_{\alpha\beta} = e^2 C\int_{\mathbf{k}} v_\alpha k_\beta f_{0\mathbf{k}}(1-f_{0\mathbf{k}}). \tag{3.21}$$

Because we are free to choose C positive and infinitely large, the conductivity can be made infinite. Note that $\delta\sigma_{\alpha\beta} = 0$ only if $S_{\alpha\beta} = \int dO_{\mathbf{k}} v_\alpha k_\beta = 0$ for any α and β, where $dO_{\mathbf{k}}$ is the solid angle element. It is easy to see that at least the diagonal components, $S_{\alpha\alpha}$, are finite. Indeed, assume that opposite is true: $S_{xx} = \int dO_{\mathbf{k}} v_x k_x = 0, S_{yy} = \int dO_{\mathbf{k}} v_y k_y = 0$ ... Adding these relations together, we obtain $\int dO_{\mathbf{k}}\,(\mathbf{v}_{\mathbf{k}}\cdot\mathbf{k}) = 0$, but this cannot happen because $\mathbf{v}_{\mathbf{k}}\cdot\mathbf{k}$ is even on $\mathbf{k}\to-\mathbf{k}$. Therefore, momentum-conserving electron-electron interaction alone cannot control the *dc* conductivity.

b. Compensated metals. There is one but important exception from this rule: a metal with closed Fermi pockets that contain equal numbers of electron and hole, which is known as a"compensated metal". However, a compensated metal is an exception of this rule, because solution (3.18) corresponds to zero current [10]. Indeed, re-write (3.20) for the extra current as

$$\delta\mathbf{j} = e^2 CT\int_{\mathbf{k}} (\mathbf{E}\cdot\mathbf{k})\mathbf{v}_{\mathbf{k}}\frac{\partial f_{0\mathbf{k}}}{\partial\varepsilon_{\mathbf{k}}} = e^2 CT\int_{\mathbf{k}} (\mathbf{E}\cdot\mathbf{k})\frac{\partial f_{0\mathbf{k}}}{\partial\mathbf{k}}, \tag{3.22}$$

Now we introduce the distribution function for holes $f^{(h)}_{0\mathbf{k}} = 1 - f_{0\mathbf{k}}$ and split the integral into two parts, going over the electron and hole pockets of the Fermi surface, respectively:

$$\delta\mathbf{j} = e^2 CT\left[\int_{\mathbf{k}\in\mathrm{eFS}} (\mathbf{E}\cdot\mathbf{k})\frac{\partial f_{0\mathbf{k}}}{\partial\mathbf{k}} - \int_{\mathbf{k}\in\mathrm{hFS}} (\mathbf{E}\cdot\mathbf{k})\frac{\partial f^{(h)}_{\mathbf{k}0}}{\partial\mathbf{k}}\right]. \tag{3.23}$$

Integrating by parts and discarding the boundary terms, which are zero because a closed Fermi surface does not cross the boundaries of the Brillouin zone, we obtain

$$\delta\mathbf{j} = e^2 CT\mathbf{E}\left[-\int_{\mathbf{k}\in\text{eFS}} + \int_{\mathbf{k}\in\text{hFS}} f_0^{(h)}\right] = e^2 CT\mathbf{E}(\mathcal{N}_h - \mathcal{N}_e), \tag{3.24}$$

where $\mathcal{N}_e$ and $\mathcal{N}_n$ are the number densities of electrons and holes. For a compensated metal, $\mathcal{N}_e = \mathcal{N}_e$ and thus $\delta\mathbf{j} = 0$. As we see, this condition does not depend on the actual shapes of pockets.

For the model case of two spherical electron and hole pockets with masses $m_\pm$, the linearized Boltzmann equation can be solved exactly, generalizing the method of Refs. [43–45], developed originally for ^{3}He. The result is the expected FL behavior [46, 47]

$$\rho = \frac{\sqrt{m_+ m_-}}{e^2\mathcal{N}}\frac{1}{\tau_{\text{ee}}} \tag{3.25}$$

where $1/\tau_{\text{ee}} = AT^2/\varepsilon_F$ and A depends on the details of the scattering probability. T^2 scaling of teh resistivity resulting from electron-hole scattering in a compensated metal is known as Baber mechanism [48].

The proof above works for systems with electron and hole pockets located in different regions of the Brillouin zone, which is the case, e.g., in Bi. However, it can be also modified to apply a zero-gap semiconductor at charge neutrality as well. As an example, consider a single Dirac cone with linear spectrum $\varepsilon_\pm = \pm v_D k$. Re-write the extra current as

$$\delta\mathbf{j} = e^2 CT\int_{\mathbf{k}} \mathbf{E}\cdot\mathbf{k}\left[\mathbf{v}_+(\mathbf{k})f'_{0+} + \mathbf{v}_-(\mathbf{k})f'_{0-}\right] \tag{3.26}$$

where

$$-f'_{0\pm} = \frac{1}{4T\cosh^2\frac{\pm v_D k-\varepsilon_F}{2T}} \tag{3.27}$$

and $\mathbf{v}_\pm(\mathbf{k}) = \pm v_D\hat{\mathbf{k}}$. Substituting the last two equations into (3.26) yields

$$\delta\mathbf{j} = \frac{1}{4}e^2 C v_D\int_{\mathbf{k}}(\mathbf{E}\cdot\mathbf{k})\hat{\mathbf{k}}\left[\frac{1}{\cosh^2\frac{v_D k-\varepsilon_F}{2T}} - \frac{1}{\cosh^2\frac{v_D k+\varepsilon_F}{2T}}\right]. \tag{3.28}$$

At the charge neutrality point (CNP), where $\varepsilon_F = 0$, the integral vanishes. Therefore, the conductivity of a Dirac system at CNP can be controlled by electron-hole interaction alone [49–51].

c. Optical conductivity. Now let's look at the oscillatory driving field, $\mathbf{E} = \mathbf{E}_0 e^{-i\Omega t}$. Accordingly, (3.17) is replaced by

$$i\Omega f_{0\mathbf{k}}(1-f_{0\mathbf{k}})g_{\mathbf{k}} + e(\mathbf{v}_{\mathbf{k}}\cdot\mathbf{E}_0)f'_{0\mathbf{k}} = \int_{\mathbf{k}'\mathbf{p}\mathbf{p}'} W_{\mathbf{k},\mathbf{p}\to\mathbf{k}'\mathbf{p}'}\left(g_{\mathbf{k}}+g_{\mathbf{p}}-g_{\mathbf{k}'}-g_{\mathbf{p}'}\right) f_{0\mathbf{k}}f_{0\mathbf{p}}\left(1-f_{0\mathbf{k}'}\right)\left(1-f_{0\mathbf{p}'}\right) \times\delta\left(\mathbf{k}+\mathbf{p}-\mathbf{k}'-\mathbf{p}'\right)\delta\left(\varepsilon_{\mathbf{k}}+\varepsilon_{\mathbf{p}}-\varepsilon_{\mathbf{k}'}-\varepsilon_{\mathbf{p}'}\right), \tag{3.29}$$

or, recalling that $f_{0\mathbf{k}}(1-f_{0\mathbf{k}}) = -Tf'_{0\mathbf{k}}$ and canceling the common factors,

$$i\Omega g_{\mathbf{k}} - \frac{e}{T}(\mathbf{v}_{\mathbf{k}}\cdot\mathbf{E}_0) = \int_{\mathbf{k}'\mathbf{p}\mathbf{p}'} W_{\mathbf{k},\mathbf{p}\to\mathbf{k}'\mathbf{p}'}\left(g_{\mathbf{k}}+g_{\mathbf{p}}-g_{\mathbf{k}'}-g_{\mathbf{p}'}\right)\frac{1-f_{0\mathbf{k}'}}{1-f_{0\mathbf{k}}}f_{0\mathbf{p}}\left(1-f_{0\mathbf{p}'}\right) \times\delta\left(\mathbf{k}+\mathbf{p}-\mathbf{k}'-\mathbf{p}'\right)\delta\left(\varepsilon_{\mathbf{k}}+\varepsilon_{\mathbf{p}}-\varepsilon_{\mathbf{k}'}-\varepsilon_{\mathbf{p}'}\right) \tag{3.30}$$

Now the freedom of adding the zero mode (3.18) is gone, and (3.30) should have a unique solution. The units of the RHS is the scattering rate. Let's denote the order-of-magnitude of this rate as $1/\tau_j$, which may or may not coincide with the Pauli rate, $1/\tau_{ee}$. When $\Omega\tau_j \gg 1$, one can iterate in the collision integral. The zeroth order iteration yields

$$g^{(0)}_{\mathbf{k}} = \frac{e(\mathbf{v}_{\mathbf{k}}\cdot\mathbf{E}_0)}{i\Omega T}. \tag{3.31}$$

The corresponding contribution to the conductivity is purely imaginary-the second term in (3.8). Substituting this back into (3.30) and iterating one more time, we obtain

$$g^{(1)}_{\mathbf{k}} = -\frac{e}{T\Omega^2}\int_{\mathbf{k}'\mathbf{p}\mathbf{p}'} W_{\mathbf{k},\mathbf{p}\to\mathbf{k}'\mathbf{p}'}\left(\mathbf{v}_{\mathbf{k}}+\mathbf{v}_{\mathbf{p}}-\mathbf{v}_{\mathbf{k}'}-\mathbf{v}_{\mathbf{p}'}\right)\cdot\mathbf{E}_0\frac{1-f_{0\mathbf{k}'}}{1-f_{0\mathbf{k}}}f_{0\mathbf{p}}\left(1-f_{0\mathbf{p}'}\right) \times\delta\left(\mathbf{k}+\mathbf{p}-\mathbf{k}'-\mathbf{p}'\right)\delta\left(\varepsilon_{\mathbf{k}}+\varepsilon_{\mathbf{p}}-\varepsilon_{\mathbf{k}'}-\varepsilon_{\mathbf{p}'}\right). \tag{3.32}$$

In a Galilean-invariant system, the combination of velocities in in the first line of the last equation vanishes, and the same will be true to all orders $1/\Omega\tau_j$. As long as $\mathbf{v}_{\mathbf{k}} \neq \mathbf{k}/m$, however, this combination is, in general, finite, and thus $g^{(1)}_{\mathbf{k}}$ will contribute to $\mathrm{Re}\sigma(\Omega)$. Therefore, the optical conductivity can be controlled by electron-electron interactions alone, as long as the system is not Galilean-invariant. The corresponding contribution to the conductivity behaves as

$$\mathrm{Re}\sigma(\Omega) \propto \frac{1}{\Omega^2\tau_j}. \tag{3.33}$$

Power-counting yields that, generically, $1/\tau_j \propto T^2$, although, as we will see later, additional conservation laws may reduce it to $1/\tau_j \propto T^4$.

Equation (3.33) looks like a high-frequency limit of the Drude formula

$$\mathrm{Re}\sigma_D(\Omega) \propto \frac{\tau_j}{1+\Omega^2\tau_j^2}, \tag{3.34}$$

which does a finite *dc* limit $\mathrm{Re}\Sigma(0) \propto \tau_j$. Nevertheless, we showed in Sec. III C 1 a that e-e interactions cannot control the *dc* conductivity, unless the metal is compensated. The resolution of this contradiction is that the conductivity of a non-Galilean Fermi liquid with momentum-conserving e-e scattering and in the absence of disorder contains two terms, singular and regular [52]:

$$\mathrm{Re}\sigma(\Omega) = D\delta(\Omega) + \sigma_{\mathrm{reg}}(\Omega, T), \tag{3.35}$$

where D denotes the Drude weight, while the $\Omega \to 0$ $\Omega \to \infty$ limits $\sigma_{\mathrm{reg}}(\Omega, T)$ coincide with the corresponding limits of the Drude conductivity in (3.34). Therefore, the conductivity is finite at any $\Omega \neq 0$ but infinite at $\Omega = 0$. Momentum-non-conserving scattering due to impurities, umklapps, phonons, etc. smears the delta function, such that the conductivity becomes finite at $\Omega = 0$ as well. For a compensated metal, $D = 0$ [52], and the regular part determines the conductivity at any Ω.

On general grounds, one would expect $1/\tau_j$ to depend on T and Ω in a symmetric way, e.g., $1/\tau_j(T, \Omega) \propto \max\{T^2, \Omega^2\}$. However, since the RHS of (3.42) does not contain Ω, the ensuing $1/\tau_j$ may depend only on T. This is a drawback of the semiclassical Boltzmann equation, which is valid only for $\Omega \ll T$. To restore duality between Ω and T one has to use either the quantum Boltzmann equation or Kubo formula.

2. *Umklapp scattering*

In the presence of lattice, momentum is conserved only up to an integer number of reciprocal lattice vectors:

$$\mathbf{k} + \mathbf{p} = \mathbf{k}' + \mathbf{p}' + n\mathbf{b}. \tag{3.36}$$

$n = 0$ corresponds to momentum-conserving or "normal" scattering, considered in the previous section. $n \neq 0$ corresponds to umklapp scattering. For umklapp scattering, (3.18) is no longer a solution of (3.17). Power-counting the collision integral, one obtains the expected Fermi-liquid scaling $\rho \propto T^2$, which is known as Landau-Pomeranchuk mechanism [40, 53].

Umklapp scattering requires two conditions. First is that the Fermi surface must be large enough to accommodate the condition $|\mathbf{k} + \mathbf{p} - \mathbf{k}' - \mathbf{p}'| \geq b$ or $k_{F\,\mathrm{max}} \geq b/4$, where $k_{F\,\mathrm{max}}$ is the longest radius of the Fermi surface. In a multi-valley system, the valleys have to be separated

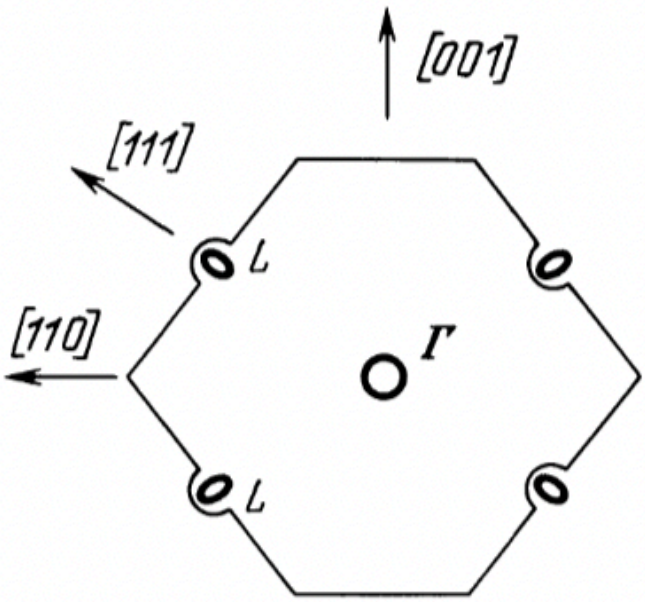

Fig. 7.9. The (110) cross section of the BZ of germanium (cf. fig. 1.1).

FIG. 15. Reproduced from Ref. [54].

by reciprocal lattice vector. This is the case, for example, in Ge, where the distance between the electron valleys, located at the L points of the Brillouin zone, is $b_{001}/2$ (cf. Fig. 15. Therefore, a simultaneous transfer of two electrons from one valley to another satisfies the umklapp condition. If the umklapp condition is not satisfied, the corresponding contribution to the resistivity is exponentially small, $\rho \propto \exp(-\Delta k/T)$, where Δk is the momentum deficit.

In the case of honeycomb lattice, shown in Fig. 16, the centers of the K and K' valleys are separated by $b/3$, which is not enough to allow for umklapp scattering at low filling. Then the Fermi surfaces has to be also larger enough to accommodate for missing momentum. If the Fermi contours are modeled by circles of radii k_F, then the largest change in momentum is achieved in a process, in which two electrons are taken from lowest point of the first valley and transferred to the highest point of the second valley. Umklapp becomes possible if [55]

$$4k_F + 2b/3 \geq b \Rightarrow k_F \geq b/12. \tag{3.37}$$

This condition can be readily satisfied in twisted bilayer graphene [56], where b is related to

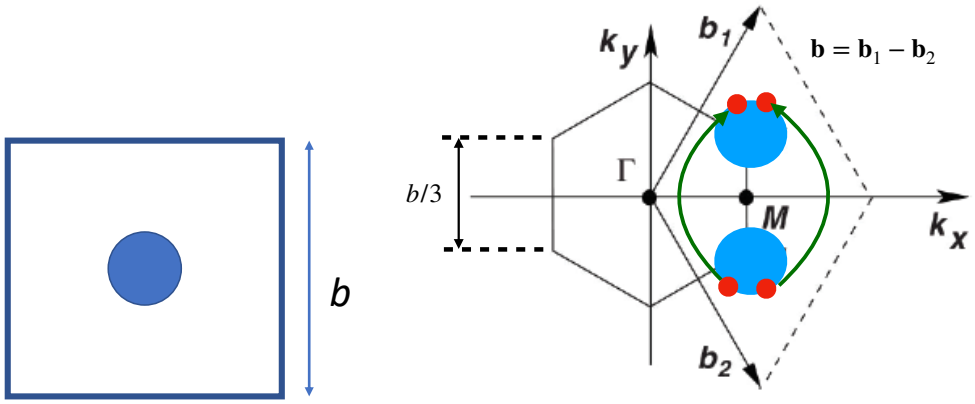

FIG. 16. Left: If the Fermi surface is too small, umklapps are forbidden. Right: An example of inter-valley umklapp process on honeycomb lattice [55].

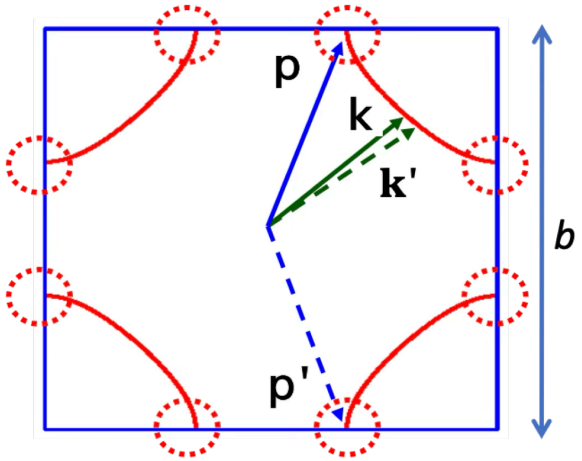

FIG. 17. Umklapp process for forward scattering [57].

the spacing of superlattice, which is significantly larger than the atomic spacing in monolayer graphene. (To determine the umklapp threshold more accurately one certainly needs to take into account anisotropy of the Fermi surface, which is significant at high filling.)

The second condition is that, even if the Fermi surface is sufficiently large, the interaction should allow large ($\sim k_F \sim b$) momentum transfers. Suppose that the opposite is true, i.e., that e-e scattering is of the forward type. Consider an umklapp process on a 2D Fermi surface shown in Fig. (17). Since momentum transfers are small, we have either $\mathbf{k} \approx \mathbf{k}'$ or $\mathbf{p} \approx \mathbf{p}'$. Accordingly, umklapp condition (3.36) needs to be satisfied at the expense of the other two momenta, e.g.,

$|\mathbf{p} - \mathbf{p}'| \approx b$, which pins $\mathbf{p}$ and $\mathbf{p}'$ to small spots near the boundaries of the Brillouin zone. In this case, umklapp contribution to the resistivity is suppressed in proportion to $\bar{q}^2/k_F^2$, where $\bar{q}$ is the typical momentum transfer [57]. This condition becomes relevant near the quantum critical points, separating the high-symmetry phase and a phase with spatially uniform order, e.g., a ferromagnet or nematic. [11]

D. What about the experiment?

Armed with understanding acquired in previous sections, we now look at several examples of T^2 scaling observed in real systems.

Figure 18 illustrates T^2 scaling of the resistivity in aluminum (left) and a heavy-fermion metal $CeAl_3$. In both cases, the Fermi surfaces are large and there is no reason to assume that the interaction is of the forward-scattering type. Therefore, we can safely attribute the T^2 behavior to umklapps, as in the Landau-Pomeranchu mechanism.

Figure 19 shows the temperature dependence of electron and hole mobilities in bismuth. Both mobilities behave as $1/T^2$, which means that the scattering rate scales as T^2. Bismuth is an archetypic compensated semi-metal, with small and equal number densities of electrons and holes: $\mathcal{N}_e = \mathcal{N}_h = 4{\times}10^{17}$ cm^{-3}, located in different regions of the BZ. Baber mechanism is fully expected to work here, as well as in other compensated semi-metals.

The two examples above fit squarely into the conventional Fermi-liquid behavior. Now, we come to a family "strange" Fermi liquids. The first example is doped quantum paraelectric (an insulator very close to ferroelectricity but never making it) $SrTiO_3$ (STO). T^2 scaling behavior in its resistivity had been observed since 1950s, but it did not cause any surprise until a seminal paper [59] pointed out that, for most of the doping range, the Fermi surface is too small to accommodate umklapp processes. And STO is not a compensated semi-metal. Yet, the resistivity exhibits a strongly pronounced T^2 behavior over a wide temperature range, which is much wider that in canonical "umklapp" materials in Fig. 18. In fact, the temperature range of the T^2 behavior is *too* wide, as it goes through a number of apparently relevant energy scales. At low doping, the T^2 behavior is observed both below and *above* the Fermi energy, indicated by an arrow in the top panel of Fig. 20. Since a Fermi-liquid behavior is supposed to strictly bounded to T below (in fact, well below) the Fermi energy, theorists (including this author) started to search for another

[11] Accidentally, two umklapp hot spots can happen to be close to each other. This case is considered in Ref. [58].

source of T^2 scaling, not related to e-e interaction. In fact, STO is a highly unusual material. Its proximity to ferroelectricity gives rise to two unusual but related properties: i) the lattice dielectric constant is very high, reaching $25,000$ at liquid helium and ii) the transverse optical phonon mode is very soft, with frequency $\omega_0 \sim 10\,\mathrm{K}$, also at helium. The first property effective eliminates the Coulomb interaction between free charge carriers. The second property makes the temperature separating equipartition and inelastic ranges of electron-phonon interaction, discussed in Sec. I B 4, to be abnormally low. An additional quirk is that electrons do not couple directly to polarization produced by a transverse optical mode: such a coupling should be of the form $\boldsymbol{\nabla}\cdot\mathbf{P}$, which is zero for transverse polarization $\mathbf{P}$. This means that single-phonon scattering is forbidden, but two-phonon scattering (described by diagrams in the lower panel of Fig. 21) is allowed. For the same reason as single-phonon scattering in the equipartition regime gives $\rho \propto T$, two-phonon scattering gives $\rho \propto T^2$ [60]. As a bonus, this model explains why E_F is not a relevant energy scale: the dependence of two-phonon scattering rate on electron momentum cancel out between the electron-phonon vertex and electron density of states, making the rate to be the same for degenerate and non-degenerate electrons. The two-phonon model describes the data in the interval $T > \omega_0$ reasonably well (at higher T, one needs to add scattering by LO phonons). In fact–and this is a problem–it describes the data even *below* ω_0, where scattering is inelastic rather than quasi-elastic. In fact, the same model should predict $\rho \propto \exp(-\omega_0/T)$ for $T \ll \omega_0$ due an exponential freeze-out of the optical phonons.

The two-phonon model comes with two falsifiable predictions. First, as discussed I B 4, one should observe the universal Lorentz ratio in the quasi-elastic regime. Instead, one observes that both the charge resistivity and thermal resistivity, $W = CT/\kappa$, scale as T^2 [61], which indicates the common origin and charge and heat transport. However, the Lorentz ratio is only about $1/3$ of the universal value, which is typical for small-angle scattering but not expected within the two-phonon mechanism. To be precise, the measurements in Ref. [61] were performed on much heavier doped samples $\mathcal{N} \sim 10^{20}\,\mathrm{cm}^{-3}$, when all three d-bands are occupied, whereas the data in Fig. **??** corresponds to much lower doping ($4\times10^{17}\,\mathrm{cm}^{-3}$), when only the lowest band is occupied. As will see in the next section, a FL-like T^2 term is expected in a disordered multi-band system.

Second, the two-phonon mechanism predicts that the energy relaxation rate is independent of T. Indeed, substituting $\tau_{\mathrm{sp}} \propto 1/T^2$ into (1.59), we obtain $\tau_\varepsilon = \mathrm{const}$. Instead, recent experiment observed that $1/\tau_\varepsilon$ increases with T [62]. Again, the experiment was performed on highly-doped samples, where the two-phonon model is not applicable. Indeed, the Bloch-Grueneisen

temperature for scattering at a dispersive optical phonon is $T_{BG} = \omega_0(q = 2k_F)$, which for STO translates into $T_{BG} = \sqrt{\omega_0^2(q=0) + (2k_F)^2 s^2}$, where $s \approx 6.6 \times 10^5$ cm/s from neutron scattering. At $n \sim 10^{20}\,\mathrm{cm}^{-3}$, $T_{BG} \sim 250\,\mathrm{K}$ which means that the data in [62] was collected in the inelastic regime. It would be fair to say the two experiments described above neither confirmed no ruled out the two-phonon mechanism, and thus a T^2 behavior in STO still remains somewhat mysterious.

As we have just seen, STO is a rather exotic material. What about something simpler, such is a plain vanilla doped semiconductor? Figure 22 shows the resistivity of just that: a doped semiconductor Bi_2O_2Se [63]. There is nothing exotic about this material, in particular, it does not have soft optical modes. Nevertheless, it does exhibit $\rho \propto T^2$ also over a wide temperature range. However, the Fermi energy in Bi_2O_2Se is much higher than in STO, and T^2 scaling does not extend into a non-degenerate range.

One more recent addition to the family of strange liquids is illustrated in Fig. 23: it's a two-dimensional electron gas (2DEG) in HgTe quantum well [64]. Again, no umklapps, no compensation, yet a T^2 behavior is still pronounced.

Finally, Fig. 24 shows unpublished data from Denis Bandurin's group at the National University of Singapore on TBG away from the magic angle [56]. Here, the story is more complicated, because, as discussed in Sec. III C 2, TBG can be gated into the regime, where umklapps are allowed. Figure 25 shows the number-density dependence of the coefficient $A_{\rho 2}$ in the relation $\rho = A_{\rho 2} T^2$. The blue curve is obtained by subtracting the T^2 term arising from the impurity part of the resistivity at finite T. [12] The vertical lines indicate umklapp thresholds calculated by Joshua Covey using a realistic band structure model. It is clear that $A_{\rho 2}$ behaves differently above and below the threshold. Therefore, the T^2 behavior above the threshold can be attributed to inter-valley umklapp scattering. An additional confirmation of the e-e origin of the T^2 term is the data obtained under THz radiation, while the lattice was kept at the lowest temperature. As shown in panel B, THz radiation increase the resistivity. Given THz is absorbed mostly by electrons, it means that in a situation when $T_e \neq T_L$, the resistivity follows the electron rather than lattice temperature. This rules out phonons as the source of the T-dependence.

However, there is also a range of densities below the umklapp threshold, where $\rho \propto T^2$, although umklapps are not allowed. Along with STO, Bi_2O_2Se, and HgTe, this range belongs to the category of strange Fermi liquids.

[12] For elastic scattering, the conductivity at finite T is related to that at finite energy of an electron via $\sigma_i(T) = \int d\varepsilon(-f_0')\sigma_i(\varepsilon)$. On its turn, $\sigma_i(\varepsilon)$ is obtained from the residual resistivity as a function of n as $\sigma_i(\varepsilon_F) = 1/\rho_i(\varepsilon_F(n))$ with $\varepsilon_F(n)$ calculated from a band structure model.

E. Non-Galilean–invariant Fermi liquids with disorder

1. *Generic case*

There is one more aspect of the story that we have discussed yet: what happens if one takes disorder, which is always present in real materials. Naively speaking, can one have a situation when the corresponding scattering rates just add up, such that

$$\rho \propto \frac{1}{\tau_{\rm imp}} + \frac{1}{\tau_{\rm ee}} = \text{const} + AT^2 \, ? \tag{3.38}$$

The answer is yes and no. Yes, in a sense that if the system is non-Galilean–invariant, e-e interaction can add a T-dependent *correction* to the resistivity, which scales, generically, T^2, but can be reduced down to T^4. No, in a sense that (3.38) works only at low enough T, when as $1/\tau_{\rm ee} \ll 1/\tau_{\rm imp}$. For $1/\tau_{\rm ee} \gg 1/\tau_{\rm imp}$, the resistivity saturates–in the absence of phonons–at another T-independent value, which is controlled only by disorder and which may or may not coincide with the residual resistivity.

Now let's go back to (3.29), put $\Omega = 0$, but add the e-i collision integral instead. As we have shown that the RTA form is good enough for weak and uniform electric fields, I choose the simplest form, applicable for point-like impurities

$$I_{ei} = \frac{f_{\mathbf{k}0} - f_{\mathbf{k}}}{\tau_{\rm imp}} = -\frac{f_{0\mathbf{k}}(1 - f_{0\mathbf{k}})g_{\mathbf{k}}}{\tau_{\rm imp}} \tag{3.39}$$

Instead of (3.30) we then obtain

$$\frac{g_{\mathbf{k}}}{\tau_{\rm imp}} - \frac{e}{T}(\mathbf{v}_{\mathbf{k}} \cdot \mathbf{E}) = \int_{\mathbf{k}'\mathbf{p}\mathbf{p}'} W_{\mathbf{k},\mathbf{p}\to\mathbf{k}'\mathbf{p}'} \left(g_{\mathbf{k}} + g_{\mathbf{p}} - g_{\mathbf{k}'} - g_{\mathbf{p}'}\right) \frac{1 - f_{0\mathbf{k}'}}{1 - f_{0\mathbf{k}}} f_{0\mathbf{p}} \left(1 - f_{0\mathbf{p}'}\right)$$
$$\times \delta\left(\mathbf{k} + \mathbf{p} - \mathbf{k}' - \mathbf{p}'\right) \delta\left(\varepsilon_{\mathbf{k}} + \varepsilon_{\mathbf{p}} - \varepsilon_{\mathbf{k}'} - \varepsilon_{\mathbf{p}'}\right). \tag{3.40}$$

As for the optical conductivity, we can iterate in I_{ee} if $1/\tau_{\rm ee} \ll 1/\tau_{\rm imp}$. The zeroth and first order iterations are given by

$$g^{(0)}_{\mathbf{k}} = \tau_{\rm imp} \frac{e(\mathbf{v}_{\mathbf{k}} \cdot \mathbf{E})}{T} \tag{3.41}$$

and

$$g^{(1)}_{\mathbf{k}} = \frac{e\tau^2_{\rm imp}}{T} \int_{\mathbf{k}'\mathbf{p}\mathbf{p}'} W_{\mathbf{k},\mathbf{p}\to\mathbf{k}'\mathbf{p}'} \left(\mathbf{v}_{\mathbf{k}} + \mathbf{v}_{\mathbf{p}} - \mathbf{v}_{\mathbf{k}'} - \mathbf{v}_{\mathbf{p}'}\right) \cdot \mathbf{E}_0 \frac{1 - f_{0\mathbf{k}'}}{1 - f_{0\mathbf{k}}} f_{0\mathbf{p}} \left(1 - f_{0\mathbf{p}'}\right)$$
$$\times \delta\left(\mathbf{k} + \mathbf{p} - \mathbf{k}' - \mathbf{p}'\right) \delta\left(\varepsilon_{\mathbf{k}} + \varepsilon_{\mathbf{p}} - \varepsilon_{\mathbf{k}'} - \varepsilon_{\mathbf{p}'}\right). \tag{3.42}$$

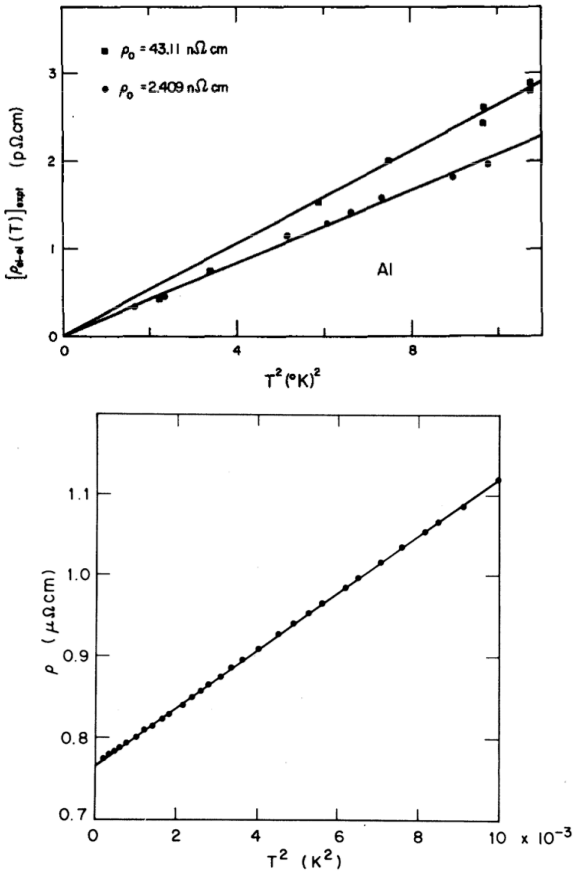

FIG. 3. Electrical resistivity of $CeAl_3$ below 100 mK, plotted against T^2.

FIG. 18. Top: Resistivity of Al. Reproduced from Ref. [65]. Bottom: Resistivity of a heavy fermion metal $CeAl_3$ below 0.1 K. Reproduced from Ref. [66].

Substituting the last result into the current, we obtain the correction to the $\sigma_{\alpha\beta}$ component of the conductivity

$$\delta\sigma_{\alpha\beta} = -\frac{2e^2\tau_{\rm imp}^2}{T}\int_{\mathbf{k},\mathbf{p},\mathbf{k}',\mathbf{p}'} W_{\mathbf{k},\mathbf{p}\to\mathbf{k}',\mathbf{p}'} f_{0\mathbf{k}} f_{0\mathbf{p}}(1-f_{0\mathbf{k}'})(1-f_{0\mathbf{p}'}) \times v_{\mathbf{k},\alpha}\left(v_{\mathbf{k},\beta}+v_{\mathbf{p},\beta}-v_{\mathbf{k}',\beta}-v_{\mathbf{p}',\beta}\right)\delta\left(\mathbf{k}+\mathbf{p}-\mathbf{k}'-\mathbf{p}'\right)\delta\left(\varepsilon_{\mathbf{k}}+\varepsilon_{\mathbf{p}}-\varepsilon_{\mathbf{k}'}-\varepsilon_{\mathbf{p}'}\right). \quad (3.43)$$

In the presence of time-reversal and inversion symmetries, the scattering kernel is symmetric with respect two permutations of the fermionic momenta. Using these symmetries, one can re-write the

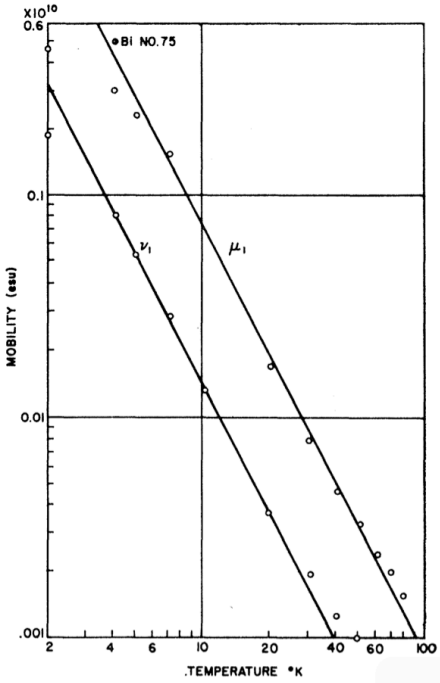

FIG. 3. Temperature variation of electron and hole mobilities for the higher conductivity sample at its greatest thickness.

FIG. 19. Mobilities of electrons (μ_1) and holes (ν_1) in a compensated semi-metal Bi. The straight lines indicate T^{-2} fits. Reproduced from Ref. [67].

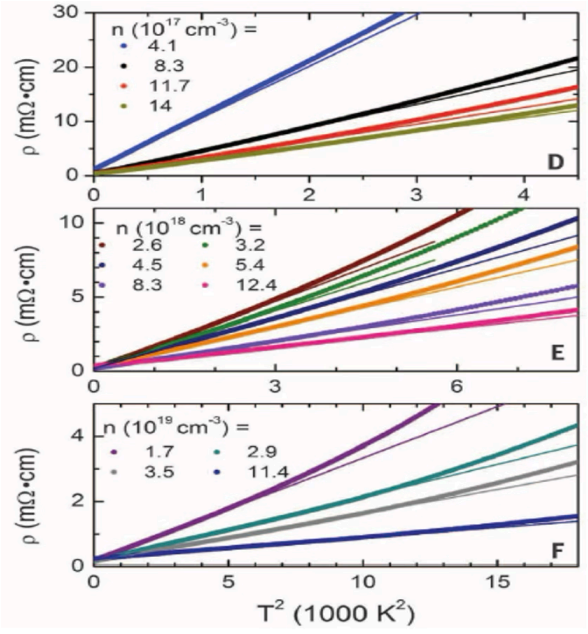

FIG. 20. Resistivity of a doped quantum paraelectric $SrTiO_3$. Reproduced from Ref. [59].

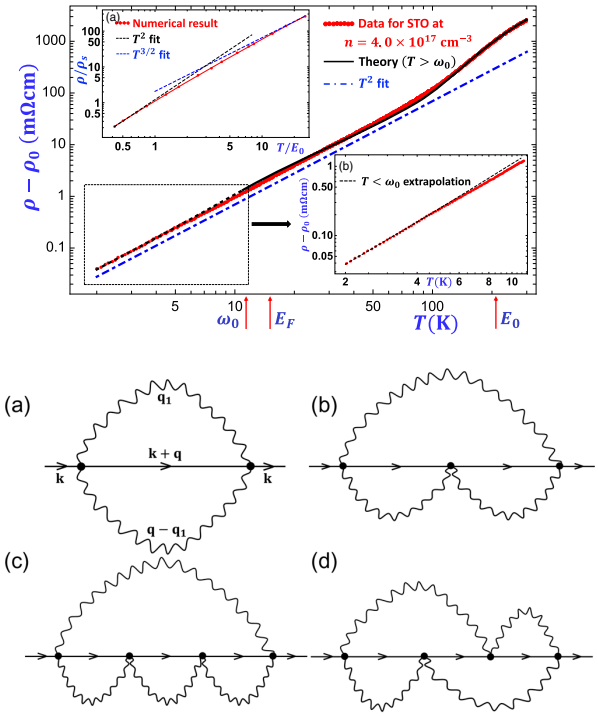

FIG. 21. Top panel.Red curve: resistivity of STO at $n = 4.0 \times 10^{17}$ cm^{-3}. Black curve: two-phonon model with an additional contribution due to scattering by LO phonons. Bottom: two-phonon diagrams for the electron self-energy. Reproduced from [60].

last equation in a more symmetric form [5, 57, 68]

$$\delta\sigma_{\alpha\beta} = -\frac{e^2\tau_{\rm imp}^2}{2T}\int_{\mathbf{k},\mathbf{p},\mathbf{k}',\mathbf{p}'} W_{\mathbf{k},\mathbf{p}\to\mathbf{k}',\mathbf{p}'} f_{0\mathbf{k}} f_{0\mathbf{p}}(1-f_{0\mathbf{k}'})(1-f_{0\mathbf{p}'}) \times \left(v_{\mathbf{k},\alpha} + v_{\mathbf{p},\alpha} - v_{\mathbf{k}',\alpha} - v_{\mathbf{p}',\alpha}\right)\left(v_{\mathbf{k},\beta} + v_{\mathbf{p},\beta} - v_{\mathbf{k}',\beta} - v_{\mathbf{p}',\beta}\right) \times\delta\left(\mathbf{k}+\mathbf{p}-\mathbf{k}'-\mathbf{p}'\right)\delta\left(\varepsilon_{\mathbf{k}}+\varepsilon_{\mathbf{p}}-\varepsilon_{\mathbf{k}'}-\varepsilon_{\mathbf{p}'}\right). \tag{3.44}$$

Let's power-count the last result. The integrals over three independent energies, e.g., $\varepsilon_{\mathbf{k}}$, $\varepsilon_{\mathbf{p}}$, and $\varepsilon_{\mathbf{k}'}$, give a factor of T^3.[13] With an additional $1/T$ factor, we obtain $\delta\sigma_{\alpha\beta} \propto T^2$. The corresponding correction to the conductivity can be written as,

$$\delta\sigma = -\sigma_{\rm imp}\frac{\tau_{\rm imp}}{\tau_j} \tag{3.45}$$

where $1/\tau_j \propto T^2$. Accordingly

$$\rho = \frac{1}{\sigma_{\rm imp} - \sigma_{\rm imp}(\tau_{\rm imp}/\tau_j)} \approx \rho_{\rm imp}\left(1+\frac{\tau_{\rm imp}}{\tau_j}\right) = \rho_{\rm imp} + \frac{d}{e^2 v_F^2 \nu_F}\frac{1}{\tau_j}. \tag{3.46}$$

[13] This is true for a generic case. Additional cancellations, arising in special cases, are discussed in Sec. III E 2.

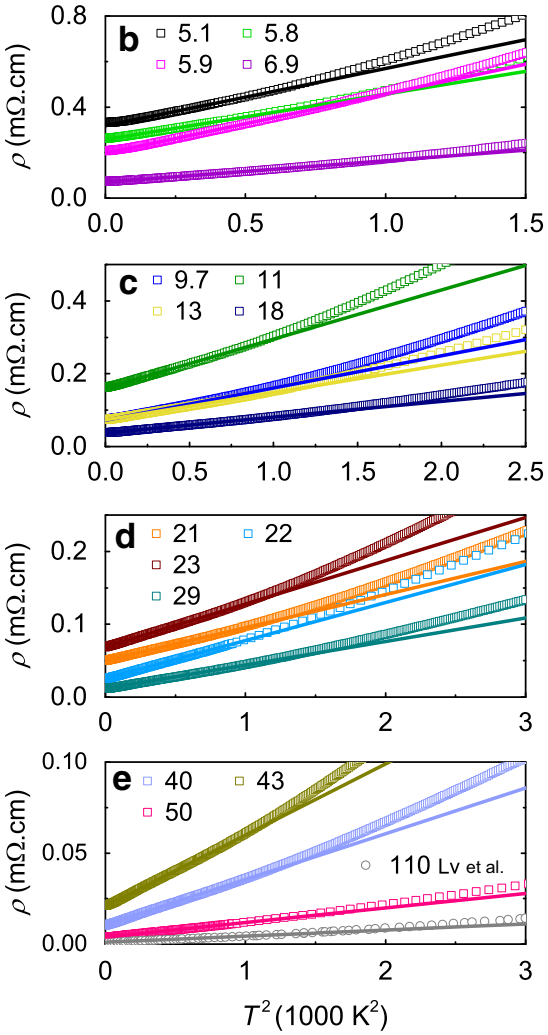

FIG. 22. Resistivity of a doped "trivial" semiconductor Bi_2O_2Se. Reproduced from Ref. [63].

Note that the last result does look like the Matthiessen rule: the e-i and e-e resistivities add up.

However, this is only the first term in the expansion in $\tau_{\rm imp}/\tau_j$. What happens in the opposite limit, when $1\tau_j \gg 1/\tau_{\rm imp}$? In this regime, e-e collisions are much more frequent than e-i ones. Consequently, e-e collision establish quasi equilibrium in the electronic system, however, they cannot fix the center-of-mass velocity. In the isotropic case, the result is especially simple. The distribution function is a Fermi function of a system moving as a whole with velocity $\mathbf{u}$:

$$f_{\mathbf{k}} = f_0(\varepsilon_{\mathbf{k}} + \mathbf{u}\cdot\mathbf{k}), \tag{3.47}$$

where $\mathbf{u}$ is independent of $\mathbf{k}$. This function nullifies the e-e collision integral due the identity

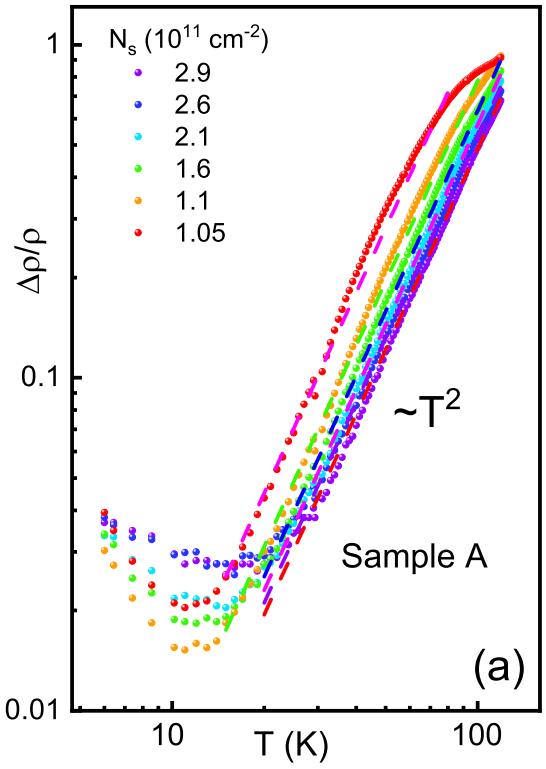

FIG. 23. Resistivity of a 2DEG in HgTe quantum well. Reproduced from Ref. [64].

known as "detailed balance",

$$f_{0\mathbf{k}} f_{0\mathbf{p}} (1 - f_{0\mathbf{k}'})(1 - f_{0\mathbf{p}'}) = f_{0\mathbf{k}'} f_{0\mathbf{p}'} (1 - f_{0\mathbf{k}})(1 - f_{0\mathbf{p}}), \tag{3.48}$$

which is valid if $\mathbf{k} + \mathbf{p} = \mathbf{k}' + \mathbf{p}'$. In equilibrium, i.e., for $\mathbf{u} = 0$, (3.48) works because $\varepsilon_{\mathbf{k}} + \varepsilon_{\mathbf{p}} = \varepsilon_{\mathbf{k}'} + \varepsilon_{\mathbf{p}'}$. However, it works also for $\mathbf{u} \neq 0$ due to momentum conservation $\mathbf{k} + \mathbf{p} = \mathbf{k}' + \mathbf{p}'$. Expanding (3.47) to linear order in $\mathbf{u}$, we obtain

$$f_{\mathbf{k}} = f_{0\mathbf{k}} + f'_{0\mathbf{k}} (\mathbf{u} \cdot \mathbf{k}), \tag{3.49}$$

which, according to (3.16), means that $g_{\mathbf{k}} = -\mathbf{u} \cdot \mathbf{k}/T$. On substituting $g_{\mathbf{k}}$ into (3.40), the RHS vanishes, and we obtain an equation for $\mathbf{u}$ [69]:

$$\mathbf{u} \cdot \mathbf{k} = -e(\mathbf{v}_{\mathbf{k}} \cdot \mathbf{E})\tau_{\text{imp}}. \tag{3.50}$$

This means that $\mathbf{u}$ is determined entirely by disorder, as if e-e interaction were absent, and the corresponding conductivity is the same as $T = 0$.

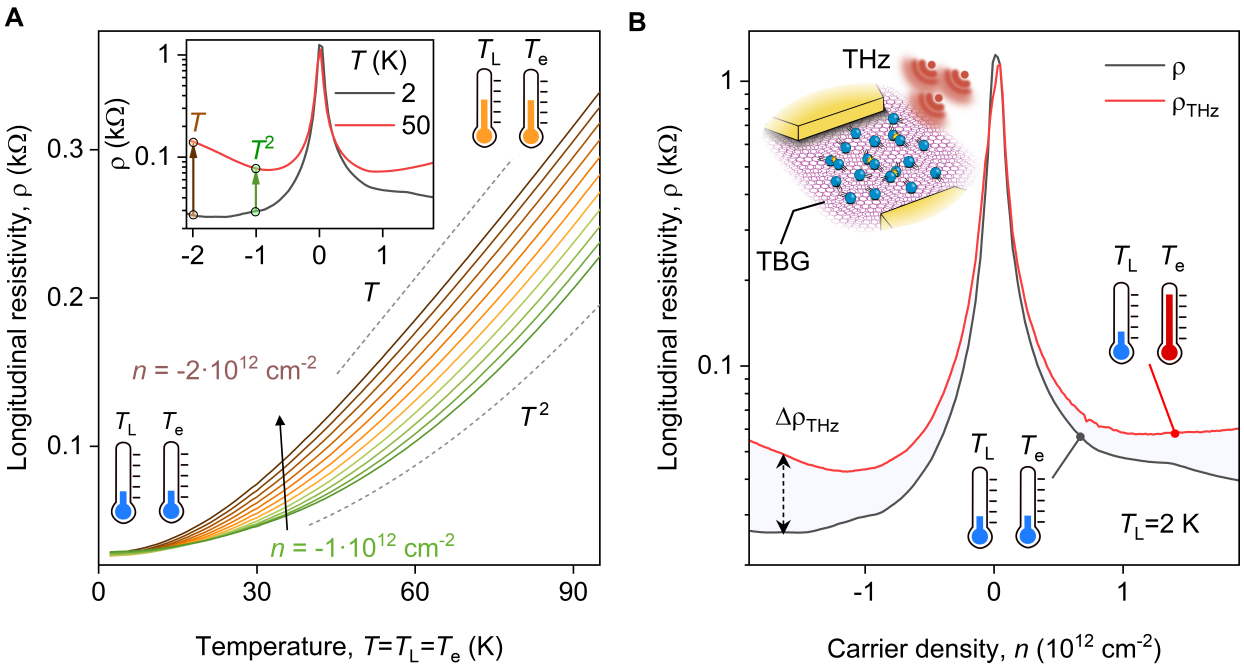

FIG. 24. **Resistivity of twisted bilayer graphene.** (**A**) Longitudinal resistivity ρ of 2° TBG as a function of temperature and carrier density n. Inset: $\rho(n)$ at representative temperatures. Arrows indicate scaling regimes with $\rho \sim T^{\alpha}$, where $\alpha = 1$ (orange) and $\alpha = 2$ (green). Thermometers indicate that both electron and lattice temperatures are varied simultaneously. (**B**) $\rho(n)$ measured in the dark and under continuous-wave illumination at 0.14 THz. Inset: schematic showing THz-driven electron heating. Thermometers indicate that THz radiation increases the electron temperature while the lattice remains intact. Reproduced from Ref. [56]

.

To summarize, ρ initially increases with T until τ_j becomes comparable to $\tau_{\rm imp}$, but then decreases back to its residual value.

For anisotropic dispersion, the analysis is more complicated. Nevertheless, using the spectral decomposition of the (non-self-adjoint) operator I_{ee}, one can show that the conductivity saturates at higher T at a value which is controlled solely by disorder [68]. The high-T limit if the conductivity is given by

$$\sigma_{\alpha\beta}|_{T\to\infty} = 2e^2\tau_{\rm imp}\nu_F \sum_{\gamma} \frac{\langle v_\alpha k_\gamma\rangle}{\langle k_\gamma^2\rangle}\langle k_\gamma v_\beta\rangle, \tag{3.51}$$

where $\langle \dots \rangle$ stands for averaging over the Fermi surface. For comparison, the residual conductivity

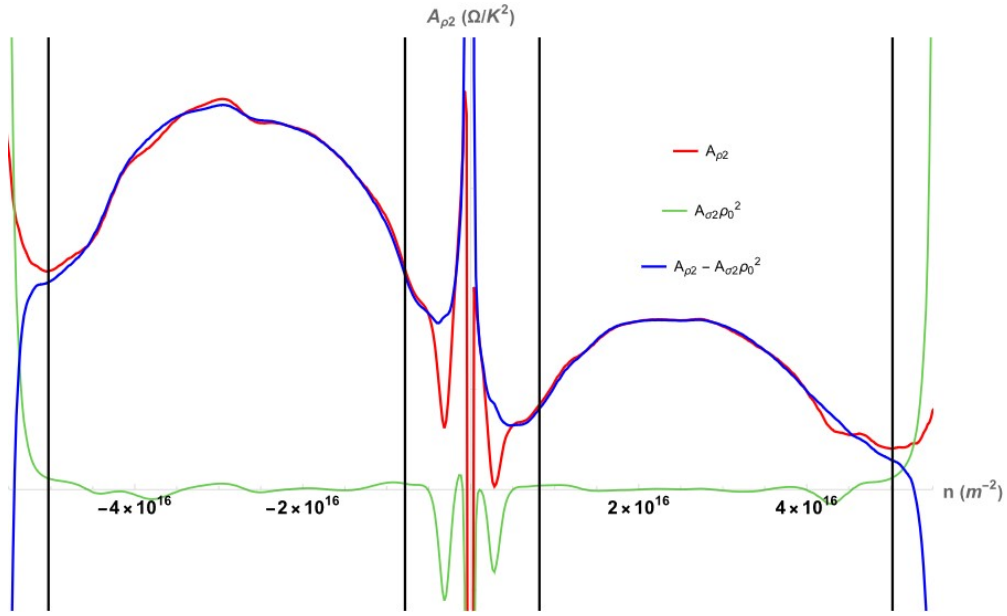

FIG. 25. Number-density dependence of the coefficient $A_{\rho 2}$ obtained by fitting the T^2 part of the resistivity into $\rho = A_{\rho 2}T^2$. Positive/negative n corresponds to electron/hole doping. Red: raw data. Blue: data after subtracting the T^2 contribution to the residual resistivity due to smearing of the Fermi function of at finite T. The vertical lines indicate umklapp thresholds, calculated using the realistic band structure model. Reproduced from [56].

at $T = 0$ is given by

$$\sigma_{\alpha\beta}|_{T\to 0} = 2e^2\tau_{\rm imp}\nu_F\langle v_\alpha v_\beta\rangle. \tag{3.52}$$

It is easy to check that, for an isotropic dispersion, $\sigma_{\alpha\beta}|_{T\to\infty} = \sigma_{\alpha\beta}|_{T\to 0}$.

The temperature dependence of the resistivity is sketched in Fig. 26. The work on exact solution of the Boltzmann equation for the isotropic case is currently in progress [70].

2. *Special cases*

There is a number of special cases when, instead of an expected T^2 correction to the residual resistivity, one obtains $T^4 \ln T$ (in 2D) or T^4 in 3D. These special cases are 1) isotropic (but non-parabolic) electron spectrum, both in 2D and 3D, and 2) a convex Fermi surface in 2D.

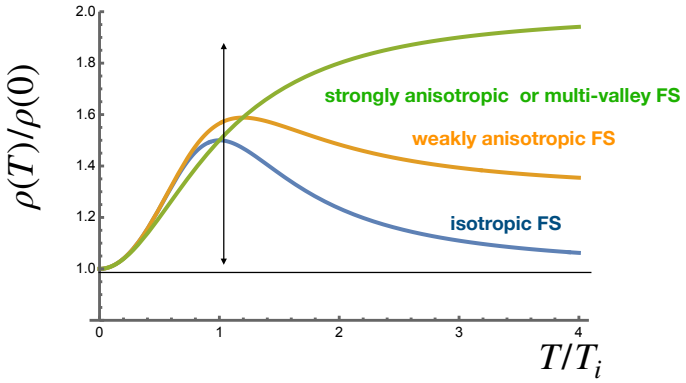

FIG. 26. Temperature dependence of the resistivity of a non-Galilean–invariant Fermi liquid with disorder. The currently available theory describes the initial increase of the resistance and its saturation at higher T. The full curves needs to be understood as a sketch.

a. Isotropic Fermi liquid. In an isotropic case, there are only diagonal components of the conductivity, which are equal to each other. with $\delta\sigma = (1/d)\sum_\alpha \delta\sigma_{\alpha\alpha}$, Eq. (3.44) becomes

$$\delta\sigma = -\frac{e^2\tau_{\rm imp}^2}{2dT}\int_{\mathbf{k},\mathbf{p},\mathbf{k}',\mathbf{p}'} W_{\mathbf{k},\mathbf{p}\to\mathbf{k}',\mathbf{p}'} f_{0\mathbf{k}} f_{0\mathbf{p}}(1-f_{0\mathbf{k}'})(1-f_{0\mathbf{p}'}) \times \left(\mathbf{v}_\mathbf{k}+\mathbf{v}_\mathbf{p}-\mathbf{v}_{\mathbf{k}'}-\mathbf{v}_{\mathbf{p}'}\right)^2 \delta\left(\mathbf{k}+\mathbf{p}-\mathbf{k}'-\mathbf{p}'\right)\delta\left(\varepsilon_\mathbf{k}+\varepsilon_\mathbf{p}-\varepsilon_{\mathbf{k}'}-\varepsilon_{\mathbf{p}'}\right).. \tag{3.53}$$

If the electron dispersion is isotropic, $\varepsilon_\mathbf{k} = \varepsilon(k)$,

$$\mathbf{v}_\mathbf{k} = \partial_\mathbf{k}\varepsilon_\mathbf{k} = \frac{\mathbf{k}}{m(k)}, \tag{3.54}$$

where $m(k) = k/\varepsilon'(k)$. If all four fermions are projected onto the Fermi surface, i..e, $k = p = k' = p' = k_F$, their masses become the same and

$$\left(\mathbf{v}_\mathbf{k}+\mathbf{v}_\mathbf{p}-\mathbf{v}_{\mathbf{k}'}-\mathbf{v}_{\mathbf{p}'}\right)^2 = \frac{1}{m^2(k_F)}\left(\mathbf{k}+\mathbf{p}-\mathbf{k}'-\mathbf{p}'\right)^2 = 0 \tag{3.55}$$

by momentum conservation. To get a final result, one needs to expand the dispersions near the Fermi surface. In 3D, this gives an additional factor of T^2, and $\delta\sigma \propto T^4$. In 2D, there is an extra log factor, arising from the 2D kinematic singularity: $\delta\sigma \propto T^4 \ln T$ [71]. The T^4 correction is likely to be masked either by eph scattering or by weak localization. For example, in a monolayer graphene $1/\tau_{\rm eph} \propto T^4$ for $T \ll T_{BG}$, see Fig. 10. Restoring the units and setting the eph coupling constant to 1, $1/\tau_{\rm eph} \sim T^4/T_{BG}^3$. On the hand, the ee momentum relaxation rate can be written as

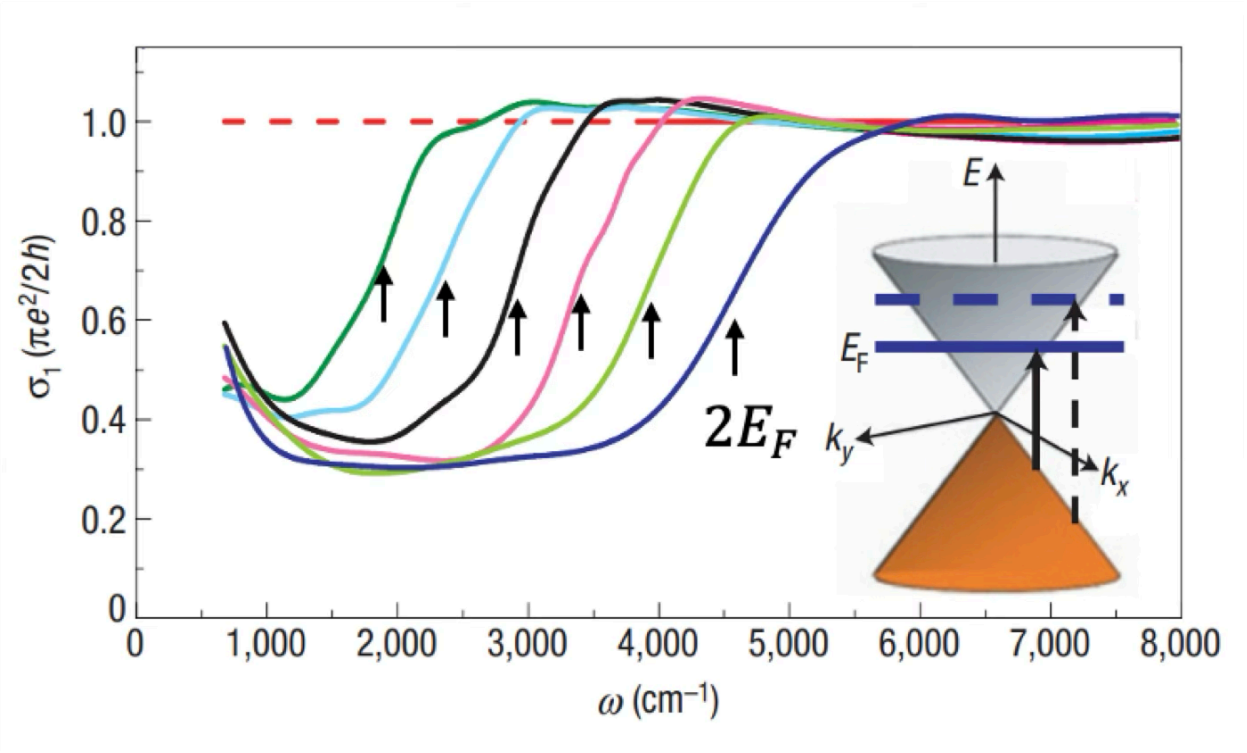

FIG. 27. The real part of the optical conductivity of monolayer graphene for different gate voltages. The vertical arrows indicate the Pauli threshold in the non-interacting system, equal to $2\varepsilon_F$. Reproduced from Ref. [73]

$1/\tau_j \sim (T^4/\varepsilon_F^3)\ln(\Lambda/T)$, where Λ is a UV cutoff, which depends on the details of the ee interaction. As long as the speed of sound is much smaller than v_F, we have $T_{BG} \ll \varepsilon_F$, and thus $1/\tau_{\rm eph} \ll 1/\tau_j$.

On the other hand, the ee contribution wins over the eph one in the optical conductivity, measured at $\Omega \gg T$ [71, 72]. In this case, the scaling $1/\tau_j \propto \Omega^4 \ln(\Lambda/\Omega)$ (in 2D) continues up to $\Omega \sim \Lambda$, whereas the eph one saturates at a frequency-independent value for $\Omega \gg T_{BG}$. The corresponding real part of the optical conductivity behaves as $\mathrm{Re}\sigma(\Omega) \propto 1/\Omega^2\tau_j \propto \Omega^2 \ln(\Lambda/\Omega)$. Figure 27 shows the real part of the optical conductivity of monolayer graphene at different gate voltages (the number density increases from the green to dark-blue curve). The vertical arrows indicate the Pauli threshold in a non-interacting graphene, equal to $2\varepsilon_F$. In the absence of any interactions, the optical conductivity would be strictly zero for $\Omega < 2\varepsilon_F$ and attain a universal value of $\pi e^2/2h$ for $\Omega > 2\varepsilon_F$ (shown by the horizontal dotted line). In reality, there is a substantial spectral weight below $2\varepsilon_F$. Part of this weight is just a Drude tail, arising from ei and eph scatterings. However, when the Drude tail becomes small, the conductivity starts to increase, presumably due to ee in-

teractions, as explained above. A detailed theory of absorption in this range, which includes not only the electron-electron but also the electron-hole interactions can be found in Ref. [72].

IV. HOMEWORK PROBLEMS FOR SECTION III

1. Derive Eq. (3.13).

2. Derive Eq. (3.17). *Hint*: when linearizing the collision integral, take an advantage of the following identity

$$f_{0\mathbf{k}} f_{0\mathbf{p}} (1 - f_{0\mathbf{k}'})(1 - f_{0\mathbf{p}'}) = f_{0\mathbf{k}'} f_{0\mathbf{p}'} (1 - f_{0\mathbf{k}})(1 - f_{0\mathbf{p}}).$$

3. Consider two spherical pockets, containing equal numbers of electrons and holes with parabolic spectra $\varepsilon_\pm = k^2/2m_\pm$. The pockets are assumed to be sufficiently far away from each other to neglect inter-pocket transfer. Electron-electron and hole-hole interactions drop out from the equations of motion, but electron-hole interaction remains. In addition, electrons and holes are scattered by impurities with mean free times $\tau_\pm$. Phenomenologically, *dc* transport in such a system can be described by coupled equations of motion

$$0 = -eE - \frac{m_+ v_+}{\tau_+} - \mathcal{N}\gamma(v_+ - v_-)$$
$$0 = +eE - \frac{m_- v_-}{\tau_-} - \mathcal{N}\gamma(v_- - v_+).$$

   The last terms in these equations describe electron-hole interactions as frictional forces, parametrized by the coefficient γ. In a Fermi liquid, $\gamma \propto T^2$. Find the *dc* conductivity and show that it remains finite in the limit $\tau_\pm \to \infty$.

Appendix A: Green's function of the Boltzmann equation

The Green's function of the Boltzmann equation for elastic scattering by point-like impurities with collision integral given by (1.7) satisfies the following equation

$$\left[\frac{\partial}{\partial t} + \mathbf{v}_\mathbf{k} \cdot \vec{\nabla}_\mathbf{r} + \frac{1}{\tau}\right] \mathcal{G}(\mathbf{k}, \mathbf{r}, t|\mathbf{k}', \mathbf{r}', t') - \frac{1}{\tau}\bar{\mathcal{G}}(k, \mathbf{r}, t|\mathbf{k}', \mathbf{r}', t) = \delta(\mathbf{k} - \mathbf{k}')\delta(\mathbf{r} - \mathbf{r}')\delta(t - t'), \quad \text{(A1)}$$

where $\bar{\mathcal{G}}(\mathbf{k}, \mathbf{r}, t|k, \mathbf{r}', t') = \int_{\hat{k}} \mathcal{G}(\mathbf{k}, \mathbf{r}, t|\mathbf{k}, \mathbf{r}', t')$ is the Green's function averaged over the directions of $\mathbf{k}'$. In a translational- and time-reversal-invariant system, $\mathcal{G}(\mathbf{k}, \mathbf{r}, t|\mathbf{k}', \mathbf{r}', t') = \mathcal{G}(\mathbf{r} - \mathbf{r}', t - t'; \mathbf{k}, \mathbf{k}')$.

Switching to the Fourier space via

$$\mathcal{G}(\mathbf{q},\omega;\mathbf{k},\mathbf{k}') = \int d^d r \int dt e^{i(\omega t-\mathbf{q}\cdot\mathbf{r})}\mathcal{G}(\mathbf{r},t;\mathbf{k},\mathbf{k}'), \tag{A2}$$

we obtain

$$i(\mathbf{q}\cdot\mathbf{v}-\omega)\mathcal{G}(\mathbf{q},\omega;\mathbf{k},\mathbf{k}') + \frac{1}{\tau}\left[\mathcal{G}(\mathbf{q},\omega;\mathbf{k},\mathbf{k}' - \bar{\mathcal{G}}(\mathbf{q},\omega;k,\mathbf{k}')\right] = \delta(\mathbf{k}-\mathbf{k}'). \tag{A3}$$

First, we solve Eq. (A3) at fixed $\bar{\mathcal{G}}$ to obtain

$$\mathcal{G}(\mathbf{q},\omega;\mathbf{k},\mathbf{k}') = \frac{\tau(\varepsilon)\delta(\mathbf{k}-\mathbf{k}') + \bar{\mathcal{G}}(\mathbf{q},\omega;k,\mathbf{k}')}{i\tau(\varepsilon)(\mathbf{v}\cdot\mathbf{q}-\omega)+1}, \tag{A4}$$

and then average Eq. (A4) over the directions of $\mathbf{k}$ to exclude $\bar{\mathcal{G}}$. This way, we arrive at

$$\mathcal{G}(\mathbf{q},\omega;\mathbf{k},\mathbf{k}') = \mathcal{G}_1(\mathbf{q},\omega;\mathbf{k},\mathbf{k}') + \mathcal{G}_2(\mathbf{q},\omega;\mathbf{k},\mathbf{k}') \tag{A5a}$$

$$\mathcal{G}_1(\mathbf{q},\omega;\mathbf{k},\mathbf{k}') = \frac{\tau(\varepsilon)\delta(\mathbf{k}-\mathbf{k}')}{1+i\tau(\varepsilon)(\mathbf{v}\cdot\mathbf{q}-\omega)} \tag{A5b}$$

$$\mathcal{G}_2(\mathbf{q},\omega;\mathbf{k},\mathbf{k}') = \frac{\tau(\varepsilon)\delta(\varepsilon-\varepsilon')}{(2\pi)^d\nu(\varepsilon)}\frac{1}{[1+i\tau(\varepsilon)(\mathbf{v}\cdot\mathbf{q}-\omega)]\,[1+i\tau(\varepsilon)(\mathbf{v}'\cdot\mathbf{q}-\omega)]}\mathcal{D}_d(\varepsilon;q,\omega), \tag{A5c}$$

where

$$\mathcal{D}_d(\varepsilon;q,\omega) = \frac{1}{1-\left\langle\frac{1}{1+i\tau(\varepsilon)(\mathbf{v}\cdot\mathbf{q}-\omega)}\right\rangle_{\hat{k}}} \tag{A6}$$

with $\langle\ldots\rangle_{\hat{k}}$ standing for averaging over the directions of $\mathbf{k}$.

The first term in Eq. (A5a) describes fast, over time τ, relaxation of the initial perturbation. This would have been the only term, had we use used the RTA collision integral from Eq. (1.8).The second term describes slow relaxation due to diffusion, which sets for $qv_F\tau \ll 1$ and $\omega\tau \ll 1$. In this regime, function $\mathcal{D}_d$ displays a diffusion pole:

$$\mathcal{D}_d(\varepsilon;q,\omega) = \frac{1}{\tau(\varepsilon)\left[D(\varepsilon)q^2 - i\omega\right]}, \tag{A7}$$

where $D(\varepsilon) = v^2(\varepsilon)\tau(\varepsilon)/d$ is the diffusion coefficient of an electron with energy ε. Note that for short-range disorder $v(\varepsilon)_{\mathbf{k}}\tau(\varepsilon) = v_{\mathrm{F}}\tau$ with $\tau \equiv \tau(\varepsilon_F)$.

Appendix B: Diffuson ladder

A dotted line in Fig. 13(h) can be related to $1/\tau_s$ by calculating the imaginary part of the self-energy. To lowest order, we need to consider only the first diagram in Fig. 5 (with the dashed line

replaced with the dotted one). The dotted line is the Fourier transform of the correlation function $u_0\delta(\mathbf{r}-\mathbf{r}')$, which just equals u_0. Then

$$\mathrm{Im}\Sigma^R(\omega=0,\mathbf{k}) = u_0^2\int_{\mathbf{k}'}\mathrm{Im}G^R_{\mathbf{k}'}(0) = -\pi u_0^2\int_{\mathbf{k}'}\delta(\varepsilon_{\mathbf{k}'}) = -\pi u_0^2\nu_F. \tag{B1}$$

Comparing Eqs. (1.32) and (1.37), we see that $\mathrm{Im}\Sigma^R = -1/2\tau_{\mathrm{sp}}$ or, for delta-correlated disorder, $\mathrm{Im}\Sigma^R = -1/2\tau_s$. Therefore, $u_0 = 1/2\pi\nu_F\tau_s$. The $-f_0'(\omega) = \delta(\omega)$ factor projects the electrons onto the Fermi surface, which means that we need to the diffuson only at $\omega = 0$. The diffuson ladder is obtained be summing the geometric series

$$\Lambda^R(q,\Omega) = u_0 + u_0^2R(q,\Omega) + u_0^3R^3(q,\Omega) + \cdots = \frac{u_0}{1-u_0R(q,\Omega)}, \tag{B2}$$

where $R(q\,\omega)$ is the "rung "of the ladder,

$$\begin{aligned} R(q,\Omega) &= \nu_F\int\frac{dO_{\mathbf{p}}}{O_d}\int d\epsilon_{\mathbf{p}}G^R_{\mathbf{p}+\mathbf{q}}(\Omega)G^A_{\mathbf{p}}(0) = 2\pi\nu_F\int\frac{dO_{\mathbf{p}}}{O_d}\frac{i}{\Omega-\mathbf{v}_{\mathbf{p}}\cdot\mathbf{q}+i/\tau_s} \\ &= 2\pi\nu_F\begin{cases} i/\sqrt{(\Omega+i/\tau_s)^2-(v_Fq)^2}, & d=2 \\ (i/2v_Fq)\ln\frac{\Omega+v_Fq+i/\tau_s}{\Omega-v_Fq+i/\tau_s} & d=3 \end{cases} \end{aligned} \tag{B3}$$

For $d = 2$, the branch of the square roo function is defined by the condition $\mathrm{Im}\sqrt{(\Omega+i/\tau_s)^2-(v_Fq)^2} > 0$. We then obtain

$$\Lambda^R_q(0) = \frac{1}{2\pi N_F\tau_s}\frac{\sqrt{(q\ell_s)^2+1}}{\sqrt{(q\ell_s)^2+1}-1} = \frac{1}{2\pi N_F\tau_s}\mathcal{D}_2(q\ell_s), \tag{B4}$$

$$\Lambda^R(q,\Omega) = \frac{1}{2\pi N_F\tau_s}\frac{1}{1-\frac{i}{\sqrt{(\Omega\tau_s+i)^2-q^2\ell_s^2}}},\ d=2 \tag{B5}$$

and

$$\Lambda^R(q,\Omega) = \frac{1}{2\pi\nu_F\tau_s}\frac{1}{1-\frac{i}{2q\ell_s}\ln\frac{\Omega\tau_s+q\ell_s+i}{\Omega\tau_s-q\ell_s+i}},\ d=3, \tag{B6}$$

where $\ell_s = v_F\tau_s$.

$$\mathcal{D}_2(a) = \frac{\sqrt{a^2+1}}{\sqrt{a^2+1}-1}. \tag{B7}$$

For $|\Omega|\tau_s \ll 1$ and $q\ell_s \ll 1$, both (B5) and (B6) exhibit the diffusion pole

$$\Lambda^R(q,\Omega) = \frac{1}{2\pi\nu_F\tau_s^2}\frac{1}{D_sq^2-i\Omega}, \tag{B8}$$

where $D_s = v_F^2 \tau_s / d$. The static limits are given by

$$\Lambda^R(q,0) = \frac{1}{2\pi N_F \tau_s} \frac{\sqrt{(q\ell_s)^2+1}}{\sqrt{(q\ell_s)^2+1}-1}, \; d=2 \tag{B9}$$

and

$$\Lambda^R(q,0) = \frac{1}{2\pi N_F \tau_s} \frac{1}{1-\frac{\tan^{-1}(q\ell_s)}{q\ell_s}}, \; d=3. \tag{B10}$$

[1] W. Kohn and J. M. Luttinger, Quantum Theory of Electrical Transport Phenomena, Phys. Rev. **108**, 590 (1957).

[2] J. M. Luttinger and W. Kohn, Quantum Theory of Electrical Transport Phenomena. II, Phys. Rev. **109**, 1892 (1958).

[3] B. I. Sturman, Collision integral for elastic scattering of electrons and phonons, Sov. Phys.-Uspekhi **27**, 881 (1984).

[4] A. D. Mirlin and P. Wölfle, Composite fermions in the fractional quantum hall effect: Transport at finite wave vector, Phys. Rev. Lett. **78**, 3717 (1997).

[5] T. Kiliptari and D. L. Maslov, Magnetoconductivity due to electron-electron interactions in a non-Galilean–invariant Fermi liquid, Phys. Rev. B **112**, 045121 (2025).

[6] F. Evers, A. D. Mirlin, D. G. Polyakov, and P. Wölfle, Quasiclassical memory effects: anomalous transport properties of two-dimensional electrons and composite fermions subject to a long-range disorder, Phys. Usp. **44**, 27 (2001).

[7] D. L. Maslov, V. I. Yudson, and C. D. Batista, Resistive anomaly near a ferromagnetic phase transition: A classical memory effect, Phys. Rev. Lett. **135**, 036301 (2025).

[8] A. V. Andreev, S. A. Kivelson, and B. Spivak, Hydrodynamic Description of Transport in Strongly Correlated Electron Systems, Phys. Rev. Lett. **106**, 256804 (2011).

[9] L. D. Landau and E. M. Lifshitz, *Classical Mechanins , Course of Theoretical Physics, v. I* (Pergamon Press, New York).

[10] E. M. Lifshitz and L. P. Pitaevskii, *Physical Kinetics, Course of Theoretical Physics, v. X* (Butterworth-Heinemann, Burlington, 1981).

[11] D. I. Pikulin, C.-Y. Hou, and C. W. J. Beenakker, Nernst effect beyond the relaxation-time approximation, Phys. Rev. B **84**, 035133 (2011).

[12] A. A. Abrikosov, L. P. Gorkov, and I. E. Dzyaloshinski, *Methods of Quantum Field Theory in Statistical Physics* (Dover, New York, 1963).

[13] B. L. Altshuler and A. G. Aronov, Electron-Electron Interactions in Disordered Systems (North-Holland, Amsterdam, 1985) p. 1.

[14] Y. Imry, *Introduction to Mesoscopic Physics* (Oxford University Press, Oxford, 2002).

[15] S. M. Girvin and K. Yang, *Modern Condensed Matter Physics* (Cambridge University Press, 2019).

[16] M. Ernst and A. Weyland, Long time behaviour of the velocity auto-correlation function in a Lorentz gas, Phys.Lett. A **34**, 39 (1971).

[17] E. Hauge, in *Transport Phenomena*, edited by G. Kirczenow and J. Marro (Springer, Berlin, 1974) p. 337.

[18] J. Wilke, A. D. Mirlin, D. G. Polyakov, F. Evers, and P. Wölfle, Zero-frequency anomaly in quasiclassical ac transport: Memory effects in a two-dimensional metal with a long-range random potential or random magnetic field, Phys. Rev. B **61**, 13774 (2000).

[19] E. Baskin, L. Magarill, and M. Entin, Sov. Phys. JETP **48**, 365 (1978).

[20] M. M. Fogler, A. Y. Dobin, V. I. Perel, and B. I. Shklovskii, Suppression of chaotic dynamics and localization of two-dimensional electrons by a weak magnetic field, Phys. Rev. B **56**, 6823 (1997).

[21] N. Ashcroft and N. Mermin, *Solid State Physics* (Saunders College, Philadelphia, 1976).

[22] A. D. Mirlin, D. G. Polyakov, and P. Wölfle, Composite Fermions in a Long-Range Random Magnetic Field: Quantum Hall Effect versus Shubnikov–de Haas Oscillations, Phys. Rev. Lett. **80**, 2429 (1998).

[23] A. D. Mirlin, J. Wilke, F. Evers, D. G. Polyakov, and P. Wölfle, Strong magnetoresistance induced by long-range disorder, Phys. Rev. Lett. **83**, 2801 (1999).

[24] M. Kaganov, I. Lifshitz, and L. Tanatarov, Relaxation between electrons and the crystalline lattice, JETP **4**, 173 (1957).

[25] D. K. Efetov and P. Kim, Controlling electron-phonon interactions in graphene at ultrahigh carrier densities, Phys. Rev. Lett. **105**, 256805 (2010).

[26] B. L. Altshuler, A. G. Aronov, and D. E. Khmelnitsky, Effects of electron-electron collisions with small energy transfers on quantum localisation, J. Phys. C: Solid State Phys. **15**, 7367 (1982).

[27] P. B. Allen, Theory of thermal relaxation of electrons in metals, Phys. Rev. Lett. **59**, 1460 (1987).

[28] W. Gerlach, On the quantum theory of the spin of the electron, Phys. Z. **33**, 953 (1932).

[29] A. Fert and I. A. Campbell, Electrical resistivity of ferromagnetic nickel and iron based alloys, Journal of Physics F: Metal Physics **6**, 849 (1976).

[30] P. De Gennes and J. Friedel, Anomalies de résistivité dans certains métaux magníques, Journal of Physics and Chemistry of Solids **4**, 71 (1958).

[31] M. E. Fisher and J. S. Langer, Resistive anomalies at magnetic critical points, Phys. Rev. Lett. **20**, 665 (1968).

[32] M. E. Fisher and A. Aharony, Scaling function for critical scattering, Phys. Rev. Lett. **31**, 1238 (1973).

[33] F. J. Wegner, Correlation functions near the critical point, Journal of Physics A: Mathematical and General **8**, 710 (1975).

[34] J. Cardy, *Scaling and Renormalization in Statistical Physics* (Cambridge University Press, 1996).

[35] M. Campostrini, M. Hasenbusch, A. Pelissetto, P. Rossi, and E. Vicari, Critical exponents and equation of state of the three-dimensional Heisenberg universality class, Phys. Rev. B **65**, 144520 (2002).

[36] M. Campostrini, M. Hasenbusch, A. Pelissetto, P. Rossi, and E. Vicari, Critical behavior of the three-dimensional XY universality class, Phys. Rev. B **63**, 214503 (2001).

[37] F. Kos, D. Poland, D. Simmons-Duffin, and A. Vichi, Precision islands in the Ising and $O(N)$ models, Journal of High Energy Physics **2016**, 36 (2016).

[38] M. Reehorst, Rigorous bounds on irrelevant operators in the 3d Ising model CFT, Journal of High Energy Physics **2022**, 177 (2022).

[39] D. L. Maslov, V. I. Yudson, and C. D. Batista, Resistive anomaly near second-order phase transition: The stochastic Liouville equation approach.

[40] D. Ter-Haar, ed., *Collected Papers of L. D. Landau* (Oxford, Pergamon, 1965).

[41] P. Sharma, A. Principi, G. Vignale, and D. L. Maslov, Optical conductivity and damping of plasmons due to electron-electron interaction, Phys. Rev. B **109**, 045431 (2024).

[42] A. A. Abrikosov, *Fundamentals of the Theory of Metals* (Noth Holland, 1988).

[43] A. A. Abrikosov and I. M. Khalatnikov, The theory of a Fermi liquid (the properties of liquid 3 He at low temperatures), Rep. Prog. Phys. **22**, 329 (1959).

[44] H. H. Jensen, H. Smith, and J. Wilkins, Exact transport coefficients for a fermi liquid, Phys. Lett. A **27**, 532 (1968).

[45] G. A. Brooker and J. Sykes, Transport properties of a fermi liquid, Phys. Rev. Lett. **21**, 279 (1968).

[46] C. A. Kukkonen and P. F. Maldague, Electron-hole scattering and the electrical resistivity of the semimetal tis_2, Phys. Rev. Lett. **37**, 782 (1976).

[47] S. Li and D. L. Maslov, Lorentz ratio of a compensated metal, Phys. Rev. B **98**, 245134 (2018).

[48] W. G. Baber, The Contribution to the Electrical Resistance of Metals from Collisions between Electrons, Proc. Royal Soc. London A **158**, 383 (1937).

[49] A. B. Kashuba, Conductivity of defectless graphene, Phys. Rev. B **78**, 085415 (2008).

[50] M. Müller, L. Fritz, and S. Sachdev, Quantum-critical relativistic magnetotransport in graphene, Phys. Rev. B **78**, 115406 (2008).

[51] M. Müller, J. Schmalian, and L. Fritz, Graphene: A nearly perfect fluid, Phys. Rev. Lett. **103**, 025301 (2009).

[52] D. L. Maslov and A. V. Chubukov, Optical response of correlated electron systems, Rep. Prog. Phys. **80**, 026503 (2017).

[53] L. Landau and I. Y. Pomeranchuk, On the properties of metals at very low temperatures, Ph. Zs. Sowjet. **10**, 649 (1936).

[54] V. F. Gantmakher and Y. B. Levinson, *Carrier Scattering in Metals and Semiconductors* (North-Holland, Amsterdam, 1987).

[55] J. Covey and D. L. Maslov, Integrals of products of Bessel functions: a perspective from the physics of Bloch electrons, Physica Scripta **100**, 045229 (2025).

[56] A. Shilov, M. Kravtsov, J. Covey, M. Kashchenko, O. Popova, X. Zhou, I.Yahniuk, T. Taniguchi, K. Watanabe, K. Novoselov, S. Ganichev, D. Svintsov, A. Principi, D. Maslov, and D. Bandurin, Interaction-limited conductivity of twisted bilayer graphene revealed by giant terahertz photoresistance, (unpublished).

[57] D. L. Maslov, V. I. Yudson, and A. V. Chubukov, Resistivity of a Non-Galilean–Invariant Fermi Liquid near Pomeranchuk Quantum Criticality, Phys. Rev. Lett. **106**, 106403 (2011).

[58] P. A. Lee, Low-temperature T-linear resistivity due to umklapp scattering from a critical mode, Phys. Rev. B **104**, 035140 (2021).

[59] X. Lin, B. Fauqué, and K. Behnia, Scalable T^2 resistivity in a small single-component Fermi surface, Science **349**, 945 (2015).

[60] A. Kumar, V. I. Yudson, and D. L. Maslov, Quasiparticle and Nonquasiparticle Transport in Doped Quantum Paraelectrics, Phys. Rev. Lett. **126**, 076601 (2021).

[61] S. Jiang, B. Fauqué, and K. Behnia, T-Square Dependence of the Electronic Thermal Resistivity of Metallic Strontium Titanate, Phys. Rev. Lett. **131**, 016301 (2023).

[62] K. S. Kumar, D. Barbalas, R. Bhandia, D. Lee, S. Varshney, B. Jalan, and N. P. Armitage, Absence of two-phonon quasi-elastic scattering in the normal state of doped $SrTiO_3$ by THz pump-probe spec-

troscopy (2025), arXiv:2501.15771.

[63] J. Wang, J. Wu, T. Wang, Z. Xu, J. Wu, W. Hu, Z. Ren, S. Liu, K. Behnia, and X. Lin, T-square resistivity without Umklapp scattering in dilute metallic Bi_2O_2Se, Nature Comm. **11**, 3846 (2020).

[64] V. M. Kovalev, M. V. Entin, Z. D. Kvon, A. D. Levin, V. A. Chitta, G. M. Gusev, and N. N. Mikhailov, Resistivity of Non-Galilean-Invariant Two-Dimensional Dirac Systems, Phys. Rev. Lett. **134**, 196303 (2025).

[65] M. Kaveh and N. Wiser, Evidence for the electron-electron scattering contribution to the electrical resistivity of aluminum, Physics Letters A **51**, 89 (1975).

[66] K. Andres, J. E. Graebner, and H. R. Ott, $4f$-virtual-bound-state formation in $ceal_3$ at low temperatures, Phys. Rev. Lett. **35**, 1779 (1975).

[67] A. N. Friedman, Some Effects of Sample Size on Electrical Transport in Bismuth, Phys. Rev. **159**, 553 (1967).

[68] H. K. Pal, V. I. Yudson, and D. L. Maslov, Resistivity of non-Galilean-invariant Fermi- and non-Fermi liquids, Lith. J. Phys. **52**, 142 (2012).

[69] R. N. Gurzhi, Hydrodynamic effects in solids at low temperature, Phys. Usp. **11**, 255 (1968).

[70] T. Kiliptari and D. L. Maslov, Resistivity of a non-Galilean–invariant Fermi liquid: Exact solution of the Boltzmann equation (unpublished).

[71] P. Sharma, A. Principi, and D. L. Maslov, Optical conductivity of a Dirac-Fermi liquid, Phys. Rev. B **104**, 045142 (2021).

[72] A. P. Goyal, P. Sharma, and D. L. Maslov, Intrinsic optical absorption in Dirac metals, Annals of Physics **456**, 169355 (2023).

[73] Z. Q. Li, E. A. Henriksen, Z. Jiang, Z. Hao, M. C. Martin, P. Kim, H. L. Stormer, and D. N. Basov, Dirac charge dynamics in graphene by infrared spectroscopy, Nature Physics **4**, 532 (2008).